

# On the Precision of Full-spectrum Fitting of Simple Stellar Populations. I. Well-sampled Populations.

Randa Asa'd<sup>1,2</sup> and Paul Goudfrooij<sup>2</sup>

<sup>1</sup>Physics Department, American University of Sharjah, P.O. Box 26666, Sharjah, UAE

<sup>2</sup>Space Telescope Science Institute, 3700 San Martin Drive, Baltimore, MD 21218, USA

Accepted XXX. Received XXX; in original form 2020 XXX

## ABSTRACT

We investigate the precision of the ages and metallicities of 21,000 mock simple stellar populations (SSPs) determined through full-spectrum fitting. The mock SSPs cover an age range of  $6.8 < \log(\text{age}/\text{yr}) < 10.2$ , for three wavelength ranges in the optical regime, using both Padova and MIST isochrone models. Random noise is added to the model spectra to achieve S/N ratios between 10 to 100 per wavelength pixel. We find that for  $\text{S/N} \geq 50$ , this technique can yield ages of SSPs to an overall precision of  $\Delta \log(\text{age}/\text{yr}) \sim 0.1$  for ages in the ranges  $7.0 \leq \log(\text{age}/\text{yr}) \leq 8.3$  and  $8.9 \leq \log(\text{age}/\text{yr}) \leq 9.4$ . For the age ranges of  $8.3 \leq \log(\text{age}/\text{yr}) \leq 8.9$  and  $\log(\text{age}/\text{yr}) \geq 9.5$ , which have significant flux contributions from asymptotic giant branch (AGB) and red giant branch (RGB) stars, respectively, the age uncertainty rises to about  $\pm 0.3$  dex. The precision of age and metallicity estimation using this method depends significantly on the S/N and the wavelength range used in the fitting. We quantify the systematic differences in age predicted by the MIST and Padova isochrone models, due to their different assumptions about stellar physics in various important (i.e., luminous) phases of stellar evolution, which needs to be taken in consideration when comparing ages of star clusters obtained using these popular models. Knowing the strengths and limitations of this technique is crucial in interpreting the results obtained for real star clusters and for deciding the optimal instrument setup before performing the observations.

**Key words:** galaxies: star clusters: general

## 1 INTRODUCTION

Determining accurate ages and metallicities of star clusters has been an important goal for both galactic and extragalactic astrophysics, because it makes it possible to study the formation and evolution of stars, stellar populations, galaxies and the universe as a whole. Star clusters are generally considered to be the best known examples of simple stellar populations (SSPs), thus providing valuable snapshots of the chemical enrichment history of the region of the galaxy where it resided at the time of its formation. While most old globular clusters are now known to host variations of abundances of several light elements (mainly He, C, N, O, Na, and Al; see [Bastian & Lardo 2018](#), for details), such variations have not yet been found in clusters younger than  $\sim 2$  Gyr (see [Martocchia et al. 2018](#)). In this paper, we simplify this situation by considering star clusters to be well described by SSP models (i.e., models constructed of stars of the same age and metallicity), and we assume solar element abundance ratios.

The most common and direct method to estimate

the age of a star cluster is to obtain a colour-magnitude diagram (CMD) of the constituent stars in the cluster and perform isochrone fitting (e.g., [Goudfrooij et al. 2011, 2014, 2017; Correnti et al. 2014; Niederhofer et al. 2015; Bastian et al. 2016; Milone et al. 2016, 2017](#)). However, for distant galaxies where star clusters cannot be resolved, we have to rely on integrated-light measurements to derive ages and metallicities, e.g., using spectra ([Ahumada et al. 2002; Puzia et al. 2005, 2006; Santos et al. 2006; Palma et al. 2008; Talavera et al. 2010; Cid Fernandes & Gonzalez Delgado 2010; Asa'd et al. 2013; Asa'd 2014; Chilingarian & Asa'd 2018](#)). Some of these studies examined the accuracy of the integrated-light method by comparing the results with results obtained from CMDs for a small number of clusters. Several SSP models (e.g., [Bruzual & Charlot 2003; Maraston 2005; Vazdekis et al. 2010; Maraston & Strömbäck 2011](#)), and different full-spectrum fitting programs (e.g., [Cid Fernandes & Gonzalez Delgado 2010; Asa'd 2014; Wilkinson et al. 2017](#)) are available for analyzing integrated-light spectra of star clusters. In this first paper of

a series aimed at providing useful insights on the accuracy and precision of the method of full-spectrum fitting of integrated-light spectra, we examine the intrinsic precision of this fitting technique in determining the age and metallicity of simple stellar populations (SSPs) of “pseudo-infinite” mass, for which the effects of stochastic fluctuations of the number of stars near the maximum stellar mass at a given SSP age are negligible. In practice this is equivalent to cluster masses  $M_{\text{cl}} \gtrsim 10^6 M_{\odot}$  (see, e.g., Cerviño & Luridiana 2004; Peshev et al. 2008). For this work, we create 21,000 mock clusters of known age and metallicity, in the range  $6.8 < \log(\text{age}/\text{yr}) < 10.2$ , with S/N ratios between 10 to 100 for three wavelength ranges in the optical regime, using both Padova and MIST isochrone models. The main question that we want to address is: How does the accuracy and precision of ages and metallicities determined from full-spectrum fitting of integrated-light spectra depend on S/N, the wavelength range, and the model used? Answering this question will not only help astronomers interpret the results they obtain with this method, but also provide useful information for deciding the optimal instrument set-up before performing such observations (like the optimal wavelength range to be observed and the minimum S/N required to extract reliable information from the data).

## 2 DATA AND METHOD

### 2.1 Mock Star Clusters

We use the flexible stellar population synthesis (FSPS) code (Conroy et al. 2009; Conroy & Gunn 2010) operated through the Python package python-FSPS (Foreman-Mackey et al. 2014) to create two sets of integrated-light spectra (units of  $L_{\odot}/\text{\AA}$ ) of SSPs with Kroupa (2001) IMF and metallicity  $[\text{Z}/\text{H}] = -0.4$  for the age range  $6.8 < \log(\text{age}) < 10.2$  in steps of 0.1 dex. The first set uses Padova isochrones (Marigo et al. 2008), while the second set uses MIST isochrones (Choi et al. 2017). In both cases we use the MILES spectral library (Sánchez-Blázquez et al. 2006; Vazdekis et al. 2010, 2016), which has a spectral resolution of  $2.5 \text{ \AA}$ . We used the metallicity  $[\text{Z}/\text{H}] = -0.4$  to mimic the average metallicity of the Large Magellanic Cloud (LMC)<sup>1</sup>. We use the default settings of python-FSPS, including the absence of nebular emission for the youngest ages, and a zero fraction of blue horizontal branch stars at old ages. For the wavelength range we choose  $3700 - 6200 \text{ \AA}$ , encompassing the range typically used in full spectrum fitting analysis in the literature (e.g., Cappellari et al. 2011; Asa'd et al. 2013, 2016; McDermid et al. 2015). We also perform the same analysis after splitting this wavelength range in two roughly equal parts,  $3700 - 5000 \text{ \AA}$  and  $5000 - 6200 \text{ \AA}$ , in order to allow one to judge both the relative sensitivity of those two wavelength regions to variations in age and/or metallicity, and the impact of using a wavelength range that is roughly twice as small, corresponding to the use of a spectral grating with roughly twice the resolving power  $R$ .

Mock cluster spectra are created by adding 30 different

<sup>1</sup> Later papers in this series will compare observed spectra of LMC clusters with SSP model predictions.

realizations of random noise, corresponding to S/N values between 10 to 100 (in steps of 10) for each SSP, thus producing a grand total of 21,000 mock clusters.

### 2.2 Method

Using FSPS, we produce a model grid that varies in both age ( $6.8 < \log(\text{age}) < 10.2$ , in steps of 0.1 dex) and metallicity ( $-1.0 < [\text{Z}/\text{H}] < 0.2$ , in steps of 0.2 dex). Our two sets of model grids are created using FSPS in order to ensure that the only difference between them is the isochrone family (Padova vs. MILES). We use the full-spectrum fitting program ASAD<sub>2</sub> (for a full description, see Asa'd et al. 2013, 2016; Asa'd 2014) to obtain the best-fitting age and metallicity using the following equation:

$$\sum_{\lambda=\lambda_{\text{initial}}}^{\lambda_{\text{final}}} \frac{[(OF)_{\lambda} - (MF)_{\lambda}]^2}{(OF)_{\lambda_{\text{norm}}}}. \quad (1)$$

where OF is the mock cluster flux, MF is the SSP model flux, and  $\lambda_{\text{norm}}$  is the wavelength at which the model and the mock cluster spectra are normalized.

## 3 RESULTS AND DISCUSSION

### 3.1 Padova Models

#### 3.1.1 Full Wavelength Range: $3700 \leq \lambda/\text{\AA} \leq 6200$

*A. Age Determinations:* Table 1 shows the mean value and its uncertainty (calculated as the standard deviation  $\sigma$ ) of the difference between the derived and the true age for each input age and S/N in this wavelength region.

To visualize the uncertainties associated with the mean derived ages, we plot the standard deviation (uncertainty) versus  $\log(\text{age})$  for all S/N ratios on the left panel of Figure 1. The uncertainties are generally largest in the age intervals  $8.3 \lesssim \log(\text{age}/\text{yr}) \lesssim 8.9$  (especially for  $S/N \lesssim 40$ ) and  $\log(\text{age}/\text{yr}) \gtrsim 9.6$ . For the latter age range, we find  $\sigma(\log(\text{age}/\text{yr})) \gtrsim 0.1$  even for the highest S/N values.

To shed more light on the accuracy of the derived ages, the top row of panels in Figure 3 shows the number of correctly recovered ages i.e., the number of times the derived age matches exactly the input age.) using our full-spectrum fitting method as a function of age. When no point is present for a certain input age it means that specific age was never correctly recovered. As might have been expected, we find that the higher the S/N, the greater the number of the correctly derived results for a given age. However, the number of correctly derived ages also depends on the age: a significant drop in the number of correctly recovered ages is seen around  $\log(\text{age}) = 8.5$  which corresponds to the asymptotic giant branch (AGB) phase transition in stellar evolution, and around  $\log(\text{age}) = 9.0 - 9.2$  which corresponds to the red giant branch (RGB) phase transition, which is confirmed by the CMDs discussed in section 3.3.2.

The second row of panels of Figure 3 shows the difference between the derived and real  $\log(\text{age})$  versus real  $\log(\text{age})$  for the entire sample. The left panels are for S/N values from 10 to 50, and the right panels are for S/N values from 60 to 100.

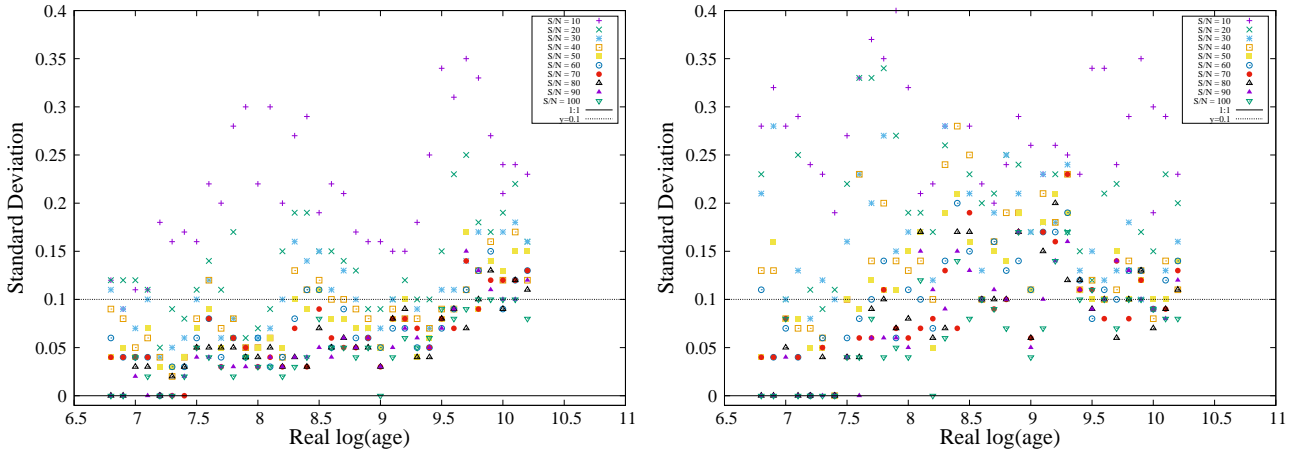


**Figure 1.** The standard deviation ( $\sigma$ ) of the differences of derived  $\log(\text{age})$  (left panel) and  $[\text{Z}/\text{H}]$  (right panel) relative to their true (input) values versus  $\log(\text{age})$  for the full mock clusters sample for all values of  $\text{S/N}$  (see boxed-in legend). The horizontal line at  $\sigma = 0.1$  is plotted to guide the eye.

In addition to illustrating and quantifying the benefit of higher  $\text{S/N}$  in age determinations from full-spectrum fitting, this figure also shows that certain age ranges are generally more susceptible to erroneous age determination than others. Specifically, concentrating on  $\text{S/N}$  values  $> 50$ , relatively large errors are found in the age ranges  $7.5 \lesssim \log(\text{age}) \lesssim 7.8$ ,  $8.5 \lesssim \log(\text{age}) \lesssim 8.9$  and  $\log(\text{age}) \gtrsim 9.1$ , corresponding to the periods during which the integrated light of SSPs is dominated by supergiant stars, AGB stars, and RGB and horizontal branch (HB) stars, respectively.

**B. Metallicity Predictions:** All our mock clusters have a metallicity of  $[\text{Z}/\text{H}] = -0.4$ , while our model clusters cover the metallicity range  $-1.0 < [\text{Z}/\text{H}] < 0.2$  in steps of 0.2 dex.

The right panel of Figure 1 shows that the uncertainties associated with the mean metallicity value are large (relative to the uncertainties for  $\log(\text{age})$ ), especially for the lower  $\text{S/N}$  values.

The third row of panels of Figure 3 shows the fraction of correctly recovered  $[\text{Z}/\text{H}]$  as function of age and  $\text{S/N}$ . Similar to the age predictions, the fraction of correctly recovered  $[\text{Z}/\text{H}]$  generally increases with increased  $\text{S/N}$ , while the age ranges with the lowest fraction of correctly recovered  $[\text{Z}/\text{H}]$  are  $8.4 \lesssim \log(\text{age}) \lesssim 8.9$  and  $\log(\text{age}) \gtrsim 9.1$ , even at the higher values of  $\text{S/N}$ . The bottom row of panels of Figure 3 shows the metallicities derived for our sample as a function of age. Note that the deviation from the real  $[\text{Z}/\text{H}]$  spans the full range considered here (i.e.,  $\pm 0.6$  dex) for spectra with  $\text{S/N} \lesssim 50$ .

Table 13 lists the mean values of  $[\text{Z}/\text{H}]$  for each  $\log(\text{age})$  and  $\text{S/N}$  ratio along with their uncertainties.

### 3.1.2 Wavelength Ranges $3700 \leq \lambda/\text{\AA} \leq 5000$ and $5000 \leq \lambda/\text{\AA} \leq 6200$

When repeating the analysis using the shorter wavelength range  $3700 \leq \lambda/\text{\AA} \leq 5000$ , Figure 4 shows that the age determinations are worse than the full wavelength range for  $\log(\text{age}) > 9.5$ , but they are actually *better* for the younger ages with  $\log(\text{age}) \lesssim 8.5$ . This likely reflects the power of the Balmer jump at  $\sim 4000\text{\AA}$  for age determination using

the full-spectrum fitting method, which is weakened when including a larger wavelength interval beyond  $5000\text{\AA}$  (see also Wilkinson et al. 2017, for a similar result). Similarly, the overall number of correctly recovered age and metallicity shown in Figure 4 are improved in the age range  $6.8 \leq \log(\text{age}) < 8.2$  for  $\text{S/N} = 100$ . Table 2 shows that the mean age is always correctly recovered for  $\text{S/N} \geq 50$ .

For the wavelength range  $5000 \leq \lambda/\text{\AA} \leq 6200$ , the results are generally significantly worse than those for the  $3700 - 5000\text{\AA}$  range, except around input  $\log(\text{age}) \sim 9.0$  for age determination, and for  $\log(\text{age}) \gtrsim 9.5$  for metallicity determination (See Figure 5). This is likely due to the dominance of RGB stars in the energy production of SSPs with ages above  $\sim 1$  Gyr, since RGB stars mainly produce light at the longer wavelengths, and many of the stronger metallicity-sensitive spectral features (e.g., MgH, Mg<sub>2</sub>, several Fe lines; see, e.g., Worthey 1994) are located beyond  $5000\text{\AA}$ .

### 3.2 MIST Models

We repeat the analysis described in Section 3.1, now using the MIST isochrone models. Looking at Figure 6 to 8, the general results remain the same as for the Padova models: results for  $\text{S/N} = 10$  are not reliable regardless of the wavelength range, the wavelength range  $5000 - 6200\text{\AA}$  should never be used for age determination, and metallicity determination from simple integrated-light spectrum fitting is not as powerful as age determination, especially for low values of  $\text{S/N}$ .

In the wavelength range  $3700 - 6200\text{\AA}$ , the fraction of correctly recovered metallicities drops beyond  $\log(\text{age}) = 8.2$  for Padova models, and at  $\log(\text{age}) = 8.4$  for MIST models. This difference in the exact age drop for MIST versus Padova is because the two models make different assumptions about stellar physics in various important (i.e., luminous) phases of stellar evolution.

In the wavelength range  $3700 - 5000\text{\AA}$ , the recovery of ages is very good with MIST models for all ages  $\leq 7.5$ ; however, the drop in recovery fraction for the older ages is steeper relative to the full wavelength range. Good recov-

ery of metallicity in this wavelength range is achieved up to  $\log(\text{age}) = 8.2$  but it has a steep gap at  $\log(\text{age}) = 7.0$  (this gap is located at  $\log(\text{age}) = 7.3$  for Padova models).

### 3.3 A Closer Look into the Differences between the Models

#### 3.3.1 Shifts in derived ages

For the analysis discussed above, the full fitting technique was applied by fitting SSP models with mock clusters built with the same SSP models, which means that we started with SSPs of known ages and metallicities and added various amounts of Poisson noise, then compared those artificial clusters with the full SSP model grid. This was done for both Padova and MIST models.

An interesting question arises: how would the results change if we perform the fitting by comparing Padova-based mock clusters with MIST models, and vice versa (i.e., MIST-based mock clusters with Padova models)? The results of this investigation is shown in Figures 9–14 and Tables 7–12. In the figures showing the number of correctly recovered ages as function of real age, when no point is present for a certain input age it means that specific age was never correctly recovered.

The results show clear differences between some derived ages and the real ones. Just to list a few such differences for the full wavelength range  $3700 \leq \lambda/\text{\AA} \leq 6200$ , when using MIST models with Padova-based mock clusters for  $\log(\text{age}) = 6.8$  we find the mean derived age to be  $\log(\text{age}) = 7.2$ , for  $\log(\text{age}) = 7.0$  the mean derived age is  $\log(\text{age}) = 6.9$ , for  $\log(\text{age}) = 7.1$  the mean derived age is  $\log(\text{age}) = 7.0$ , and for  $\log(\text{age}) = 7.2$  the mean derived age is  $\log(\text{age}) = 7.0$ .

Overall, this shift effect is less significant for analysis based on the wavelength range  $3700 \leq \lambda/\text{\AA} \leq 5000$ . We find a shift of  $\Delta \log(\text{age}/\text{yr}) \sim +0.1$  within the age range  $7.1 \leq \log(\text{age}/\text{yr}) \leq 7.6$ , except for  $\log(\text{age}/\text{yr}) = 7.3$  and 7.5 (that is, the real age is greater than the mean derived age). This shift is  $+0.2$  for  $\log(\text{age}) = 7.7$ , 7.8, and 7.9, it is  $+0.1$  for  $\log(\text{age}) = 8.1$ , 8.2, and 8.3, and it is  $-0.1$  for the range  $9.4 \leq \log(\text{age}) \leq 9.7$ . This shift is evident for the highest S/N ratios, confirming that the shift is not due to the bad quality of the data. The shift is present in all wavelength ranges. This effect will be discussed in details in section 3.3.2.

When using Padova models with MIST-based mock clusters, the shift observed in the range  $3700 \leq \lambda/\text{\AA} \leq 5000$  is again than that in the range  $3700 \leq \lambda/\text{\AA} \leq 6200$ , especially in the age range  $7.5 \leq \log(\text{age}) \leq 8.5$ . In fact, in the range  $3700 \leq \lambda/\text{\AA} \leq 6200$ , none of the ages in the range  $7.5 < \log(\text{age}) < 8.5$  were correctly recovered. As shown in the plots of (derived–real) versus real age, the shifts are very large for  $7.5 < \log(\text{age}) < 8.5$ , with values ranging up to  $-0.7$  to  $-0.9$ . An interesting observation is that there is almost a linear correlation between the shift and the age in the range  $7.5 \leq \log(\text{age}) \leq 8.8$ , with the shift decreasing almost linearly with increasing age. The slope of this linear correlation is about 0.7. However, when looking at the results in the wavelength range  $3700 \leq \lambda/\text{\AA} \leq 5000$ , the typical shift within this age range is only  $-0.3$  except for shifts of  $-0.5$  and  $-0.6$  for  $\log(\text{age}) = 8.3$  and 8.4, respectively.

In the age range  $9.3 \leq \log(\text{age}) \leq 9.7$ , we find that the

shift is almost never less than  $+0.2$  when using the wavelength range  $3700 \leq \lambda/\text{\AA} \leq 5000$ . However, the shifts fluctuate when using the full wavelength range  $3700 \leq \lambda/\text{\AA} \leq 6200$ .

The main conclusion of this comparison exercise is that for a given observed integrated-light spectrum of an SSP, different models can predict significantly different ages, especially in some age ranges as detailed above. This point will be discussed and elaborated on real clusters in an upcoming paper.

#### 3.3.2 CMDs of Padova and MIST isochrones

Figure 15 compares the Padova and MIST isochrones in  $V$  vs.  $B - R$  CMDs from  $\log(\text{age}) = 7.0$  to 10.1, using  $[Z/\text{H}] = -0.4$ .

In each of these sets we note that there are certain age ranges where not much is changing in the shape of the isochrone from one age to the next, which makes it challenging to obtain an accurate age determination in those age ranges. Good examples of such age ranges for the Padova isochrones are  $7.5 < \log(\text{age}) < 7.9$ , just before the AGB starts growing. Another example is the range  $8.5 < \log(\text{age}) < 8.9$ , just before the RGB starts growing.

This is also observed in MIST isochrones, except that the exact ages differ somewhat from one model to the other, because two models make different assumptions about stellar physics in various important (luminous) phases of stellar evolution. The main differences between the MIST and Padova isochrones in the age range studied here are: (i) differences in the onset and extent of the blue loop of core helium burning stars at young ages ( $\log(\text{age}/\text{yr}) \lesssim 7.8$ ); (ii) the growth of the AGB and then RGB occur a bit earlier in the MIST isochrones than in the Padova ones; and (iii) the luminosities of carbon stars in the thermally pulsing AGB, which are significantly higher for the Padova isochrones (for details, see Marigo et al. 2008; Choi et al. 2016). We also note that the MIST isochrones include post-AGB evolution and the Padova ones do not, but this is not relevant for a typical star cluster given the very small numbers of post-AGB stars and the speed with which such stars move through the optically luminous part of the CMD (see, e.g., Brown et al. 2000).

The differences mentioned above explain the shifts seen between ages of mock clusters built using one SSP model and fit by another one. For example, when fitting Padova-based clusters with MIST models, the model predicts  $\log(\text{age}) = 7.2$  for the real  $\log(\text{age}) = 6.8$  which is likely caused by the “blue loop” of supergiants which starts significantly earlier in the Padova models than in the MIST models.

## 4 CAN FIXING THE METALLICITY IMPROVE THE DERIVED AGE?

So far all analysis was done by varying both age and metallicity. Solving for fewer unknowns would certainly improve the fitting, however, when applying this technique to typical observations, neither the age nor the metallicity is known. In the previous sections we saw that age determination using the full-spectrum fitting technique can be successful to an accuracy of 0.1 dex (up to  $\log(\text{age}/\text{yr}) \sim 9.5$ ), however,

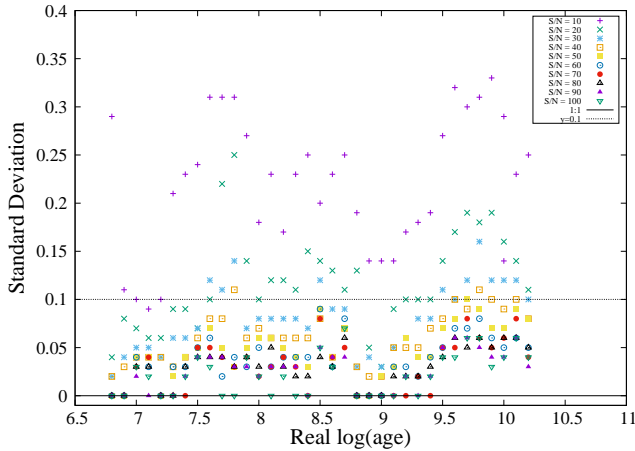


**Figure 2.** The standard deviation ( $\sigma$ ) for derived  $\log(\text{age})$  minus real  $\log(\text{age})$ , at a fixed  $[Z/\text{H}] = -0.4$  (see discussion in Section 4). The horizontal line at  $\sigma = 0.1$  is plotted to guide the eye.

the metallicity determination is not as good, especially for lower S/N. It is then interesting to study the case of using models of fixed metallicity, and explore whether the age determination is improved.

As mentioned in section 2, all our mock clusters have metallicity  $[Z/\text{H}] = -0.4$ . Assuming that the metallicity is unknown, we created Padova models for the same age range, but for a fixed solar metallicity. We applied the full spectrum fitting and analyzed the results. We then repeated the analysis with Padova models of fixed metallicity  $[Z/\text{H}] = -0.8$ .

The results are shown in figures 16. When solar metallicity is used, over all ages are underestimated. The strongest underestimation is for  $\log(\text{age}) > 9.5$ . Using the wavelength range  $3700 \leq \lambda/\text{\AA} \leq 5000$  with high S/N reduces the underestimation of age.

The opposite effect is seen when using  $[Z/\text{H}] = -0.8$ . Most ages are overestimated, however this is slightly improved for high S/N when using the wavelength range  $3700 \leq \lambda/\text{\AA} \leq 6200$ . See Beasley et al. (2002) and Asa'd et al. (2016) for more discussion on the effect of metallicity.

When using  $[Z/\text{H}] = -0.4$ , the overall age determination improves compared to the results when the metallicity is unknown a priori. Figure 2 shows that this is especially the case for  $\log(\text{age}/\text{yr}) \geq 8.0$  (compare with Figure 1). In fact, for  $S/N > 30$ , the standard deviation ( $\sigma$ ) is found to stay  $< 0.1$  for all ages. The overall improvement in  $\sigma$  relative to the case of letting metallicity be a free parameter is of order factors of 1.5–2 depending on the input age.

## 5 THE ROLE OF EXTINCTION

Although several recently developed full-spectrum fitting techniques do not directly fit for extinction (e.g., Chilingarian et al. 2007; Larsen et al. 2012; Hernandez et al. 2017), it is important to note that age and extinction do affect the shape of spectra in a similar way, especially when the spectral range does not include a strong break such as the Balmer jump.

In this section we discuss the effect of including extinction as a free parameter on the fitting results obtained on

our mock clusters. This is done by allowing our fitting technique to apply the Cardelli et al. (1989) extinction law with  $R_V = 3.1$ , using the range of  $E(\text{B}-\text{V})$  from 0.0 to 0.5, in steps of 0.01. We perform this analysis by comparing Padova model clusters with the Padova isochrone models for the full wavelength range  $3700 \leq \lambda/\text{\AA} \leq 6200$ .

We start with analyzing the case of fixed metallicity. Here we use the models with the same metallicity as the mock clusters in order to constrain that variable in the fitting procedure. The left panel of Figure 17 shows  $\log(\text{age})$  obtained when accounting for extinction versus  $\log(\text{age})$  obtained without accounting for extinction.

Overall, we find that ages are correctly retrieved for the higher S/N ratios (above  $\sim 50$ ). However, for the lower S/N ratios, there is a tendency to fit somewhat younger ages when reddening is a variable in the fitting. This tendency is strongest in the age range  $7.8 < \log(\text{age}) < 8.5$ , and is also apparent for  $\log(\text{age}) \gtrsim 9.5$ . This tendency is however not seen for the youngest ages ( $\log(\text{age}) \lesssim 7.5$ ), which is probably mainly due to the prominent Balmer jump at those ages.

We repeat this analysis by letting all parameters (age, metallicity and reddening) vary. The results are shown in the right panel of Figure 17. It turns out that this extra degree of freedom does not worsen the tendency to fit slightly younger ages along with small amounts of extinction, nor does it change the age ranges where this tendency is observed in any significant way.

## 6 SUMMARY

In this work we used synthetic spectra of 21,000 artificial star clusters spanning an age range of  $6.8 < \log(\text{age}) < 10.2$ , with S/N ratios between 10 to 100 using isochrone models of both Padova and MIST to analyze the accuracy and precision of ages and metallicities of SSPs obtained from full-spectrum fitting in three wavelength intervals. Our results can be summarized in the following points:

(A) Overall, this method can be used in obtaining ages of simple stellar populations to a precision of 0.1 dex (i.e.,  $\sim 25\%$ ) in the age range  $7.0 \leq \log(\text{age}/\text{yr}) \leq 9.5$ , provided that  $S/N \geq 50$ . Metallicity determinations using this technique are however generally not as precise. For  $S/N \gtrsim 50$ , typical standard deviations  $\sigma$  for  $[Z/\text{H}]$  range between  $\sim 0.05$  dex and 0.20 dex, depending on the age, and worse for lower S/N.

(B) Age determinations using the full wavelength range  $3700 \leq \lambda/\text{\AA} \leq 6200$  are generally not as precise as those obtained for the narrower range  $3700 \leq \lambda/\text{\AA} \leq 5000$ . This likely reflects the power of the 4000 Å Balmer jump for age determination, which is diluted when including more spectral range on the long-wavelength end of the optical range.

(C) For optical integrated-light spectra of SSPs with  $S/N \leq 50$ , full-spectrum fitting yields significant age uncertainties in the age ranges  $8.2 \leq \log(\text{age}/\text{yr}) \leq 8.8$  and  $\log(\text{age}/\text{yr}) \gtrsim 9.5$  (for the Padova models). This is due to the fact that the shape of the CMD does not change significantly with age in those intervals.

(D) There is no significant difference in the precision of age and metallicity determination when using MIST models or Padova models for clusters based on the same models.

## 6 Asa'd & Goudfrooij

(E) MIST and Padova isochrones make different assumptions about stellar physics in various important (i.e., luminous) phases of stellar evolution (e.g., the onsets of the supergiants, AGB, and RGB phases). We quantify the impact of these differences to the derived ages as a function of age, finding significant differences in the age ranges  $7.5 \lesssim \log(\text{age}/\text{yr}) \lesssim 8.5$  and  $9.3 \lesssim \log(\text{age}/\text{yr}) \lesssim 9.7$ . This issue needs to be taken in consideration when comparing SSP ages obtained by full-spectrum fitting using different models.

(F) When using models of fixed metallicity to predict the age, ages are generally underestimated when using models of higher metallicities than the mock clusters' metallicity, and overestimated when using models of lower metallicity than the mock clusters.

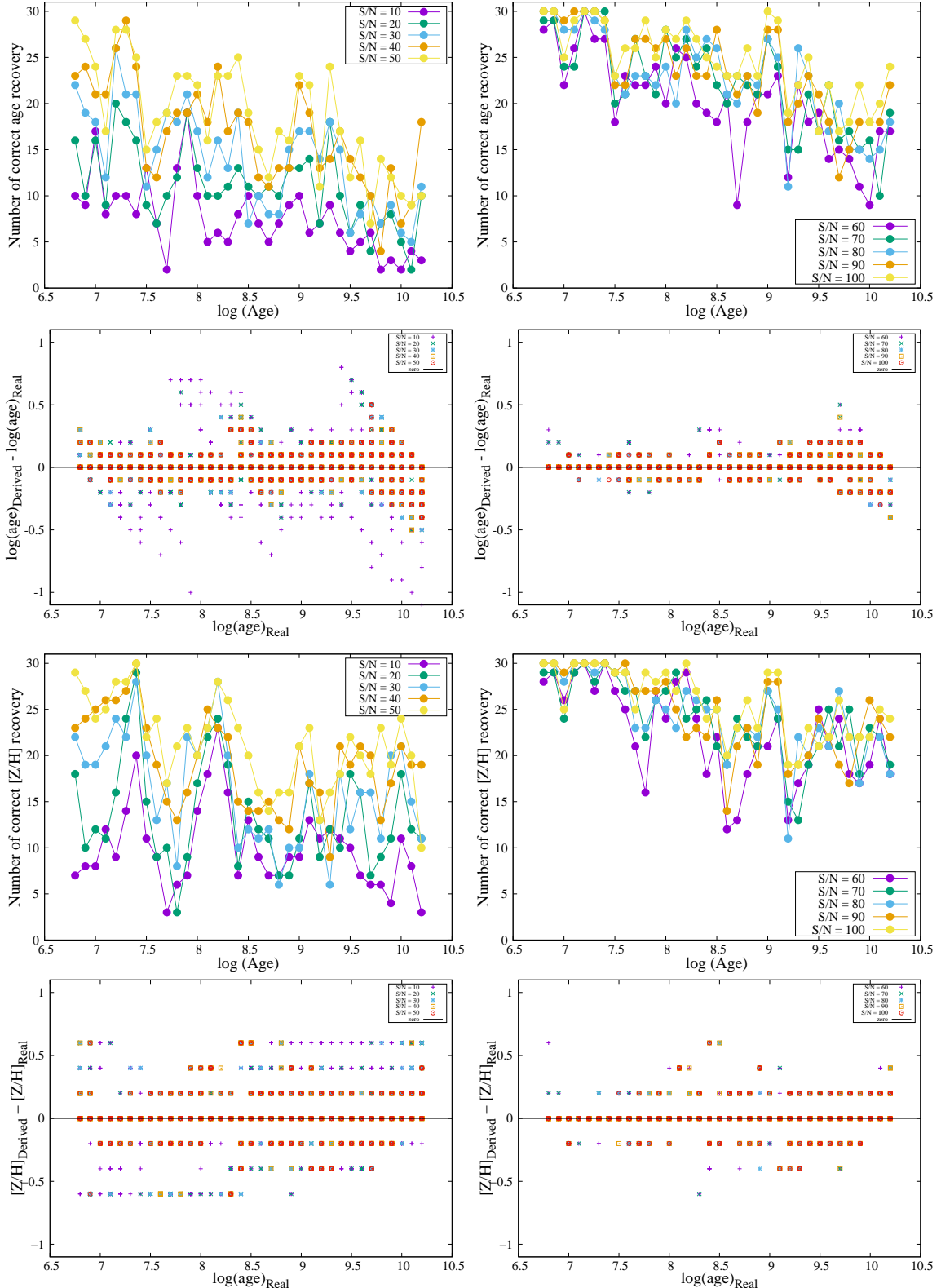
(G) We assess the effect of including extinction as an additional free parameter in full-spectrum fitting to the accuracy of age and metallicity determination, using a range  $0.0 \leq E(B-V) \leq 0.5$ . Overall, we find that ages are correctly retrieved to within 0.1 dex for spectra with S/N  $\gtrsim 50$ . However, for lower S/N ratios, there is a tendency to fit younger ages (by  $\Delta \log(\text{age}/\text{yr}) \lesssim 0.7$ , depending on the age) when extinction is a variable in the fitting.

## ACKNOWLEDGMENTS

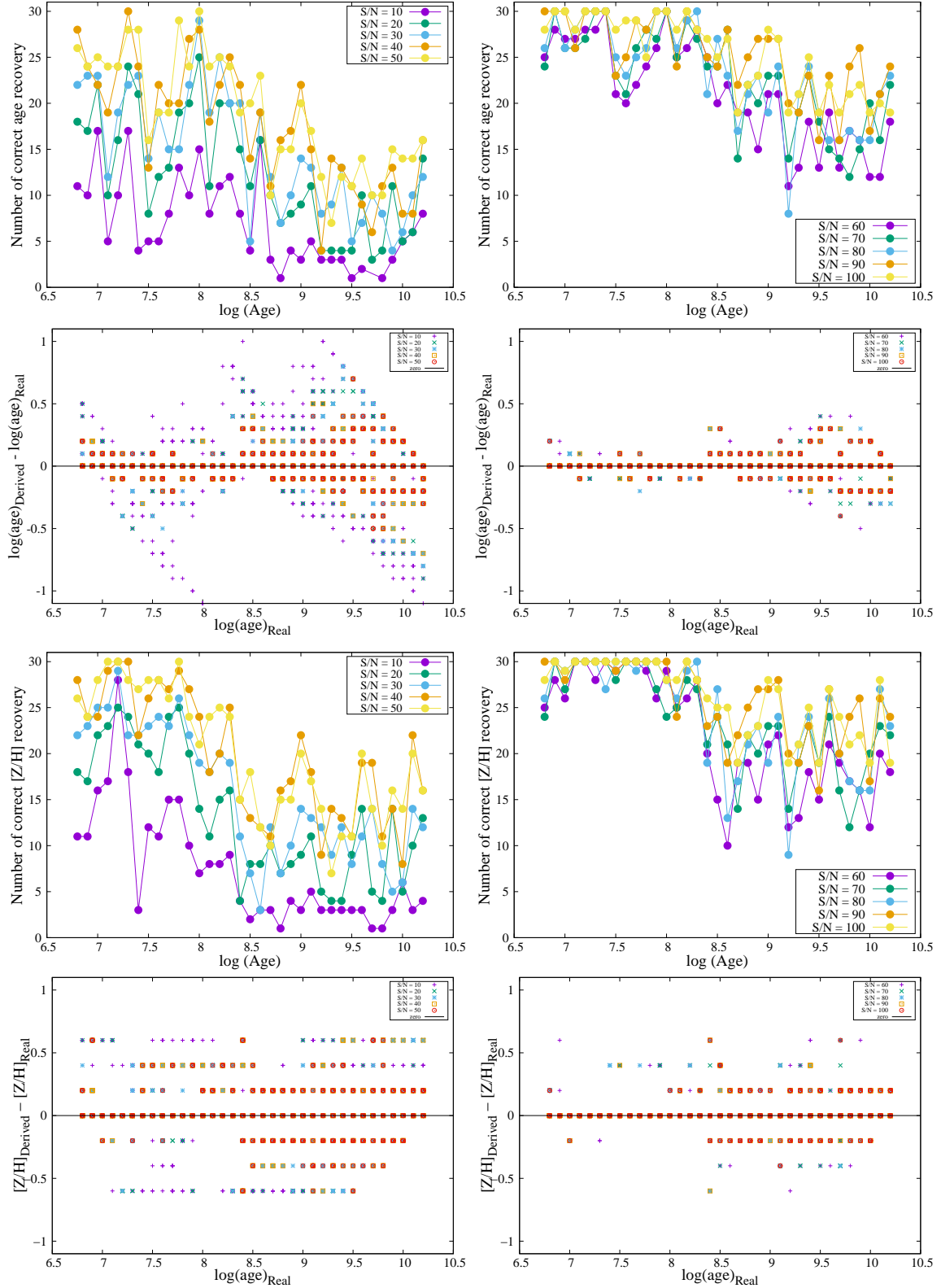
R.A. thanks the Space Telescope Science Institute for a sabbatical visitorship including travel and subsistence support as well as access to their science cluster computer facilities. This work is supported in part by the EFRG18-SET-CAS-74 and FRG19-M-S77 (Grant P.I., R. Asa'd) from American University of Sharjah. R.A. is grateful to Benjamin Johnson for useful discussions on using python-FSPS.

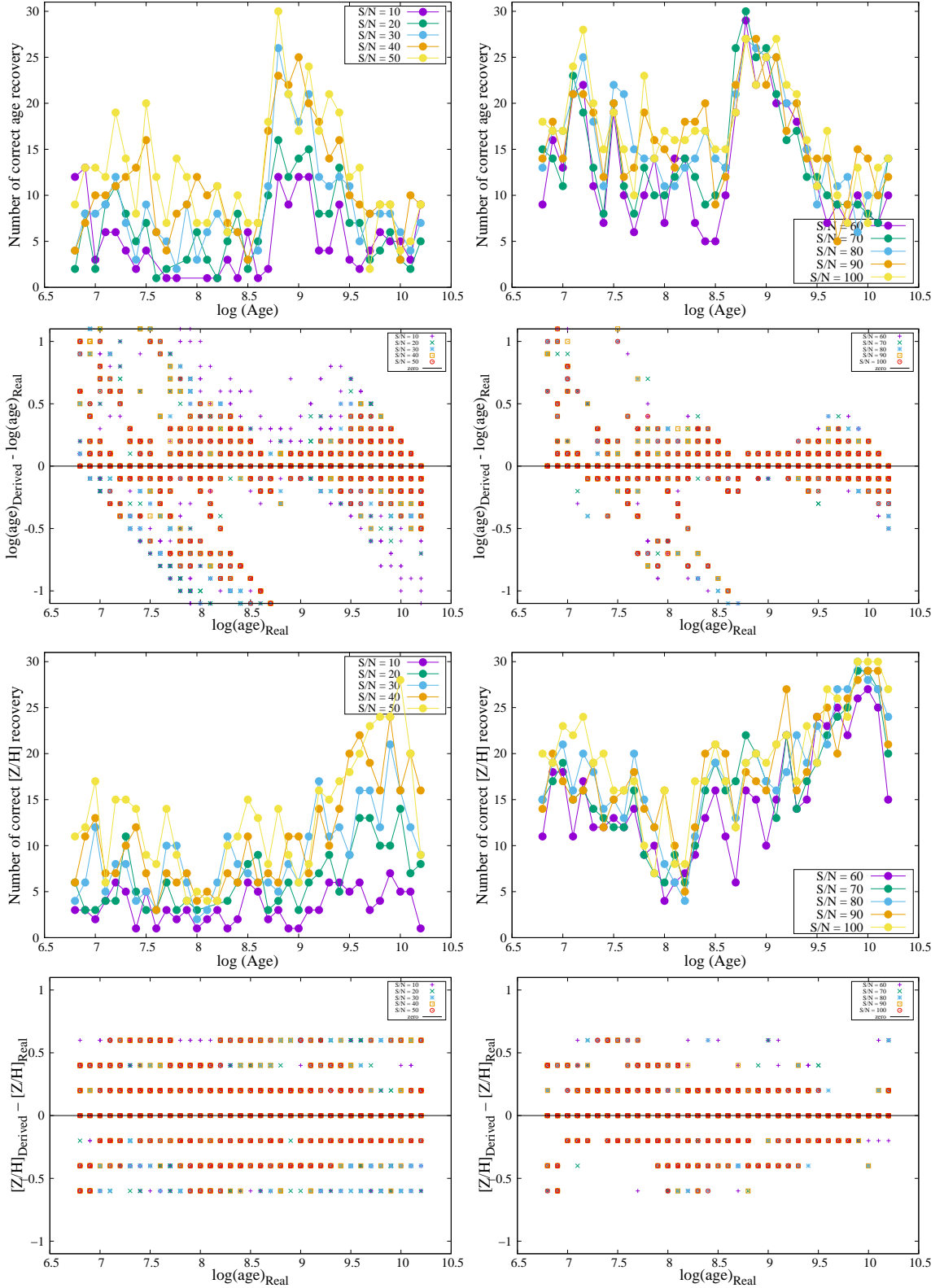
## REFERENCES

- Ahumada A. V., Claria J. J., Bica E., Dutra C. M., 2002, *A&A*, **393**, 855  
 Asa'd R. S., 2014, *MNRAS*, **445**, 1679  
 Asa'd R. S., Hanson M. M., Ahumada A. V., 2013, *PASP*, **125**, 1304  
 Asa'd R. S., Vazdekis A., Zeinelabdin S., 2016, *MNRAS*, **457**, 2151  
 Bastian N., Lardo C., 2018, *ARA&A*, **56**, 83  
 Bastian N., et al., 2016, *MNRAS*, **460**, L20  
 Beasley M. A., Hoyle F., Sharples R. M., 2002, *MNRAS*, **336**, 168  
 Brown T. M., Bowers C. W., Kimble R. A., Sweigart A. V., Ferguson H. C., 2000, *ApJ*, **532**, 308  
 Bruzual G., Charlot S., 2003, *MNRAS*, **344**, 1000  
 Cappellari M., et al., 2011, *MNRAS*, **413**, 813  
 Cardelli J. A., Clayton G. C., Mathis J. S., 1989, *ApJ*, **345**, 245  
 Cerviño M., Luridiana V., 2004, *A&A*, **413**, 145  
 Chilingarian I. V., Asa'd R., 2018, *ApJ*, **858**, 63  
 Chilingarian I., Prugniel P., Sil'Chenko O., Koleva M., 2007, in Vazdekis A., Peletier R., eds, IAU Symposium Vol. 241, Stellar Populations as Building Blocks of Galaxies. pp 175–176 ([arXiv:0709.3047](https://arxiv.org/abs/0709.3047)), doi:[10.1017/S1743921307007752](https://doi.org/10.1017/S1743921307007752)  
 Choi J., Dotter A., Conroy C., Cantiello M., Paxton B., Johnson B. D., 2016, *ApJ*, **823**, 102  
 Choi J., Conroy C., Byler N., 2017, *ApJ*, **838**, 159  
 Cid Fernandes R., Gonzalez Delgado R. M., 2010, *MNRAS*, **403**, 780  
 Conroy C., Gunn J. E., 2010, *ApJ*, **712**, 833  
 Conroy C., Gunn J. E., White M., 2009, *ApJ*, **699**, 486  
 Correnti M., Goudfrooij P., Kalirai J. S., Girardi L., Puzia T. H., Kerber L., 2014, *ApJ*, **793**, 121  
 Foreman-Mackey D., Sick J., Johnson B., 2014, python-fsp: Python bindings to FSPS (v0.1.1), doi:[10.5281/zenodo.12157](https://doi.org/10.5281/zenodo.12157)  
<https://doi.org/10.5281/zenodo.12157>  
 Goudfrooij P., Puzia T. H., Kozhurina-Platais V., Chandar R., 2011, *ApJ*, **737**, 3  
 Goudfrooij P., et al., 2014, *ApJ*, **797**, 35  
 Goudfrooij P., Girardi L., Correnti M., 2017, *ApJ*, **846**, 22  
 Hernandez S., Larsen S., Trager S., Groot P., Kaper L., 2017, *A&A*, **603**, A119  
 Kroupa P., 2001, *MNRAS*, **322**, 231  
 Larsen S. S., Brodie J. P., Strader J., 2012, *A&A*, **546**, A53  
 Maraston C., 2005, *MNRAS*, **362**, 799  
 Maraston C., Strömbäck G., 2011, *MNRAS*, **418**, 2785  
 Marigo P., Girardi L., Bressan A., Groenewegen M. A. T., Silva L., Granato G. L., 2008, *A&A*, **482**, 883  
 Martocchia S., et al., 2018, *MNRAS*, **477**, 4696  
 McDermid R. M., et al., 2015, *MNRAS*, **448**, 3484  
 Milone A. P., Marino A. F., D'Antona F., Bedin L. R., Da Costa G. S., Jerjen H., Mackey A. D., 2016, *MNRAS*, **458**, 4368  
 Milone A. P., et al., 2017, *MNRAS*, **465**, 4363  
 Niederhofer F., Hilker M., Bastian N., Silva-Villa E., 2015, *A&A*, **575**, A62  
 Palma T., Ahumada A., Claria J., Bica E., 2008, *Astronomische Nachrichten*, **329**, 392  
 Peshev P. M., Goudfrooij P., Puzia T. H., Chandar R., 2008, *MNRAS*, **385**, 1535  
 Puzia T. H., Kissler-Patig M., Thomas D., Maraston C., Saglia R. P., Bender R., Goudfrooij P., Hempel M., 2005, *A&A*, **439**, 997  
 Puzia T. H., Kissler-Patig M., Goudfrooij P., 2006, *ApJ*, **648**, 383  
 Sánchez-Blázquez P., et al., 2006, *MNRAS*, **371**, 703  
 Santos J. F. C., Claria J. J., Ahumada A. V., Bica E., Piatti A. E., Parisi M. C., 2006, *A&A*, **448**, 1023  
 Talavera M., Ahumada A., Santos J., Clariá J., Bica E., Parisi M., Torres M., 2010, *Astronomische Nachrichten*, **331**, 323  
 Vazdekis A., Sánchez-Blázquez P., Falcón-Barroso J., Cenarro A. J., Beasley M. A., Cardiel N., Gorgas J., Peletier R. F., 2010, *MNRAS*, **404**, 1639  
 Vazdekis A., Koleva M., Ricciardelli E., Röck B., Falcón-Barroso J., 2016, *MNRAS*, **463**, 3409  
 Wilkinson D. M., Maraston C., Goddard D., Thomas D., Parikh T., 2017, *MNRAS*, **472**, 4297  
 Worthey G., 1994, *ApJS*, **95**, 107

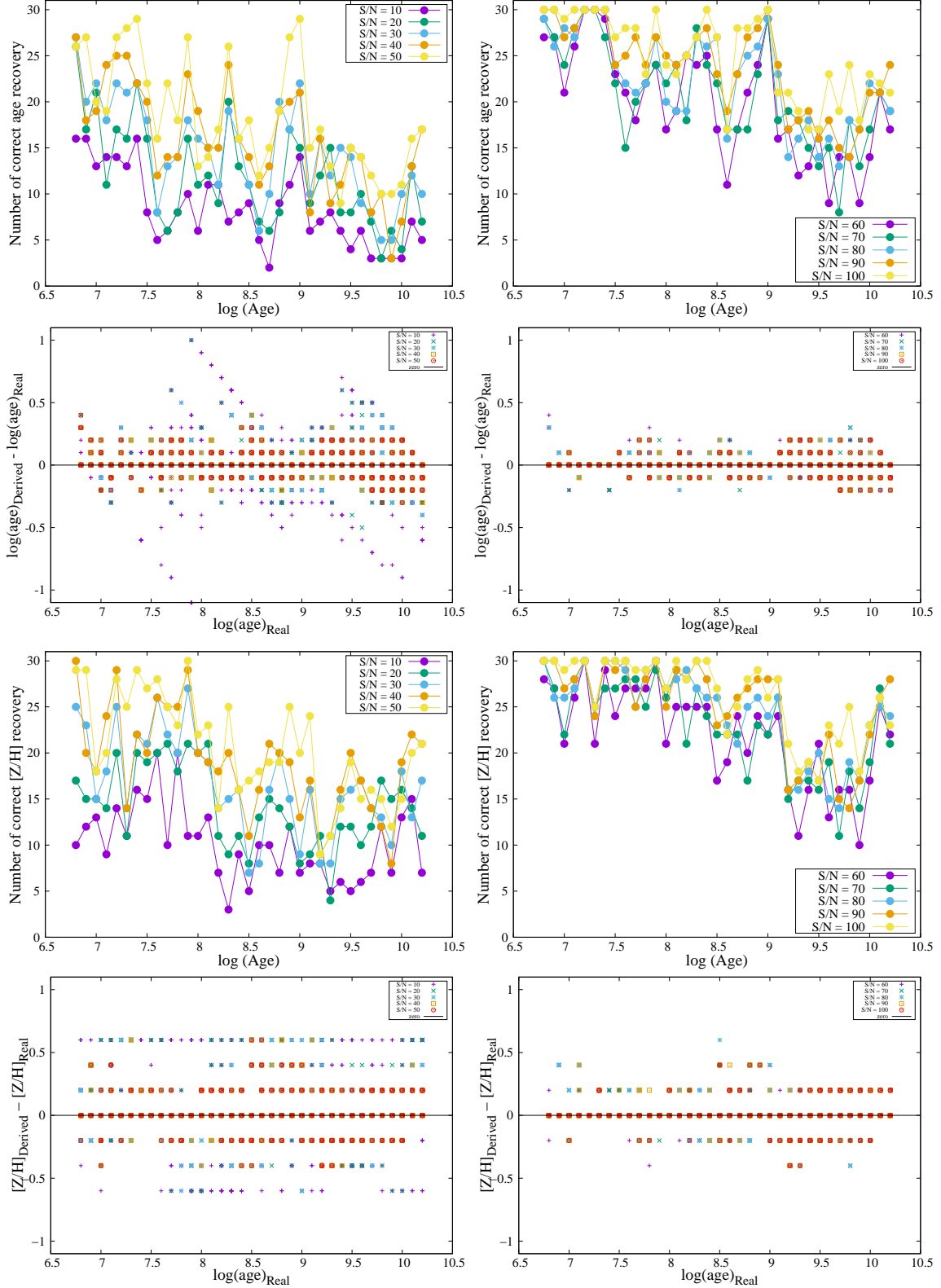


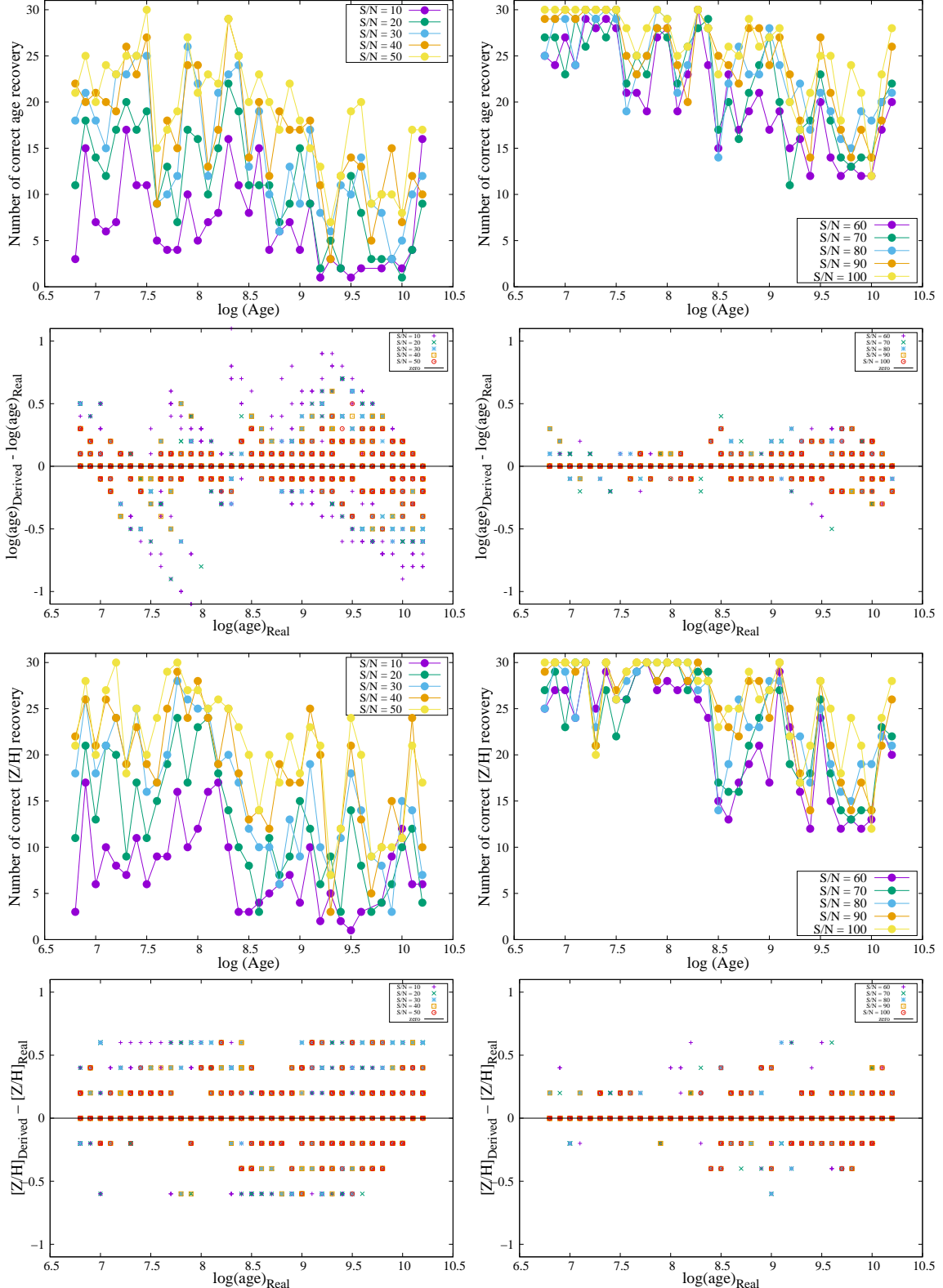
**Figure 3.** The results obtained with the full-spectrum fitting technique in the range  $3700 \leq \lambda/\text{\AA} \leq 6200$  using Padova isochrone models. The left panels show the results for  $10 \leq \text{S/N} \leq 50$  and the right panels do so for  $60 \leq \text{S/N} \leq 100$ . The first panel shows the number of correctly recovered age as a function of input age. The second panel shows  $(\text{Derived log(age)} - \text{Real log(age)})$  versus Real log(age). The third panel shows the number of correctly recovered metallicity as a function of log(age). The fourth panel shows  $(\text{Derived metallicity} - \text{Real metallicity})$  versus Real log(age).

**Figure 4.** -PADOVA- The same as figure 3 for the range  $3700 \leq \lambda/\text{\AA} \leq 5000$

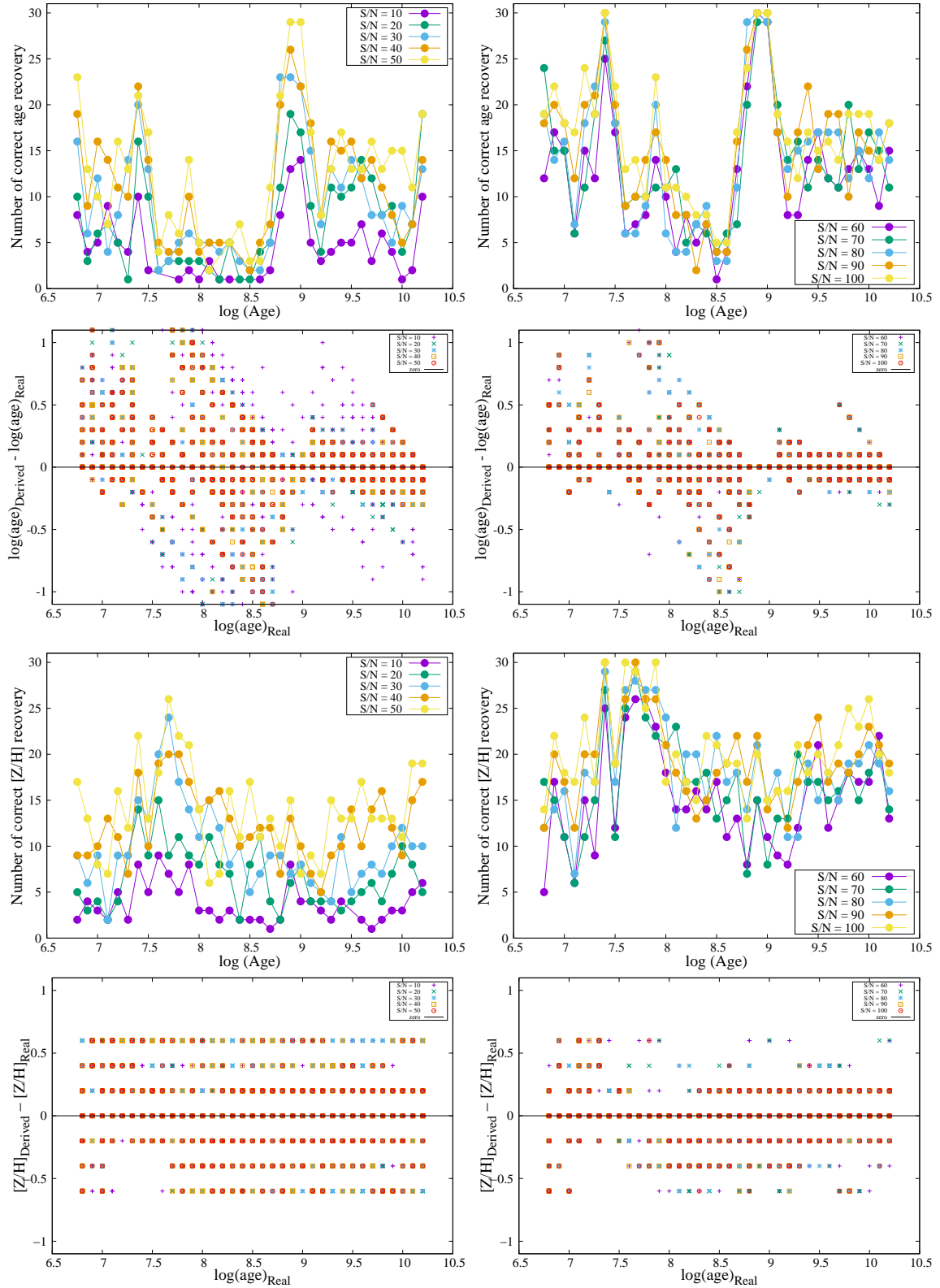


**Figure 5.** -PADOVA- The same as figure 3 for the range  $5000 \leq \lambda/\text{\AA} \leq 6200$

**Figure 6.** The same as figure 3 using MIST models



**Figure 7.** The same as figure 6 for the range  $3700 \leq \lambda/\text{\AA} \leq 5000$

**Figure 8.** The same as 6 for  $5000 \leq \lambda/\text{\AA} \leq 6200$

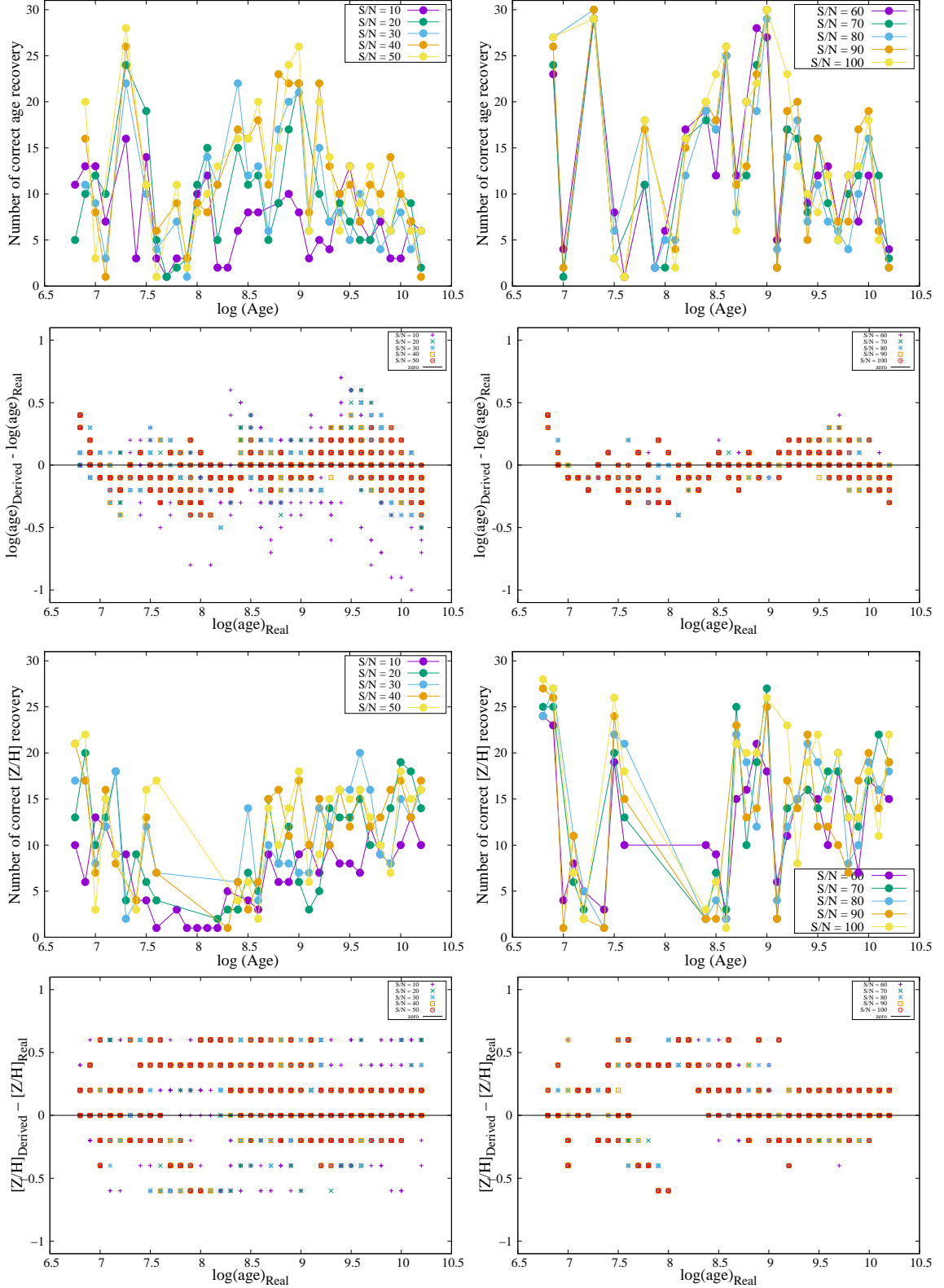


**Figure 9.** The same as figure 3 for the range  $3700 \leq \lambda/\text{\AA} \leq 6200$  using MIST models and Padova mock clusters

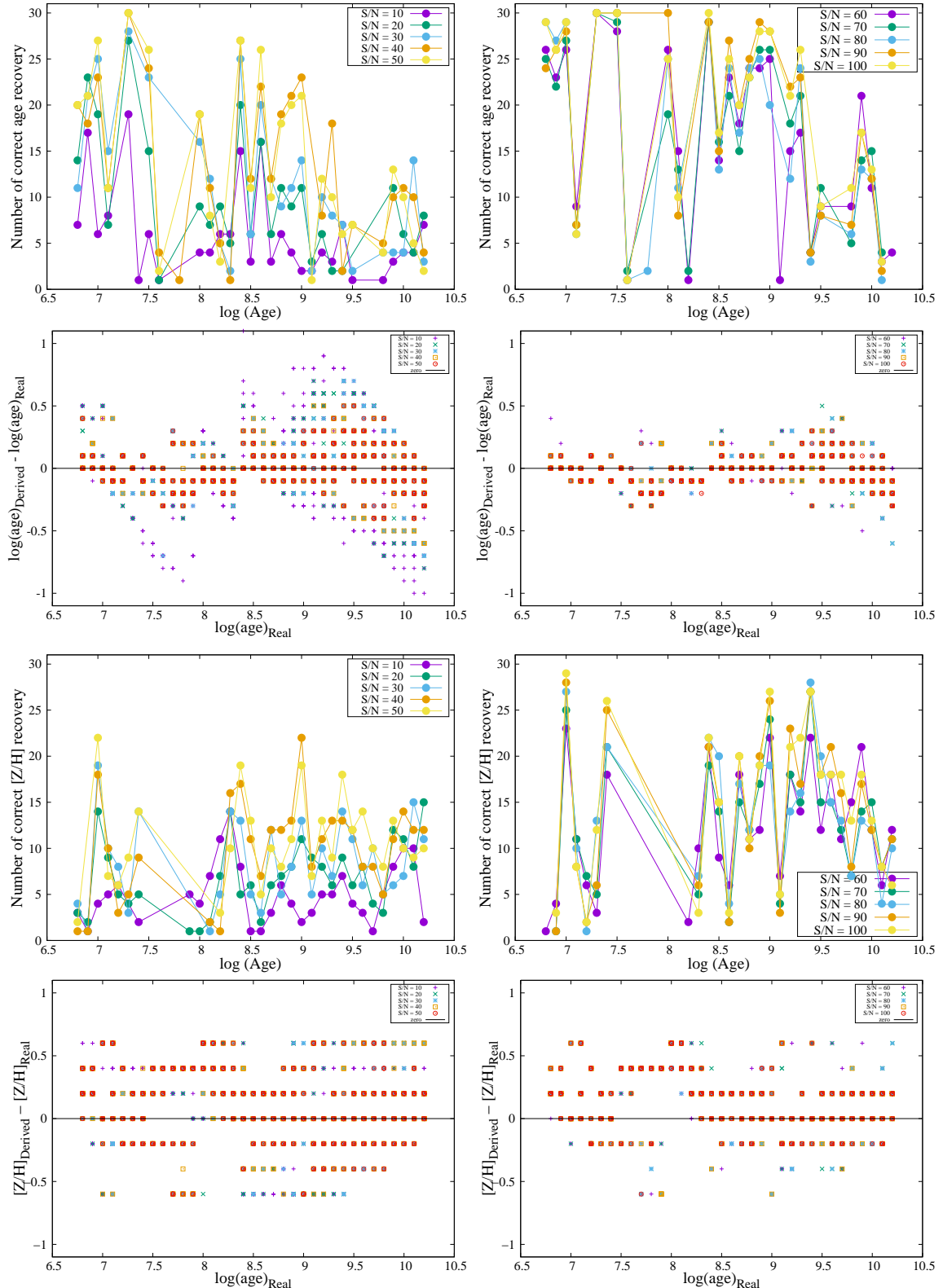


**Figure 10.** The same as figure 9 for the range  $3700 \leq \lambda/\text{\AA} \leq 5000$

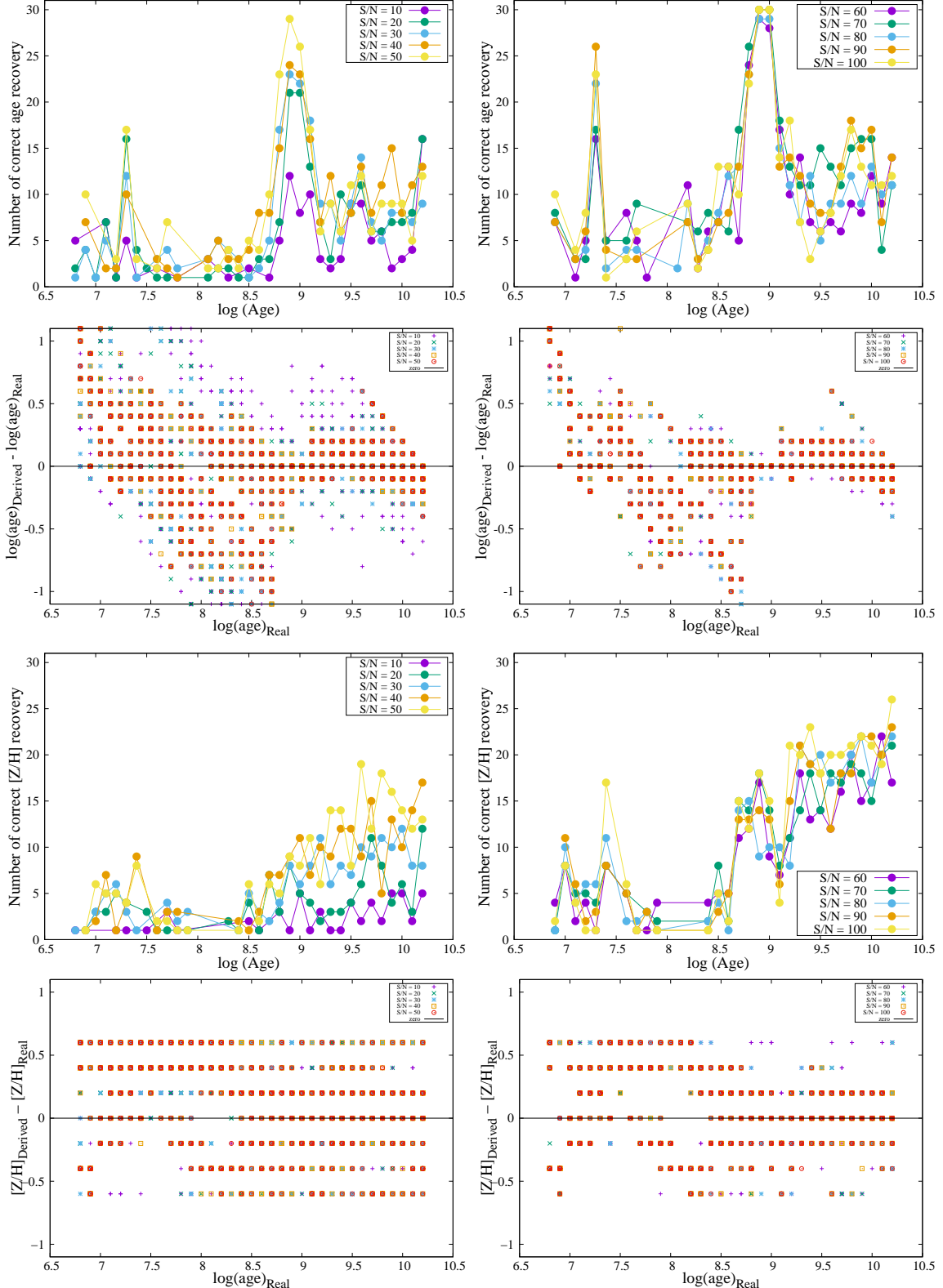
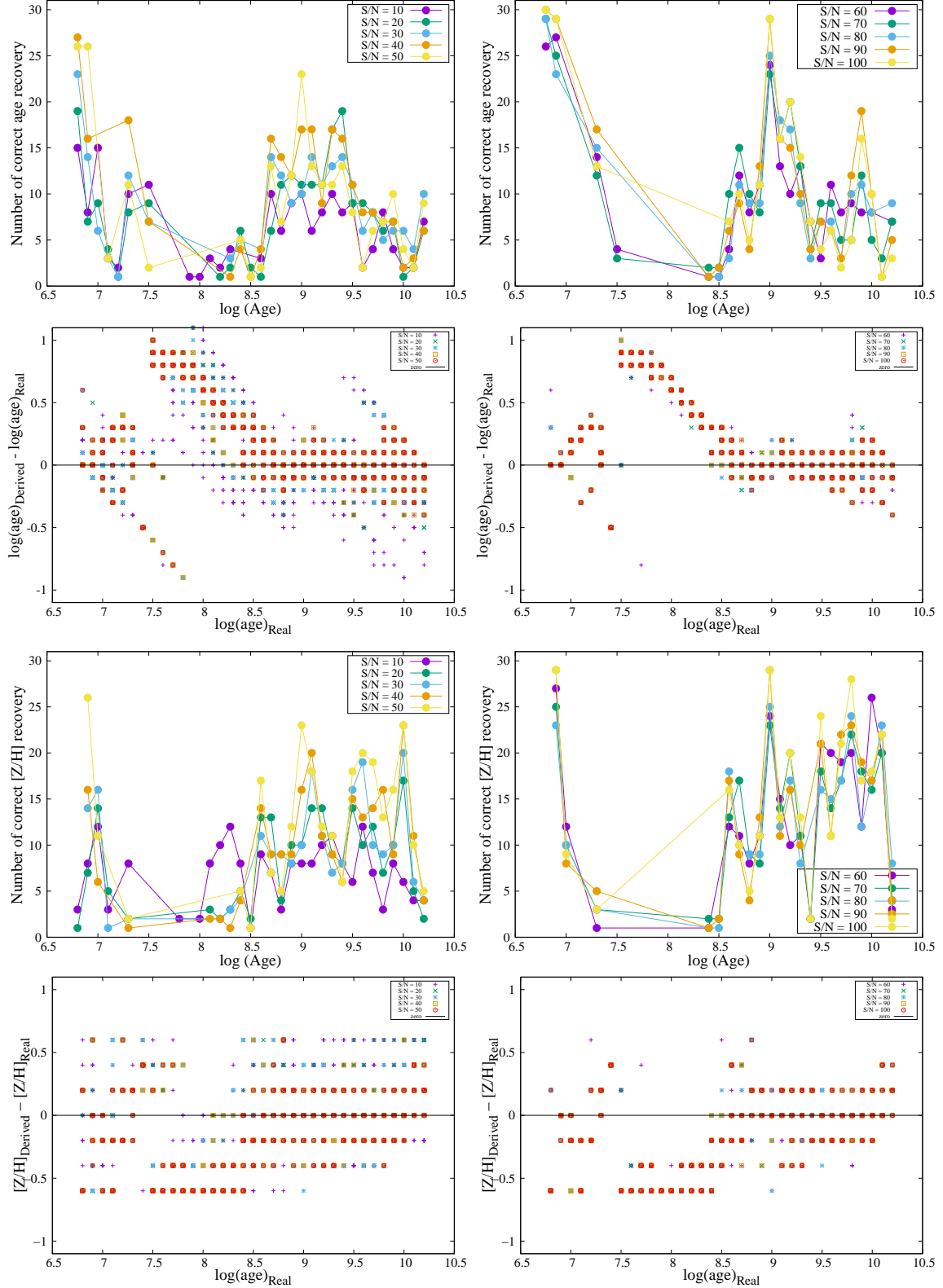
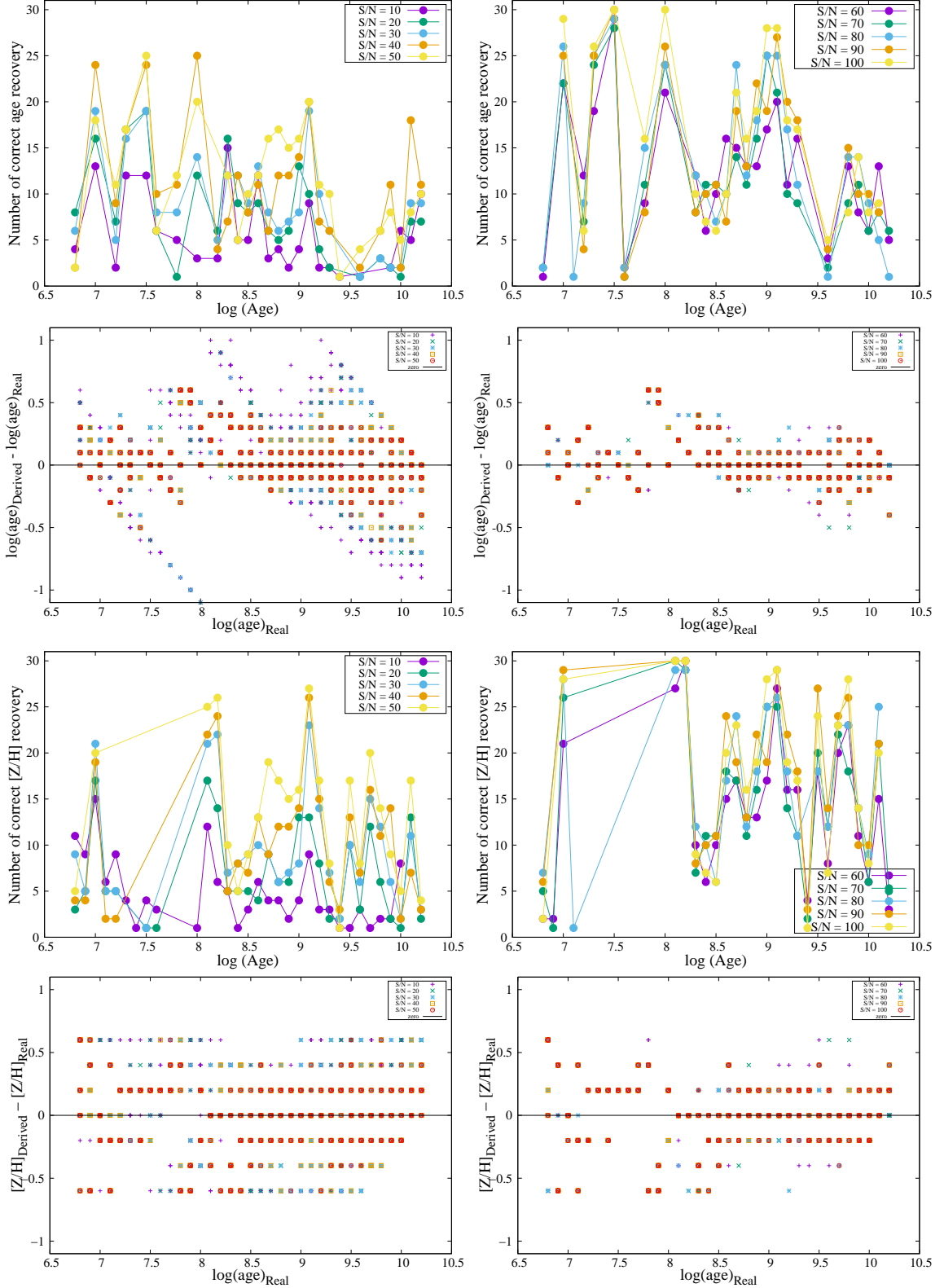


Figure 11. The same as figure 9 for the range  $5000 \leq \lambda/\text{\AA} \leq 6200$



**Figure 12.** The same as figure 3 for the range  $3700 \leq \lambda/\text{\AA} \leq 6200$  using Padova models and MIST mock clusters



**Figure 13.** The same as figure 12, now for the range  $3700 \leq \lambda/\text{\AA} \leq 5000$

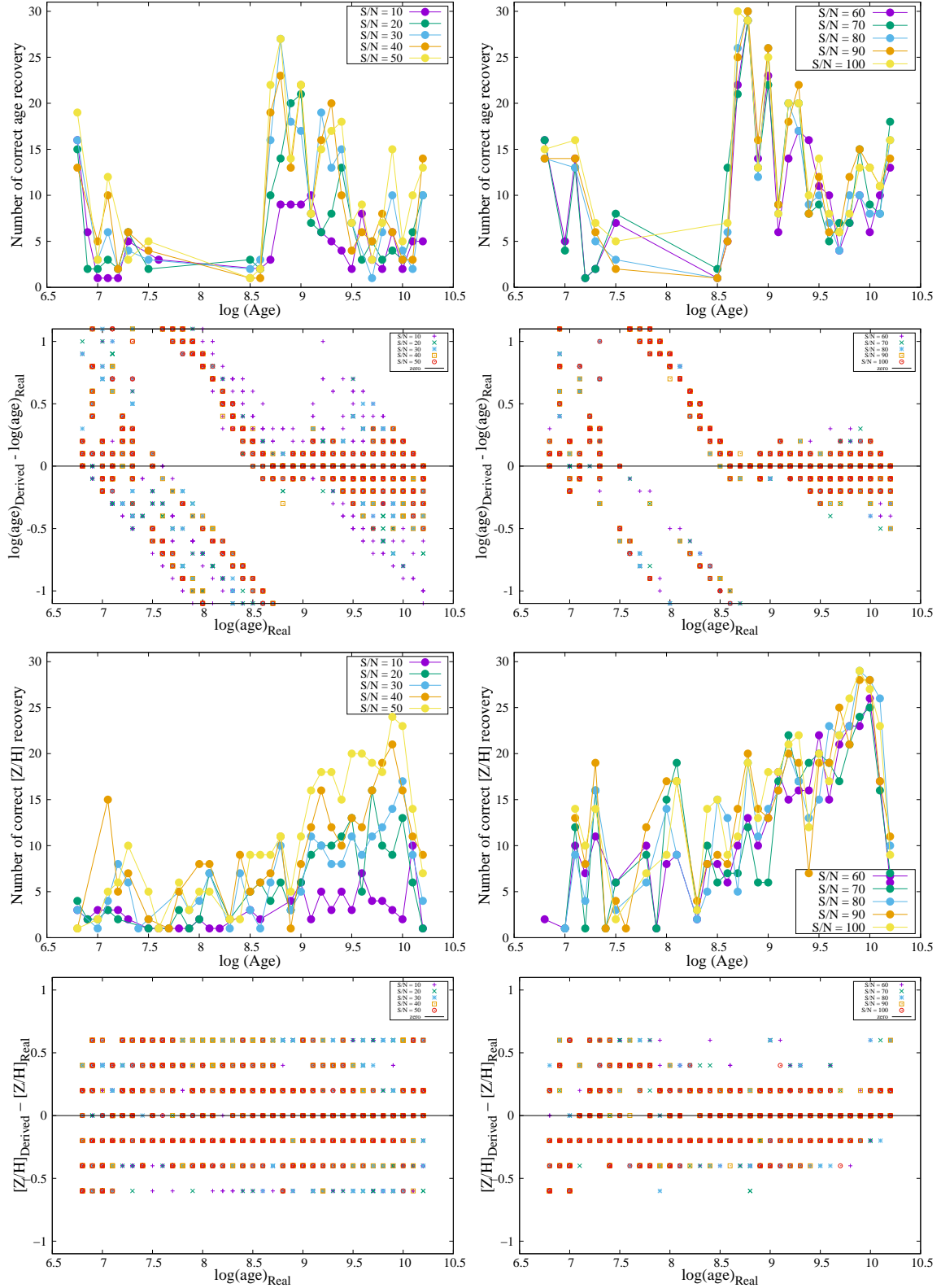


**Figure 14.** The same as figure 12, now for the range  $5000 \leq \lambda/\text{\AA} \leq 6200$

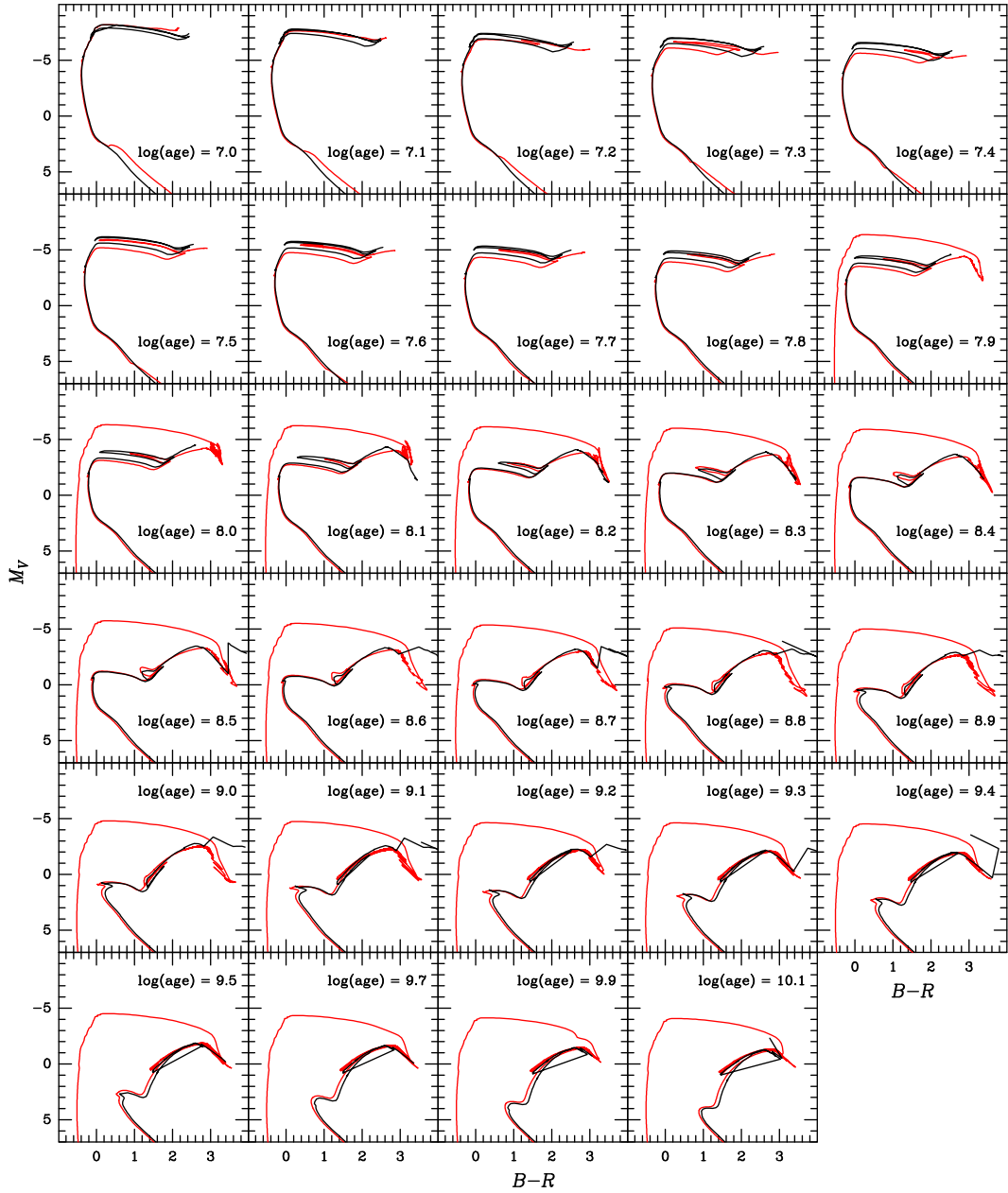


**Figure 15.**  $V$  vs.  $B - R$  CMDs from  $\log(\text{age}) = 7.0$  to  $10.1$ , using  $[Z/H] = -0.4$ . Black lines represent Padova isochrones while red lines represent MIST isochrones.

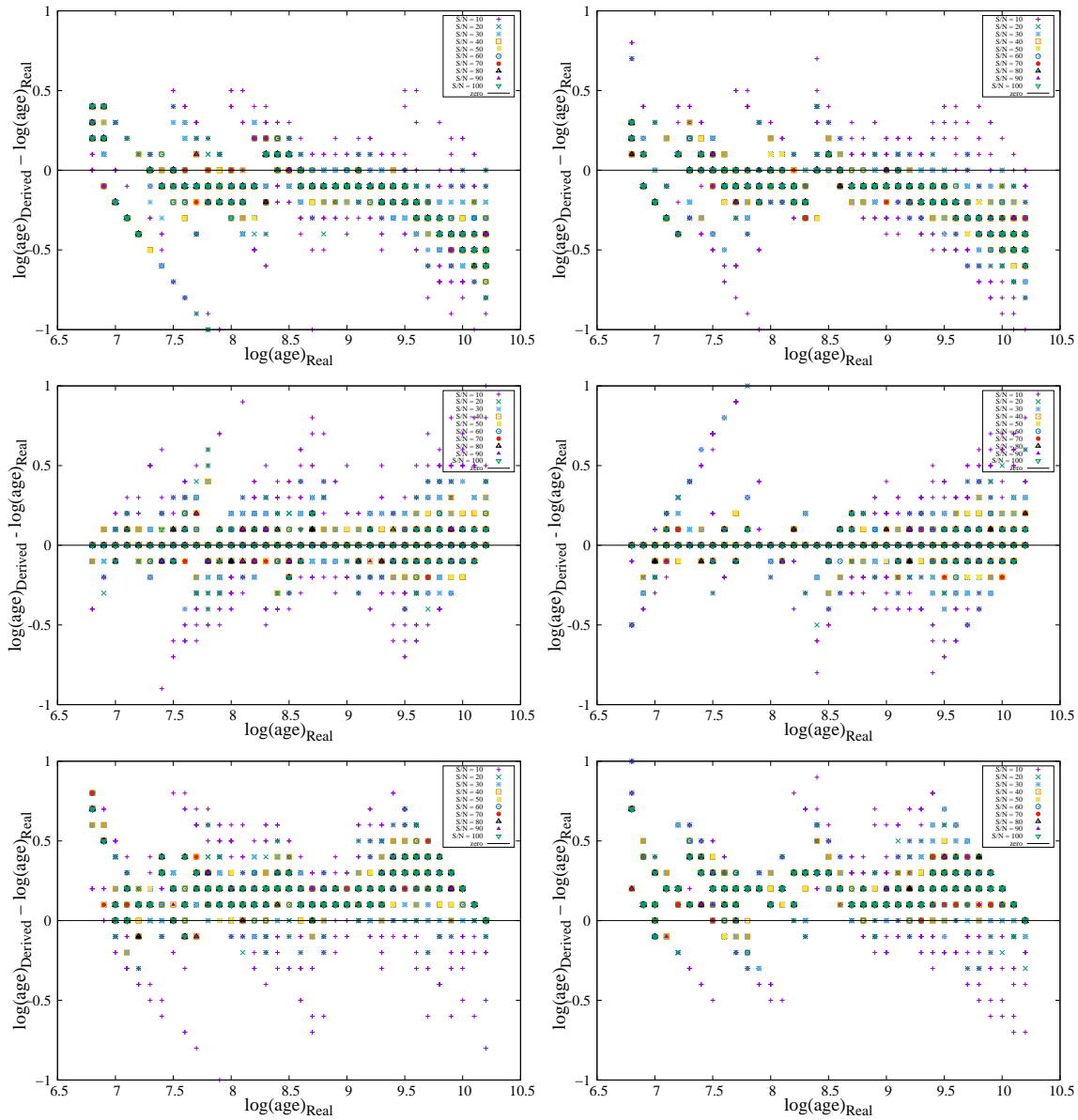


**Figure 16.** (Derived – real)  $\log(\text{age})$  as a function of  $\log(\text{age})$ , with metallicity fixed. Top panel:  $[Z/\text{H}] = 0.0$ , middle panel:  $[Z/\text{H}] = -0.4$ , and bottom panel:  $[Z/\text{H}] = -0.8$ . 3700 – 6200 Å (left), 3700 – 5000 Å (right)

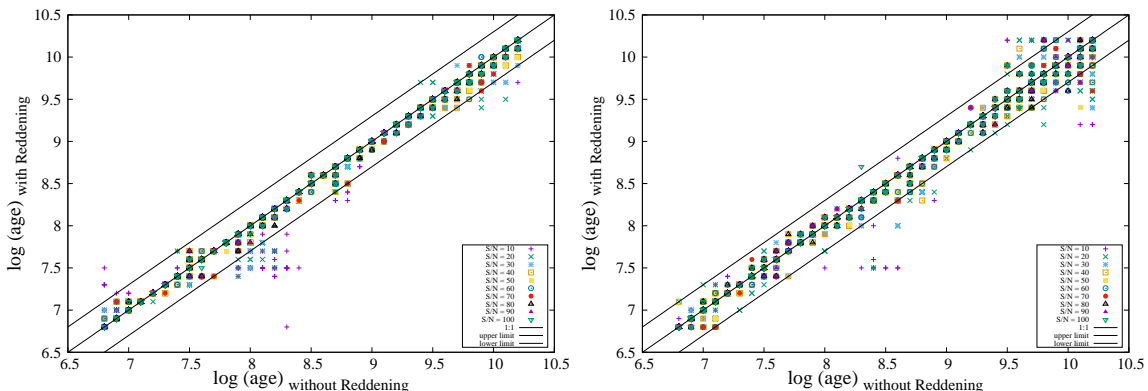


**Figure 17.**  $\log(\text{age})$  obtained when accounting for extinction versus  $\log(\text{age})$  obtained without accounting for extinction while keeping constant metallicity (left panel) and while varying metallicity (right panel)

**Table 1.** Results on age determination - Padova - wavelength:  $3700 - 6200 \text{ \AA}$ 

S/N	6.8	6.9	7.0	7.1	7.2	7.3	7.4	7.5	7.6	7.7
10.0	$6.9 \pm 0.12$	$7.0 \pm 0.09$	$7.0 \pm 0.11$	$7.0 \pm 0.11$	$7.2 \pm 0.18$	$7.3 \pm 0.16$	$7.35 \pm 0.17$	$7.5 \pm 0.16$	$7.6 \pm 0.22$	$7.65 \pm 0.2$
20.0	$6.8 \pm 0.12$	$6.9 \pm 0.12$	$7.0 \pm 0.12$	$7.1 \pm 0.11$	$7.2 \pm 0.05$	$7.3 \pm 0.09$	$7.4 \pm 0.08$	$7.5 \pm 0.11$	$7.6 \pm 0.14$	$7.7 \pm 0.11$
30.0	$6.8 \pm 0.11$	$6.9 \pm 0.09$	$7.0 \pm 0.07$	$7.1 \pm 0.1$	$7.2 \pm 0.04$	$7.3 \pm 0.05$	$7.4 \pm 0.06$	$7.5 \pm 0.1$	$7.6 \pm 0.12$	$7.7 \pm 0.06$
40.0	$6.8 \pm 0.09$	$6.9 \pm 0.08$	$7.0 \pm 0.05$	$7.1 \pm 0.06$	$7.2 \pm 0.04$	$7.3 \pm 0.02$	$7.4 \pm 0.04$	$7.5 \pm 0.08$	$7.6 \pm 0.12$	$7.7 \pm 0.07$
50.0	$6.8 \pm 0.04$	$6.9 \pm 0.05$	$7.0 \pm 0.04$	$7.1 \pm 0.07$	$7.2 \pm 0.03$	$7.3 \pm 0.03$	$7.4 \pm 0.04$	$7.5 \pm 0.07$	$7.6 \pm 0.09$	$7.7 \pm 0.05$
60.0	$6.8 \pm 0.06$	$6.9 \pm 0.04$	$7.0 \pm 0.04$	$7.1 \pm 0.04$	$7.2 \pm 0.0$	$7.3 \pm 0.03$	$7.4 \pm 0.03$	$7.5 \pm 0.06$	$7.6 \pm 0.08$	$7.7 \pm 0.04$
70.0	$6.8 \pm 0.04$	$6.9 \pm 0.04$	$7.0 \pm 0.04$	$7.1 \pm 0.04$	$7.2 \pm 0.0$	$7.3 \pm 0.0$	$7.4 \pm 0.0$	$7.5 \pm 0.05$	$7.6 \pm 0.08$	$7.7 \pm 0.03$
80.0	$6.8 \pm 0.0$	$6.9 \pm 0.0$	$7.0 \pm 0.03$	$7.1 \pm 0.03$	$7.2 \pm 0.0$	$7.3 \pm 0.02$	$7.4 \pm 0.03$	$7.5 \pm 0.05$	$7.6 \pm 0.05$	$7.7 \pm 0.05$
90.0	$6.8 \pm 0.0$	$6.9 \pm 0.0$	$7.0 \pm 0.02$	$7.1 \pm 0.0$	$7.2 \pm 0.0$	$7.3 \pm 0.0$	$7.4 \pm 0.02$	$7.5 \pm 0.04$	$7.6 \pm 0.04$	$7.7 \pm 0.03$
100.0	$6.8 \pm 0.0$	$6.9 \pm 0.0$	$7.0 \pm 0.04$	$7.1 \pm 0.02$	$7.2 \pm 0.0$	$7.3 \pm 0.0$	$7.4 \pm 0.02$	$7.5 \pm 0.05$	$7.6 \pm 0.04$	$7.7 \pm 0.03$
S/N	7.8	7.9	8.0	8.1	8.2	8.3	8.4	8.5	8.6	8.7
10.0	$7.8 \pm 0.28$	$7.9 \pm 0.3$	$8.0 \pm 0.22$	$8.05 \pm 0.3$	$8.15 \pm 0.2$	$8.3 \pm 0.27$	$8.4 \pm 0.29$	$8.5 \pm 0.19$	$8.5 \pm 0.22$	$8.5 \pm 0.21$
20.0	$7.75 \pm 0.17$	$7.9 \pm 0.06$	$8.0 \pm 0.07$	$8.0 \pm 0.09$	$8.2 \pm 0.15$	$8.3 \pm 0.19$	$8.4 \pm 0.19$	$8.5 \pm 0.15$	$8.6 \pm 0.15$	$8.7 \pm 0.14$
30.0	$7.8 \pm 0.08$	$7.9 \pm 0.05$	$8.0 \pm 0.06$	$8.05 \pm 0.07$	$8.2 \pm 0.1$	$8.3 \pm 0.16$	$8.4 \pm 0.14$	$8.5 \pm 0.15$	$8.55 \pm 0.11$	$8.7 \pm 0.13$
40.0	$7.8 \pm 0.08$	$7.9 \pm 0.05$	$8.0 \pm 0.05$	$8.1 \pm 0.06$	$8.2 \pm 0.04$	$8.3 \pm 0.13$	$8.4 \pm 0.11$	$8.5 \pm 0.12$	$8.6 \pm 0.1$	$8.7 \pm 0.1$
50.0	$7.8 \pm 0.06$	$7.9 \pm 0.04$	$8.0 \pm 0.05$	$8.1 \pm 0.06$	$8.2 \pm 0.05$	$8.3 \pm 0.1$	$8.4 \pm 0.09$	$8.5 \pm 0.11$	$8.6 \pm 0.08$	$8.7 \pm 0.08$
60.0	$7.8 \pm 0.06$	$7.9 \pm 0.04$	$8.0 \pm 0.06$	$8.1 \pm 0.03$	$8.2 \pm 0.04$	$8.3 \pm 0.08$	$8.4 \pm 0.11$	$8.5 \pm 0.11$	$8.6 \pm 0.05$	$8.7 \pm 0.09$
70.0	$7.8 \pm 0.06$	$7.9 \pm 0.05$	$8.0 \pm 0.03$	$8.1 \pm 0.04$	$8.2 \pm 0.03$	$8.3 \pm 0.07$	$8.4 \pm 0.03$	$8.5 \pm 0.09$	$8.6 \pm 0.06$	$8.7 \pm 0.05$
80.0	$7.8 \pm 0.05$	$7.9 \pm 0.04$	$8.0 \pm 0.04$	$8.1 \pm 0.05$	$8.2 \pm 0.03$	$8.3 \pm 0.04$	$8.4 \pm 0.03$	$8.5 \pm 0.07$	$8.6 \pm 0.05$	$8.7 \pm 0.06$
90.0	$7.8 \pm 0.03$	$7.9 \pm 0.03$	$8.0 \pm 0.03$	$8.1 \pm 0.04$	$8.2 \pm 0.03$	$8.3 \pm 0.04$	$8.4 \pm 0.04$	$8.5 \pm 0.05$	$8.6 \pm 0.04$	$8.7 \pm 0.06$
100.0	$7.8 \pm 0.02$	$7.9 \pm 0.04$	$8.0 \pm 0.03$	$8.1 \pm 0.03$	$8.2 \pm 0.02$	$8.3 \pm 0.03$	$8.4 \pm 0.04$	$8.5 \pm 0.08$	$8.6 \pm 0.05$	$8.7 \pm 0.05$
S/N	8.8	8.9	9.0	9.1	9.2	9.3	9.4	9.5	9.6	9.7
10.0	$8.7 \pm 0.17$	$8.9 \pm 0.16$	$9.0 \pm 0.16$	$9.1 \pm 0.15$	$9.2 \pm 0.15$	$9.3 \pm 0.18$	$9.5 \pm 0.25$	$9.6 \pm 0.34$	$9.5 \pm 0.31$	$9.7 \pm 0.35$
20.0	$8.7 \pm 0.13$	$8.9 \pm 0.09$	$9.0 \pm 0.09$	$9.1 \pm 0.1$	$9.2 \pm 0.12$	$9.3 \pm 0.1$	$9.5 \pm 0.1$	$9.6 \pm 0.15$	$9.6 \pm 0.23$	$9.85 \pm 0.25$
30.0	$8.8 \pm 0.1$	$8.9 \pm 0.07$	$9.0 \pm 0.07$	$9.1 \pm 0.1$	$9.2 \pm 0.08$	$9.3 \pm 0.09$	$9.4 \pm 0.07$	$9.6 \pm 0.11$	$9.7 \pm 0.11$	$9.8 \pm 0.14$
40.0	$8.8 \pm 0.09$	$8.9 \pm 0.08$	$9.0 \pm 0.05$	$9.1 \pm 0.09$	$9.2 \pm 0.08$	$9.35 \pm 0.08$	$9.4 \pm 0.07$	$9.5 \pm 0.09$	$9.7 \pm 0.09$	$9.8 \pm 0.11$
50.0	$8.8 \pm 0.07$	$8.9 \pm 0.07$	$9.0 \pm 0.05$	$9.1 \pm 0.08$	$9.2 \pm 0.1$	$9.3 \pm 0.04$	$9.4 \pm 0.06$	$9.5 \pm 0.08$	$9.6 \pm 0.09$	$9.8 \pm 0.17$
60.0	$8.8 \pm 0.06$	$8.9 \pm 0.06$	$9.0 \pm 0.05$	$9.1 \pm 0.07$	$9.2 \pm 0.07$	$9.3 \pm 0.05$	$9.4 \pm 0.05$	$9.5 \pm 0.07$	$9.6 \pm 0.09$	$9.75 \pm 0.11$
70.0	$8.8 \pm 0.05$	$8.9 \pm 0.06$	$9.0 \pm 0.03$	$9.1 \pm 0.08$	$9.2 \pm 0.08$	$9.3 \pm 0.07$	$9.4 \pm 0.05$	$9.5 \pm 0.08$	$9.6 \pm 0.07$	$9.7 \pm 0.14$
80.0	$8.8 \pm 0.05$	$8.9 \pm 0.05$	$9.0 \pm 0.03$	$9.1 \pm 0.08$	$9.2 \pm 0.09$	$9.3 \pm 0.04$	$9.4 \pm 0.04$	$9.5 \pm 0.08$	$9.6 \pm 0.09$	$9.7 \pm 0.07$
90.0	$8.8 \pm 0.05$	$8.9 \pm 0.06$	$9.0 \pm 0.03$	$9.1 \pm 0.05$	$9.2 \pm 0.07$	$9.3 \pm 0.06$	$9.4 \pm 0.05$	$9.5 \pm 0.07$	$9.6 \pm 0.09$	$9.7 \pm 0.15$
100.0	$8.8 \pm 0.04$	$8.9 \pm 0.05$	$9.0 \pm 0.0$	$9.1 \pm 0.04$	$9.2 \pm 0.06$	$9.3 \pm 0.05$	$9.4 \pm 0.06$	$9.5 \pm 0.09$	$9.6 \pm 0.08$	$9.7 \pm 0.09$
S/N	9.8	9.9	10.0	10.1	10.2					
10.0	$9.7 \pm 0.33$	$9.75 \pm 0.27$	$9.8 \pm 0.24$	$9.85 \pm 0.24$	$9.9 \pm 0.23$					
20.0	$9.85 \pm 0.18$	$9.9 \pm 0.17$	$10.0 \pm 0.21$	$9.8 \pm 0.22$	$10.0 \pm 0.16$					
30.0	$9.9 \pm 0.17$	$9.95 \pm 0.14$	$10.0 \pm 0.19$	$9.9 \pm 0.18$	$10.1 \pm 0.16$					
40.0	$9.9 \pm 0.13$	$9.9 \pm 0.16$	$10.0 \pm 0.17$	$10.1 \pm 0.17$	$10.2 \pm 0.12$					
50.0	$9.8 \pm 0.09$	$9.9 \pm 0.14$	$10.0 \pm 0.12$	$10.1 \pm 0.15$	$10.0 \pm 0.15$					
60.0	$9.8 \pm 0.13$	$9.9 \pm 0.15$	$9.95 \pm 0.13$	$10.1 \pm 0.12$	$10.2 \pm 0.13$					
70.0	$9.8 \pm 0.09$	$9.9 \pm 0.12$	$10.0 \pm 0.09$	$10.1 \pm 0.12$	$10.2 \pm 0.13$					
80.0	$9.8 \pm 0.1$	$9.9 \pm 0.13$	$10.0 \pm 0.12$	$10.1 \pm 0.12$	$10.2 \pm 0.11$					
90.0	$9.8 \pm 0.13$	$9.9 \pm 0.11$	$10.0 \pm 0.09$	$10.1 \pm 0.1$	$10.2 \pm 0.12$					
100.0	$9.8 \pm 0.1$	$9.9 \pm 0.1$	$10.0 \pm 0.1$	$10.1 \pm 0.1$	$10.2 \pm 0.08$					

**Table 2.** Results - Padova - wavelength: 3700-5000

S/N	6.8	6.9	7.0	7.1	7.2	7.3	7.4	7.5	7.6	7.7
10.0	6.9±0.21	7.0±0.12	7.0±0.1	7.05±0.12	7.2±0.13	7.3±0.16	7.3±0.16	7.35±0.31	7.5±0.3	7.7±0.28
20.0	6.8±0.13	6.9±0.08	7.0±0.07	7.1±0.08	7.2±0.17	7.3±0.14	7.4±0.1	7.5±0.14	7.5±0.07	7.7±0.11
30.0	6.8±0.09	6.9±0.06	7.0±0.04	7.1±0.08	7.2±0.09	7.3±0.09	7.4±0.08	7.5±0.1	7.6±0.1	7.7±0.11
40.0	6.8±0.05	6.9±0.07	7.0±0.04	7.1±0.06	7.2±0.04	7.3±0.0	7.4±0.06	7.5±0.07	7.6±0.05	7.7±0.08
50.0	6.8±0.07	6.9±0.04	7.0±0.04	7.1±0.04	7.2±0.04	7.3±0.03	7.4±0.03	7.5±0.06	7.6±0.06	7.7±0.09
60.0	6.8±0.08	6.9±0.04	7.0±0.03	7.1±0.03	7.2±0.03	7.3±0.03	7.4±0.0	7.5±0.05	7.6±0.05	7.7±0.04
70.0	6.8±0.08	6.9±0.0	7.0±0.03	7.1±0.04	7.2±0.03	7.3±0.0	7.4±0.0	7.5±0.05	7.6±0.05	7.7±0.03
80.0	6.8±0.07	6.9±0.0	7.0±0.03	7.1±0.03	7.2±0.0	7.3±0.0	7.4±0.0	7.5±0.04	7.6±0.04	7.7±0.05
90.0	6.8±0.0	6.9±0.0	7.0±0.0	7.1±0.04	7.2±0.0	7.3±0.0	7.4±0.0	7.5±0.05	7.6±0.04	7.7±0.02
100.0	6.8±0.05	6.9±0.0	7.0±0.0	7.1±0.03	7.2±0.0	7.3±0.0	7.4±0.0	7.5±0.03	7.6±0.02	7.7±0.02
S/N	7.8	7.9	8.0	8.1	8.2	8.3	8.4	8.5	8.6	8.7
10.0	7.8±0.24	7.8±0.29	8.0±0.38	8.05±0.24	8.2±0.21	8.3±0.33	8.5±0.29	8.8±0.22	8.6±0.16	8.75±0.19
20.0	7.8±0.1	7.9±0.07	8.0±0.08	8.1±0.08	8.2±0.08	8.3±0.15	8.45±0.21	8.6±0.17	8.6±0.14	8.7±0.1
30.0	7.75±0.08	7.9±0.04	8.0±0.04	8.1±0.05	8.2±0.05	8.3±0.09	8.4±0.13	8.6±0.16	8.6±0.11	8.7±0.08
40.0	7.8±0.05	7.9±0.03	8.0±0.05	8.1±0.05	8.2±0.04	8.3±0.04	8.4±0.1	8.6±0.15	8.6±0.08	8.7±0.09
50.0	7.8±0.02	7.9±0.04	8.0±0.0	8.1±0.04	8.2±0.04	8.3±0.04	8.4±0.09	8.5±0.11	8.6±0.05	8.7±0.08
60.0	7.8±0.04	7.9±0.03	8.0±0.0	8.1±0.04	8.2±0.03	8.3±0.03	8.4±0.06	8.5±0.11	8.6±0.06	8.7±0.06
70.0	7.8±0.03	7.9±0.03	8.0±0.0	8.1±0.04	8.2±0.02	8.3±0.03	8.4±0.08	8.5±0.09	8.6±0.03	8.7±0.07
80.0	7.8±0.03	7.9±0.0	8.0±0.0	8.1±0.03	8.2±0.02	8.3±0.0	8.4±0.07	8.5±0.08	8.6±0.04	8.7±0.07
90.0	7.8±0.03	7.9±0.0	8.0±0.0	8.1±0.04	8.2±0.0	8.3±0.03	8.4±0.06	8.5±0.06	8.6±0.03	8.7±0.05
100.0	7.8±0.04	7.9±0.0	8.0±0.0	8.1±0.03	8.2±0.0	8.3±0.03	8.4±0.03	8.5±0.08	8.6±0.03	8.7±0.06
S/N	8.8	8.9	9.0	9.1	9.2	9.3	9.4	9.5	9.6	9.7
10.0	8.7±0.22	8.9±0.3	9.05±0.3	9.1±0.39	9.15±0.4	9.2±0.43	9.25±0.48	9.4±0.48	10.0±0.43	10.0±0.47
20.0	8.7±0.1	8.9±0.17	9.0±0.15	9.1±0.24	9.3±0.28	9.4±0.27	9.4±0.33	9.4±0.39	9.6±0.27	10.0±0.33
30.0	8.8±0.1	8.9±0.09	9.0±0.09	9.1±0.13	9.2±0.15	9.3±0.21	9.4±0.31	9.5±0.27	9.75±0.25	9.7±0.25
40.0	8.8±0.08	8.9±0.06	9.0±0.05	9.1±0.12	9.2±0.14	9.3±0.14	9.4±0.19	9.5±0.22	9.55±0.17	9.8±0.17
50.0	8.8±0.07	8.9±0.07	9.0±0.06	9.1±0.12	9.2±0.08	9.35±0.12	9.4±0.16	9.5±0.22	9.6±0.18	9.7±0.24
60.0	8.8±0.06	8.9±0.07	9.0±0.05	9.1±0.09	9.2±0.1	9.3±0.09	9.4±0.15	9.5±0.15	9.6±0.16	9.7±0.15
70.0	8.8±0.05	8.9±0.06	9.0±0.05	9.1±0.07	9.2±0.07	9.3±0.08	9.4±0.08	9.5±0.14	9.6±0.14	9.7±0.19
80.0	8.8±0.06	8.9±0.05	9.0±0.06	9.1±0.05	9.2±0.09	9.3±0.06	9.4±0.09	9.5±0.11	9.6±0.13	9.7±0.12
90.0	8.8±0.04	8.9±0.03	9.0±0.03	9.1±0.03	9.2±0.06	9.3±0.06	9.4±0.09	9.5±0.13	9.6±0.1	9.7±0.12
100.0	8.8±0.05	8.9±0.05	9.0±0.03	9.1±0.05	9.2±0.06	9.3±0.06	9.4±0.07	9.5±0.1	9.6±0.1	9.7±0.11
S/N	9.8	9.9	10.0	10.1	10.2					
10.0	10.0±0.46	9.9±0.46	10.0±0.38	9.95±0.42	10.0±0.35					
20.0	10.0±0.39	9.9±0.31	10.0±0.3	10.1±0.3	10.1±0.28					
30.0	9.8±0.32	9.75±0.28	9.8±0.28	10.1±0.24	10.1±0.25					
40.0	9.8±0.27	9.9±0.19	10.0±0.22	10.15±0.14	10.2±0.15					
50.0	9.8±0.23	9.9±0.15	10.0±0.15	10.1±0.12	10.2±0.11					
60.0	9.8±0.15	9.9±0.16	10.0±0.17	10.1±0.13	10.2±0.09					
70.0	9.8±0.16	9.9±0.14	10.0±0.12	10.1±0.11	10.2±0.09					
80.0	9.8±0.13	9.9±0.14	10.0±0.14	10.1±0.09	10.2±0.09					
90.0	9.8±0.09	9.9±0.07	10.0±0.13	10.1±0.08	10.2±0.08					
100.0	9.8±0.11	9.9±0.1	10.0±0.12	10.1±0.07	10.2±0.1					

**Table 3.** Results - Padova - wavelength: 5000-6200

S/N	6.8	6.9	7.0	7.1	7.2	7.3	7.4	7.5	7.6	7.7
10.0	6.9±0.55	6.9±0.64	7.05±0.67	7.0±0.37	7.0±0.5	7.2±0.66	7.2±0.66	7.3±0.69	7.25±0.54	7.2±0.68
20.0	7.7±0.56	7.3±0.58	7.2±0.56	7.1±0.46	7.2±0.56	7.25±0.33	7.5±0.52	7.45±0.58	7.35±0.46	7.5±0.57
30.0	7.8±0.52	7.3±0.56	7.2±0.35	7.1±0.4	7.2±0.35	7.3±0.32	7.45±0.28	7.5±0.52	7.5±0.52	7.7±0.45
40.0	8.0±0.52	7.2±0.5	7.2±0.4	7.2±0.25	7.15±0.33	7.3±0.14	7.4±0.37	7.5±0.36	7.5±0.38	7.7±0.42
50.0	7.75±0.55	7.0±0.44	7.1±0.4	7.1±0.26	7.2±0.23	7.3±0.25	7.4±0.2	7.5±0.29	7.5±0.29	7.6±0.34
60.0	7.8±0.58	6.9±0.51	7.1±0.32	7.1±0.13	7.2±0.14	7.3±0.14	7.5±0.18	7.5±0.2	7.5±0.26	7.6±0.32
70.0	7.1±0.58	7.0±0.33	7.1±0.37	7.1±0.12	7.2±0.13	7.3±0.14	7.4±0.17	7.5±0.1	7.5±0.1	7.65±0.27
80.0	7.7±0.6	6.9±0.51	7.0±0.31	7.1±0.05	7.2±0.08	7.3±0.1	7.4±0.16	7.5±0.2	7.6±0.16	7.7±0.31
90.0	7.7±0.6	6.9±0.36	7.1±0.32	7.1±0.05	7.2±0.11	7.3±0.11	7.45±0.13	7.5±0.21	7.5±0.14	7.7±0.27
100.0	6.8±0.6	6.9±0.36	7.0±0.29	7.1±0.11	7.2±0.03	7.3±0.12	7.4±0.13	7.5±0.2	7.6±0.14	7.7±0.31
S/N	7.8	7.9	8.0	8.1	8.2	8.3	8.4	8.5	8.6	8.7
10.0	7.35±0.7	7.25±0.73	7.4±0.73	7.3±0.69	7.3±0.74	7.5±0.78	7.3±0.77	8.45±0.81	7.4±0.73	7.3±0.78
20.0	7.8±0.64	7.8±0.6	8.0±0.5	7.7±0.53	7.5±0.56	8.3±0.65	8.35±0.72	8.45±0.67	8.0±0.71	7.6±0.81
30.0	7.2±0.51	7.9±0.43	8.0±0.41	8.05±0.41	8.2±0.51	8.4±0.52	8.4±0.6	8.55±0.56	7.6±0.64	8.5±0.7
40.0	7.8±0.42	7.9±0.28	8.0±0.32	8.1±0.35	8.2±0.35	8.3±0.49	8.4±0.51	8.4±0.53	8.6±0.55	8.7±0.48
50.0	7.8±0.33	7.9±0.35	8.0±0.28	8.0±0.3	8.2±0.4	8.4±0.4	8.4±0.45	8.5±0.43	8.5±0.47	8.7±0.33
60.0	7.8±0.37	7.9±0.36	8.0±0.26	8.1±0.21	8.2±0.38	8.35±0.47	8.5±0.47	8.5±0.41	8.6±0.36	8.7±0.48
70.0	7.8±0.35	7.8±0.32	8.0±0.21	8.0±0.24	8.2±0.33	8.3±0.34	8.4±0.4	8.5±0.22	8.6±0.31	8.7±0.06
80.0	7.8±0.37	7.9±0.31	8.0±0.15	8.1±0.24	8.2±0.27	8.3±0.33	8.4±0.27	8.5±0.26	8.6±0.32	8.7±0.2
90.0	7.8±0.29	7.9±0.22	8.0±0.2	8.1±0.21	8.2±0.2	8.3±0.21	8.4±0.18	8.5±0.25	8.6±0.32	8.7±0.05
100.0	7.8±0.16	7.9±0.27	8.0±0.21	8.1±0.17	8.2±0.29	8.3±0.11	8.4±0.27	8.5±0.1	8.6±0.2	8.7±0.07
S/N	8.8	8.9	9.0	9.1	9.2	9.3	9.4	9.5	9.6	9.7
10.0	8.8±0.78	8.9±0.88	9.0±0.76	9.1±0.62	9.2±0.71	9.4±0.85	9.4±0.26	9.6±0.31	9.5±0.6	9.6±0.69
20.0	8.8±0.71	8.9±0.59	9.0±0.38	9.1±0.41	9.2±0.13	9.4±0.1	9.4±0.12	9.5±0.27	9.6±0.25	9.8±0.3
30.0	8.8±0.23	8.9±0.05	9.0±0.06	9.1±0.05	9.2±0.09	9.3±0.1	9.4±0.16	9.5±0.19	9.6±0.22	9.8±0.17
40.0	8.8±0.3	8.9±0.35	9.0±0.04	9.1±0.05	9.2±0.07	9.3±0.07	9.4±0.1	9.6±0.12	9.6±0.21	9.85±0.17
50.0	8.8±0.0	8.9±0.05	9.0±0.06	9.1±0.04	9.2±0.07	9.3±0.05	9.4±0.1	9.5±0.17	9.6±0.17	9.85±0.17
60.0	8.8±0.02	8.9±0.05	9.0±0.04	9.1±0.05	9.2±0.05	9.3±0.06	9.4±0.11	9.6±0.1	9.7±0.13	9.8±0.12
70.0	8.8±0.0	8.9±0.04	9.0±0.04	9.1±0.05	9.2±0.06	9.3±0.06	9.4±0.11	9.5±0.12	9.6±0.12	9.75±0.13
80.0	8.8±0.03	8.9±0.03	9.0±0.04	9.1±0.04	9.2±0.06	9.3±0.06	9.4±0.1	9.5±0.1	9.6±0.12	9.8±0.09
90.0	8.8±0.03	8.9±0.03	9.0±0.04	9.1±0.04	9.2±0.06	9.3±0.06	9.4±0.11	9.55±0.08	9.6±0.1	9.9±0.12
100.0	8.8±0.03	8.9±0.05	9.0±0.04	9.1±0.03	9.2±0.05	9.3±0.05	9.4±0.08	9.6±0.09	9.6±0.07	9.8±0.1
S/N	9.8	9.9	10.0	10.1	10.2					
10.0	9.75±0.75	9.9±0.57	9.85±0.37	9.9±0.57	9.9±0.56					
20.0	9.7±0.24	9.8±0.24	9.9±0.18	9.9±0.18	10.05±0.15					
30.0	9.8±0.18	9.9±0.21	9.9±0.19	9.95±0.19	9.95±0.19					
40.0	9.8±0.16	9.9±0.15	9.9±0.17	10.05±0.17	10.1±0.17					
50.0	9.9±0.14	9.95±0.15	10.05±0.16	10.1±0.11	10.05±0.16					
60.0	9.9±0.14	9.9±0.13	10.0±0.12	10.1±0.13	10.1±0.15					
70.0	9.8±0.12	9.9±0.11	10.0±0.12	10.1±0.12	10.1±0.14					
80.0	9.85±0.1	9.9±0.12	10.0±0.11	10.1±0.11	10.1±0.14					
90.0	9.85±0.08	9.9±0.08	10.0±0.11	10.1±0.1	10.1±0.07					
100.0	9.85±0.1	9.9±0.07	10.0±0.11	10.1±0.1	10.1±0.08					

**Table 4.** Results - MIST - wavelength: 3700-6200

S/N	6.8	6.9	7.0	7.1	7.2	7.3	7.4	7.5	7.6	7.7
10.0	6.8±0.14	6.9±0.09	7.0±0.08	7.0±0.1	7.3±0.1	7.3±0.09	7.4±0.25	7.55±0.13	7.5±0.2	7.8±0.33
20.0	6.8±0.12	6.9±0.08	7.0±0.08	7.0±0.09	7.2±0.1	7.3±0.11	7.4±0.09	7.5±0.08	7.6±0.1	7.9±0.14
30.0	6.8±0.09	6.9±0.08	7.0±0.05	7.1±0.06	7.2±0.09	7.3±0.09	7.4±0.09	7.5±0.06	7.6±0.1	7.8±0.09
40.0	6.8±0.09	6.9±0.07	7.0±0.09	7.1±0.04	7.2±0.05	7.3±0.07	7.4±0.09	7.5±0.06	7.6±0.09	7.75±0.09
50.0	6.8±0.11	6.9±0.05	7.0±0.08	7.1±0.06	7.2±0.05	7.3±0.03	7.4±0.04	7.5±0.04	7.6±0.08	7.7±0.08
60.0	6.8±0.1	6.9±0.03	7.0±0.06	7.1±0.03	7.2±0.0	7.3±0.0	7.4±0.04	7.5±0.04	7.6±0.06	7.7±0.07
70.0	6.8±0.05	6.9±0.03	7.0±0.05	7.1±0.03	7.2±0.0	7.3±0.0	7.4±0.06	7.5±0.04	7.6±0.07	7.7±0.06
80.0	6.8±0.05	6.9±0.03	7.0±0.03	7.1±0.03	7.2±0.0	7.3±0.0	7.4±0.0	7.5±0.04	7.6±0.05	7.7±0.07
90.0	6.8±0.0	6.9±0.0	7.0±0.03	7.1±0.03	7.2±0.0	7.3±0.0	7.4±0.0	7.5±0.04	7.6±0.04	7.7±0.05
100.0	6.8±0.0	6.9±0.0	7.0±0.02	7.1±0.0	7.2±0.0	7.3±0.0	7.4±0.0	7.5±0.03	7.6±0.03	7.7±0.04
S/N	7.8	7.9	8.0	8.1	8.2	8.3	8.4	8.5	8.6	8.7
10.0	7.9±0.19	7.9±0.59	8.0±0.37	8.1±0.33	8.2±0.27	8.3±0.29	8.4±0.28	8.5±0.21	8.65±0.19	8.65±0.19
20.0	7.9±0.08	7.9±0.2	7.9±0.1	8.1±0.13	8.2±0.14	8.3±0.16	8.4±0.12	8.6±0.16	8.6±0.14	8.7±0.12
30.0	7.85±0.11	7.9±0.07	8.0±0.06	8.1±0.12	8.2±0.08	8.3±0.12	8.4±0.1	8.6±0.12	8.6±0.13	8.7±0.1
40.0	7.8±0.09	7.9±0.05	8.0±0.05	8.1±0.11	8.2±0.07	8.3±0.04	8.4±0.1	8.6±0.1	8.6±0.1	8.7±0.08
50.0	7.8±0.08	7.9±0.03	7.9±0.05	8.1±0.07	8.2±0.07	8.3±0.03	8.4±0.08	8.5±0.09	8.6±0.08	8.7±0.07
60.0	7.8±0.08	7.9±0.04	8.0±0.05	8.1±0.07	8.2±0.04	8.3±0.04	8.4±0.04	8.5±0.08	8.6±0.1	8.7±0.06
70.0	7.8±0.07	7.9±0.05	8.0±0.04	8.1±0.04	8.2±0.06	8.3±0.03	8.4±0.04	8.5±0.04	8.6±0.07	8.7±0.06
80.0	7.8±0.06	7.9±0.03	8.0±0.05	8.1±0.07	8.2±0.05	8.3±0.03	8.4±0.04	8.5±0.05	8.6±0.07	8.7±0.05
90.0	7.8±0.05	7.9±0.03	8.0±0.04	8.1±0.04	8.2±0.04	8.3±0.03	8.4±0.03	8.5±0.05	8.6±0.06	8.7±0.05
100.0	7.8±0.06	7.9±0.0	8.0±0.04	8.1±0.04	8.2±0.04	8.3±0.03	8.4±0.0	8.5±0.03	8.6±0.07	8.7±0.03
S/N	8.8	8.9	9.0	9.1	9.2	9.3	9.4	9.5	9.6	9.7
10.0	8.8±0.2	8.9±0.14	9.0±0.12	9.1±0.15	9.2±0.19	9.35±0.17	9.5±0.28	9.55±0.26	9.6±0.3	9.65±0.36
20.0	8.75±0.14	8.9±0.07	9.0±0.1	9.2±0.1	9.2±0.12	9.3±0.11	9.5±0.13	9.5±0.16	9.6±0.21	9.7±0.17
30.0	8.8±0.06	8.9±0.06	9.0±0.08	9.2±0.06	9.2±0.11	9.4±0.11	9.4±0.08	9.5±0.08	9.6±0.14	9.6±0.17
40.0	8.8±0.07	8.9±0.05	9.0±0.05	9.2±0.05	9.2±0.08	9.4±0.11	9.5±0.09	9.5±0.08	9.6±0.09	9.6±0.11
50.0	8.8±0.06	8.9±0.03	9.0±0.02	9.15±0.05	9.2±0.08	9.4±0.08	9.5±0.09	9.5±0.07	9.6±0.09	9.65±0.1
60.0	8.8±0.06	8.9±0.04	9.0±0.02	9.1±0.06	9.2±0.08	9.35±0.1	9.4±0.1	9.5±0.07	9.6±0.1	9.7±0.13
70.0	8.8±0.06	8.9±0.04	9.0±0.02	9.1±0.05	9.2±0.07	9.3±0.09	9.4±0.09	9.5±0.07	9.6±0.08	9.6±0.13
80.0	8.8±0.04	8.9±0.03	9.0±0.02	9.1±0.04	9.2±0.09	9.3±0.07	9.4±0.09	9.5±0.08	9.6±0.08	9.6±0.09
90.0	8.8±0.03	8.9±0.03	9.0±0.0	9.1±0.04	9.2±0.08	9.3±0.07	9.4±0.08	9.5±0.08	9.6±0.06	9.7±0.1
100.0	8.8±0.03	8.9±0.02	9.0±0.0	9.1±0.05	9.2±0.07	9.3±0.09	9.4±0.08	9.5±0.06	9.6±0.05	9.7±0.08
S/N	9.8	9.9	10.0	10.1	10.2					
10.0	9.7±0.26	9.8±0.25	9.9±0.29	10.0±0.14	10.0±0.2					
20.0	9.7±0.21	9.9±0.19	10.1±0.14	10.1±0.11	10.1±0.1					
30.0	9.7±0.17	9.85±0.17	10.0±0.13	10.1±0.11	10.1±0.09					
40.0	9.75±0.13	9.8±0.14	10.0±0.15	10.1±0.1	10.2±0.09					
50.0	9.75±0.14	9.9±0.12	10.0±0.15	10.1±0.09	10.2±0.06					
60.0	9.8±0.11	9.8±0.09	10.0±0.11	10.1±0.08	10.2±0.05					
70.0	9.8±0.13	9.9±0.12	10.0±0.11	10.1±0.07	10.2±0.06					
80.0	9.8±0.1	9.9±0.07	10.0±0.1	10.1±0.06	10.2±0.07					
90.0	9.75±0.09	9.9±0.07	10.0±0.08	10.1±0.06	10.2±0.05					
100.0	9.8±0.05	9.9±0.08	10.0±0.09	10.1±0.06	10.2±0.05					

**Table 5.** Results - MIST - wavelength: 3700-5000

S/N	6.8	6.9	7.0	7.1	7.2	7.3	7.4	7.5	7.6	7.7
10.0	7.15±0.21	6.95±0.15	7.0±0.22	6.95±0.17	7.2±0.21	7.3±0.21	7.3±0.21	7.4±0.2	7.5±0.23	7.7±0.41
20.0	6.9±0.2	6.9±0.11	7.0±0.12	7.1±0.15	7.2±0.16	7.3±0.11	7.4±0.15	7.5±0.14	7.5±0.11	7.7±0.21
30.0	6.8±0.13	6.9±0.08	7.0±0.06	7.1±0.13	7.2±0.15	7.3±0.04	7.4±0.11	7.5±0.07	7.5±0.09	7.7±0.18
40.0	6.8±0.12	6.9±0.08	7.0±0.05	7.1±0.11	7.2±0.12	7.3±0.03	7.4±0.08	7.5±0.06	7.5±0.1	7.7±0.12
50.0	6.8±0.12	6.9±0.06	7.0±0.06	7.1±0.08	7.2±0.04	7.3±0.04	7.4±0.08	7.5±0.0	7.6±0.07	7.7±0.06
60.0	6.8±0.1	6.9±0.07	7.0±0.03	7.1±0.05	7.2±0.02	7.3±0.03	7.4±0.04	7.5±0.03	7.6±0.05	7.7±0.06
70.0	6.8±0.08	6.9±0.05	7.0±0.05	7.1±0.04	7.2±0.03	7.3±0.02	7.4±0.06	7.5±0.0	7.6±0.04	7.7±0.04
80.0	6.8±0.09	6.9±0.04	7.0±0.02	7.1±0.04	7.2±0.0	7.3±0.02	7.4±0.0	7.5±0.02	7.6±0.05	7.7±0.05
90.0	6.8±0.05	6.9±0.04	7.0±0.0	7.1±0.02	7.2±0.0	7.3±0.0	7.4±0.0	7.5±0.0	7.6±0.04	7.7±0.04
100.0	6.8±0.0	6.9±0.0	7.0±0.0	7.1±0.0	7.2±0.0	7.3±0.0	7.4±0.0	7.5±0.0	7.6±0.03	7.7±0.04
S/N	7.8	7.9	8.0	8.1	8.2	8.3	8.4	8.5	8.6	8.7
10.0	7.75±0.49	7.9±0.45	8.1±0.27	8.1±0.28	8.15±0.28	8.3±0.45	8.5±0.21	8.6±0.18	8.65±0.13	8.7±0.15
20.0	7.8±0.21	7.9±0.13	8.0±0.16	8.1±0.1	8.15±0.08	8.3±0.07	8.4±0.11	8.6±0.17	8.7±0.11	8.7±0.11
30.0	7.8±0.16	7.9±0.05	8.0±0.05	8.1±0.08	8.2±0.05	8.3±0.09	8.4±0.08	8.6±0.16	8.6±0.11	8.7±0.1
40.0	7.8±0.12	7.9±0.08	8.0±0.04	8.1±0.08	8.2±0.05	8.3±0.04	8.4±0.08	8.6±0.15	8.6±0.08	8.7±0.08
50.0	7.8±0.05	7.9±0.03	8.0±0.06	8.1±0.05	8.2±0.05	8.3±0.04	8.4±0.08	8.5±0.12	8.6±0.06	8.7±0.06
60.0	7.8±0.06	7.9±0.03	8.0±0.03	8.1±0.06	8.2±0.04	8.3±0.0	8.4±0.08	8.55±0.11	8.6±0.06	8.7±0.07
70.0	7.8±0.04	7.9±0.03	8.0±0.03	8.1±0.04	8.2±0.03	8.3±0.04	8.4±0.04	8.5±0.11	8.6±0.07	8.7±0.08
80.0	7.8±0.04	7.9±0.0	8.0±0.02	8.1±0.05	8.2±0.04	8.3±0.0	8.4±0.05	8.6±0.1	8.6±0.06	8.7±0.04
90.0	7.8±0.04	7.9±0.03	8.0±0.03	8.1±0.04	8.2±0.05	8.3±0.0	8.4±0.05	8.5±0.06	8.6±0.04	8.7±0.05
100.0	7.8±0.03	7.9±0.0	8.0±0.02	8.1±0.04	8.2±0.03	8.3±0.0	8.4±0.05	8.5±0.08	8.6±0.04	8.7±0.04
S/N	8.8	8.9	9.0	9.1	9.2	9.3	9.4	9.5	9.6	9.7
10.0	8.7±0.2	8.9±0.24	9.0±0.3	9.1±0.27	9.3±0.38	9.35±0.41	9.95±0.48	9.1±0.49	9.5±0.43	9.95±0.47
20.0	8.8±0.1	8.9±0.11	9.0±0.14	9.1±0.17	9.25±0.27	9.3±0.23	9.3±0.34	9.5±0.3	9.6±0.31	9.7±0.3
30.0	8.8±0.11	8.9±0.08	9.0±0.16	9.1±0.14	9.3±0.17	9.3±0.19	9.4±0.16	9.5±0.24	9.6±0.23	9.7±0.25
40.0	8.8±0.06	8.9±0.06	9.0±0.1	9.1±0.1	9.2±0.13	9.5±0.18	9.4±0.14	9.5±0.15	9.6±0.15	9.7±0.24
50.0	8.8±0.07	8.9±0.05	9.0±0.07	9.1±0.08	9.2±0.12	9.3±0.13	9.4±0.15	9.5±0.17	9.6±0.12	9.7±0.19
60.0	8.8±0.06	8.9±0.05	9.0±0.07	9.1±0.05	9.2±0.09	9.3±0.09	9.4±0.14	9.5±0.13	9.6±0.15	9.7±0.16
70.0	8.8±0.05	8.9±0.04	9.0±0.05	9.1±0.07	9.2±0.1	9.3±0.07	9.4±0.1	9.5±0.08	9.6±0.15	9.7±0.16
80.0	8.8±0.05	8.9±0.04	9.0±0.04	9.1±0.05	9.2±0.07	9.3±0.07	9.4±0.1	9.5±0.09	9.6±0.11	9.7±0.12
90.0	8.8±0.03	8.9±0.03	9.0±0.05	9.1±0.03	9.2±0.05	9.3±0.06	9.4±0.09	9.5±0.05	9.6±0.09	9.7±0.1
100.0	8.8±0.02	8.9±0.03	9.0±0.03	9.1±0.03	9.2±0.06	9.3±0.07	9.4±0.07	9.5±0.06	9.6±0.07	9.7±0.13
S/N	9.8	9.9	10.0	10.1	10.2					
10.0	9.6±0.44	10.1±0.32	10.05±0.34	10.15±0.36	10.2±0.32					
20.0	9.85±0.32	10.1±0.26	9.9±0.28	10.0±0.22	10.0±0.22					
30.0	9.8±0.26	9.85±0.23	10.0±0.19	10.05±0.18	10.05±0.18					
40.0	9.8±0.22	9.9±0.13	10.1±0.17	10.1±0.16	10.1±0.11					
50.0	9.8±0.19	9.9±0.12	10.0±0.16	10.1±0.12	10.2±0.1					
60.0	9.8±0.12	9.9±0.12	10.0±0.15	10.1±0.08	10.2±0.09					
70.0	9.8±0.17	9.9±0.12	10.0±0.14	10.1±0.06	10.2±0.09					
80.0	9.8±0.11	9.9±0.07	10.0±0.09	10.1±0.06	10.2±0.09					
90.0	9.8±0.12	9.9±0.07	10.0±0.13	10.1±0.08	10.2±0.07					
100.0	9.8±0.06	9.9±0.07	10.0±0.13	10.1±0.07	10.2±0.05					

**Table 6.** Results - MIST - wavelength: 5000-6200

S/N	6.8	6.9	7.0	7.1	7.2	7.3	7.4	7.5	7.6	7.7
10.0	7.0±0.53	7.1±0.62	7.25±0.59	7.3±0.41	7.25±0.69	7.5±0.69	7.4±1.0	7.7±0.86	7.5±0.85	7.5±0.83
20.0	7.0±0.46	7.3±0.45	7.1±0.36	7.3±0.45	7.4±0.59	7.7±0.39	7.4±0.76	7.5±0.67	7.65±0.67	8.65±0.69
30.0	6.8±0.26	7.4±0.5	7.0±0.39	7.4±0.39	7.4±0.41	7.3±0.34	7.4±0.71	7.5±0.48	7.6±0.52	7.9±0.49
40.0	6.8±0.2	7.4±0.45	7.0±0.15	7.1±0.18	7.2±0.28	7.4±0.25	7.4±0.51	7.5±0.43	7.6±0.5	7.9±0.53
50.0	6.8±0.19	7.35±0.57	7.0±0.2	7.3±0.25	7.2±0.26	7.55±0.3	7.4±0.72	7.5±0.15	7.6±0.4	7.7±0.44
60.0	7.0±0.19	6.9±0.56	7.0±0.16	7.5±0.21	7.2±0.28	7.4±0.2	7.4±0.42	7.5±0.15	7.6±0.23	7.8±0.42
70.0	6.8±0.18	7.15±0.55	7.0±0.16	7.3±0.21	7.2±0.29	7.3±0.21	7.4±0.06	7.5±0.13	7.6±0.33	7.7±0.3
80.0	6.8±0.21	7.4±0.38	7.0±0.17	7.25±0.21	7.2±0.28	7.3±0.2	7.4±0.04	7.5±0.12	7.6±0.14	7.7±0.28
90.0	6.8±0.2	6.9±0.54	7.0±0.13	7.15±0.21	7.2±0.25	7.3±0.16	7.4±0.0	7.5±0.13	7.6±0.2	7.6±0.13
100.0	6.8±0.22	6.9±0.5	7.0±0.14	7.1±0.13	7.2±0.15	7.3±0.2	7.4±0.0	7.5±0.09	7.6±0.15	7.7±0.2
S/N	7.8	7.9	8.0	8.1	8.2	8.3	8.4	8.5	8.6	8.7
10.0	8.15±0.78	7.9±0.94	7.5±0.81	8.0±0.81	7.95±0.75	7.6±0.81	8.15±0.8	8.25±0.81	8.65±0.67	8.6±0.75
20.0	7.9±0.6	8.35±0.66	8.3±0.58	8.05±0.63	8.25±0.59	8.4±0.51	8.2±0.57	8.7±0.61	8.65±0.65	8.6±0.65
30.0	7.9±0.46	8.2±0.5	8.05±0.39	8.1±0.41	8.1±0.45	8.3±0.59	8.55±0.5	8.5±0.6	8.6±0.49	8.7±0.59
40.0	7.9±0.41	8.3±0.48	8.1±0.32	8.05±0.43	8.1±0.32	8.3±0.42	8.5±0.48	8.65±0.41	8.7±0.46	8.7±0.41
50.0	7.9±0.3	7.9±0.45	8.1±0.34	8.0±0.29	8.05±0.42	8.3±0.37	8.4±0.38	8.7±0.36	8.65±0.49	8.7±0.35
60.0	7.9±0.31	7.9±0.42	8.0±0.21	8.0±0.26	8.2±0.28	8.2±0.34	8.4±0.41	8.7±0.36	8.6±0.37	8.7±0.39
70.0	7.8±0.37	7.9±0.43	8.0±0.27	8.1±0.14	8.1±0.27	8.4±0.32	8.4±0.27	8.4±0.35	8.55±0.31	8.55±0.29
80.0	7.8±0.21	7.9±0.3	8.0±0.19	8.0±0.25	8.1±0.22	8.25±0.33	8.35±0.36	8.6±0.25	8.65±0.34	8.7±0.21
90.0	7.8±0.26	7.9±0.29	8.0±0.14	8.0±0.17	8.2±0.25	8.2±0.24	8.4±0.32	8.5±0.33	8.5±0.3	8.7±0.22
100.0	7.8±0.3	7.9±0.2	8.0±0.15	8.1±0.18	8.2±0.18	8.3±0.2	8.4±0.29	8.5±0.29	8.6±0.31	8.7±0.1
S/N	8.8	8.9	9.0	9.1	9.2	9.3	9.4	9.5	9.6	9.7
10.0	8.65±0.84	8.9±0.83	9.0±0.85	9.1±0.77	9.2±0.49	9.4±0.62	9.5±0.86	9.5±0.8	9.6±0.72	9.65±0.84
20.0	8.7±0.67	8.9±0.49	9.0±0.41	9.2±0.36	9.2±0.49	9.35±0.13	9.4±0.1	9.5±0.11	9.6±0.11	9.7±0.19
30.0	8.8±0.14	8.9±0.45	9.0±0.3	9.15±0.12	9.2±0.13	9.35±0.09	9.5±0.05	9.5±0.07	9.55±0.1	9.65±0.17
40.0	8.8±0.35	8.9±0.05	9.0±0.41	9.1±0.11	9.2±0.11	9.3±0.07	9.4±0.07	9.5±0.07	9.6±0.08	9.7±0.08
50.0	8.8±0.26	8.9±0.04	9.0±0.02	9.1±0.1	9.1±0.09	9.4±0.08	9.4±0.07	9.5±0.07	9.6±0.09	9.7±0.11
60.0	8.8±0.12	8.9±0.0	9.0±0.02	9.1±0.09	9.2±0.12	9.4±0.06	9.5±0.05	9.5±0.07	9.6±0.08	9.7±0.13
70.0	8.8±0.14	8.9±0.04	9.0±0.02	9.1±0.09	9.2±0.09	9.3±0.06	9.5±0.06	9.5±0.07	9.6±0.08	9.7±0.17
80.0	8.8±0.04	8.9±0.0	9.0±0.02	9.1±0.07	9.2±0.1	9.3±0.08	9.4±0.05	9.5±0.07	9.6±0.07	9.7±0.06
90.0	8.8±0.09	8.9±0.0	9.0±0.0	9.1±0.06	9.2±0.11	9.3±0.07	9.4±0.05	9.5±0.07	9.6±0.06	9.7±0.06
100.0	8.8±0.13	8.9±0.0	9.0±0.0	9.1±0.06	9.2±0.1	9.4±0.1	9.4±0.06	9.5±0.07	9.6±0.07	9.7±0.12
S/N	9.8	9.9	10.0	10.1	10.2					
10.0	9.8±0.82	9.9±0.72	10.1±0.72	10.2±0.26	10.1±1.09					
20.0	9.8±0.25	9.85±0.2	10.0±0.19	10.1±0.13	10.2±0.06					
30.0	9.8±0.21	9.9±0.16	10.0±0.14	10.0±0.12	10.1±0.11					
40.0	9.8±0.17	9.95±0.14	10.0±0.13	10.1±0.12	10.1±0.08					
50.0	9.8±0.2	9.9±0.12	10.0±0.09	10.1±0.1	10.2±0.06					
60.0	9.8±0.14	9.9±0.1	10.0±0.09	10.1±0.09	10.15±0.07					
70.0	9.8±0.1	9.9±0.11	10.0±0.06	10.1±0.09	10.1±0.07					
80.0	9.8±0.13	9.9±0.07	9.95±0.08	10.1±0.06	10.1±0.06					
90.0	9.8±0.16	9.9±0.07	10.0±0.08	10.1±0.07	10.2±0.06					
100.0	9.8±0.09	9.9±0.06	10.0±0.06	10.1±0.07	10.2±0.05					

**Table 7.** Results - MIST models Padova clusters - wavelength: 3700-6200

S/N	6.8	6.9	7.0	7.1	7.2	7.3	7.4	7.5	7.6	7.7
10.0	6.9±0.15	6.9±0.11	6.95±0.06	7.0±0.07	7.05±0.11	7.3±0.09	7.3±0.12	7.5±0.15	7.5±0.18	7.6±0.15
20.0	7.1±0.15	7.05±0.12	6.9±0.06	7.0±0.07	7.0±0.1	7.3±0.04	7.3±0.09	7.5±0.1	7.5±0.14	7.6±0.13
30.0	7.2±0.08	7.0±0.1	6.9±0.06	7.0±0.07	7.0±0.06	7.3±0.07	7.3±0.09	7.4±0.13	7.5±0.12	7.6±0.12
40.0	7.2±0.05	6.9±0.08	6.9±0.04	7.0±0.04	7.0±0.05	7.3±0.03	7.3±0.08	7.4±0.09	7.5±0.12	7.6±0.13
50.0	7.2±0.05	6.9±0.07	6.9±0.03	7.0±0.02	7.0±0.03	7.3±0.03	7.3±0.08	7.3±0.09	7.3±0.1	7.6±0.13
60.0	7.2±0.04	6.9±0.05	6.9±0.03	7.0±0.0	7.0±0.03	7.3±0.02	7.3±0.07	7.3±0.09	7.4±0.13	7.6±0.13
70.0	7.2±0.04	6.9±0.05	6.9±0.02	7.0±0.0	7.0±0.02	7.3±0.02	7.3±0.08	7.3±0.07	7.4±0.13	7.8±0.11
80.0	7.2±0.04	6.9±0.05	6.9±0.0	7.0±0.0	7.0±0.0	7.3±0.0	7.3±0.1	7.3±0.08	7.3±0.1	7.8±0.13
90.0	7.2±0.03	6.9±0.03	6.9±0.03	7.0±0.0	7.0±0.02	7.3±0.0	7.3±0.07	7.3±0.06	7.35±0.08	7.8±0.1
100.0	7.2±0.03	6.9±0.03	6.9±0.0	7.0±0.0	7.0±0.02	7.3±0.02	7.3±0.1	7.3±0.06	7.3±0.08	7.8±0.12
S/N	7.8	7.9	8.0	8.1	8.2	8.3	8.4	8.5	8.6	8.7
10.0	7.65±0.15	7.7±0.21	7.95±0.14	8.0±0.15	8.0±0.07	8.2±0.19	8.35±0.22	8.6±0.18	8.5±0.19	8.5±0.23
20.0	7.7±0.15	7.7±0.15	8.0±0.18	8.05±0.12	8.1±0.12	8.2±0.06	8.4±0.11	8.5±0.12	8.6±0.11	8.7±0.13
30.0	7.6±0.16	7.7±0.17	7.8±0.18	8.0±0.1	8.1±0.11	8.2±0.05	8.4±0.05	8.6±0.06	8.6±0.08	8.6±0.11
40.0	7.6±0.14	7.7±0.19	7.9±0.18	8.0±0.11	8.1±0.07	8.1±0.05	8.4±0.07	8.5±0.07	8.6±0.06	8.6±0.09
50.0	7.6±0.12	7.6±0.2	7.7±0.18	8.0±0.08	8.1±0.07	8.1±0.05	8.4±0.05	8.5±0.06	8.6±0.05	8.6±0.08
60.0	7.6±0.13	7.6±0.19	7.7±0.18	8.0±0.05	8.2±0.07	8.1±0.05	8.4±0.05	8.6±0.06	8.6±0.04	8.6±0.09
70.0	7.6±0.11	7.6±0.2	7.7±0.18	8.0±0.09	8.2±0.06	8.1±0.03	8.4±0.05	8.5±0.05	8.6±0.04	8.6±0.07
80.0	7.8±0.12	7.6±0.21	7.7±0.15	8.0±0.07	8.1±0.05	8.1±0.03	8.4±0.05	8.5±0.05	8.6±0.04	8.6±0.07
90.0	7.8±0.1	7.6±0.22	7.7±0.14	8.0±0.03	8.15±0.06	8.1±0.03	8.4±0.05	8.5±0.05	8.6±0.03	8.6±0.07
100.0	7.8±0.11	7.6±0.19	7.7±0.15	8.0±0.03	8.2±0.05	8.1±0.04	8.4±0.05	8.5±0.04	8.6±0.03	8.6±0.07
S/N	8.8	8.9	9.0	9.1	9.2	9.3	9.4	9.5	9.6	9.7
10.0	8.8±0.16	8.9±0.16	9.0±0.13	9.1±0.18	9.2±0.18	9.4±0.23	9.5±0.22	9.6±0.23	9.65±0.29	9.7±0.32
20.0	8.8±0.13	8.9±0.08	9.0±0.07	9.2±0.11	9.2±0.15	9.4±0.1	9.5±0.09	9.6±0.15	9.7±0.21	9.8±0.2
30.0	8.8±0.07	8.9±0.05	9.0±0.07	9.15±0.09	9.2±0.09	9.4±0.07	9.5±0.07	9.6±0.12	9.65±0.13	9.7±0.14
40.0	8.8±0.06	8.9±0.04	9.0±0.04	9.1±0.09	9.2±0.07	9.4±0.09	9.5±0.08	9.6±0.1	9.7±0.12	9.7±0.09
50.0	8.85±0.05	8.9±0.04	9.0±0.03	9.2±0.08	9.2±0.06	9.4±0.08	9.5±0.07	9.6±0.09	9.7±0.09	9.7±0.11
60.0	8.8±0.05	8.9±0.03	9.0±0.03	9.2±0.07	9.2±0.08	9.3±0.08	9.5±0.08	9.6±0.08	9.6±0.12	9.8±0.11
70.0	8.9±0.06	8.9±0.04	9.0±0.0	9.2±0.07	9.2±0.08	9.3±0.08	9.5±0.07	9.5±0.08	9.7±0.09	9.8±0.11
80.0	8.8±0.05	8.9±0.05	9.0±0.02	9.2±0.08	9.3±0.08	9.3±0.1	9.5±0.07	9.6±0.07	9.7±0.1	9.8±0.07
90.0	8.9±0.06	8.9±0.04	9.0±0.0	9.2±0.06	9.2±0.06	9.3±0.09	9.5±0.06	9.5±0.08	9.6±0.1	9.7±0.11
100.0	8.8±0.05	8.9±0.04	9.0±0.0	9.2±0.06	9.2±0.07	9.4±0.09	9.5±0.06	9.6±0.06	9.65±0.07	9.8±0.08
S/N	9.8	9.9	10.0	10.1	10.2					
10.0	9.75±0.26	9.8±0.27	9.9±0.24	9.95±0.21	10.0±0.19					
20.0	9.7±0.17	9.9±0.2	10.0±0.13	10.0±0.13	10.0±0.12					
30.0	9.7±0.19	9.9±0.18	10.0±0.17	9.95±0.12	10.1±0.11					
40.0	9.8±0.13	9.9±0.12	9.9±0.12	9.95±0.1	10.1±0.1					
50.0	9.7±0.1	9.8±0.13	10.0±0.12	10.0±0.09	10.0±0.12					
60.0	9.8±0.11	9.8±0.12	9.9±0.11	10.0±0.1	10.05±0.1					
70.0	9.8±0.1	9.9±0.09	10.0±0.12	10.0±0.08	10.1±0.1					
80.0	9.75±0.13	9.8±0.08	10.0±0.11	10.0±0.08	10.1±0.1					
90.0	9.8±0.14	9.9±0.08	10.0±0.09	9.9±0.08	10.1±0.09					
100.0	9.8±0.1	9.8±0.05	10.0±0.11	9.9±0.08	10.1±0.08					

**Table 8.** Results - MIST models Padova clusters - wavelength: 3700-5000

S/N	6.8	6.9	7.0	7.1	7.2	7.3	7.4	7.5	7.6	7.7
10.0	6.9±0.21	6.9±0.17	7.0±0.23	7.0±0.2	7.3±0.13	7.3±0.18	7.3±0.16	7.3±0.25	7.3±0.24	7.5±0.33
20.0	6.9±0.15	6.9±0.1	7.0±0.14	7.0±0.14	7.3±0.14	7.3±0.11	7.3±0.09	7.45±0.1	7.5±0.1	7.5±0.22
30.0	6.9±0.13	6.9±0.06	7.0±0.04	7.1±0.11	7.1±0.11	7.3±0.05	7.3±0.09	7.5±0.08	7.5±0.13	7.5±0.19
40.0	6.8±0.08	6.9±0.07	7.0±0.09	7.0±0.1	7.2±0.11	7.3±0.0	7.3±0.06	7.5±0.08	7.5±0.1	7.5±0.15
50.0	6.8±0.1	6.9±0.05	7.0±0.03	7.0±0.05	7.3±0.1	7.3±0.0	7.3±0.09	7.5±0.07	7.5±0.09	7.5±0.17
60.0	6.8±0.08	6.9±0.05	7.0±0.03	7.0±0.05	7.3±0.1	7.3±0.0	7.3±0.08	7.5±0.05	7.5±0.04	7.5±0.16
70.0	6.8±0.04	6.9±0.04	7.0±0.03	7.0±0.04	7.1±0.09	7.3±0.0	7.3±0.07	7.5±0.04	7.5±0.06	7.5±0.07
80.0	6.8±0.02	6.9±0.03	7.0±0.02	7.0±0.04	7.1±0.1	7.3±0.0	7.3±0.09	7.5±0.0	7.5±0.02	7.5±0.1
90.0	6.8±0.04	6.9±0.03	7.0±0.03	7.0±0.04	7.1±0.1	7.3±0.0	7.3±0.06	7.5±0.0	7.5±0.04	7.5±0.02
100.0	6.8±0.02	6.9±0.03	7.0±0.02	7.0±0.04	7.3±0.1	7.3±0.0	7.3±0.04	7.5±0.0	7.5±0.04	7.5±0.07
S/N	7.8	7.9	8.0	8.1	8.2	8.3	8.4	8.5	8.6	8.7
10.0	7.7±0.28	7.8±0.28	7.95±0.28	8.0±0.14	8.0±0.13	8.2±0.13	8.45±0.29	8.7±0.19	8.6±0.14	8.75±0.16
20.0	7.7±0.21	7.7±0.16	8.0±0.11	8.0±0.09	8.1±0.08	8.2±0.09	8.4±0.17	8.6±0.12	8.6±0.13	8.6±0.1
30.0	7.7±0.14	7.75±0.16	8.0±0.07	8.0±0.06	8.1±0.06	8.2±0.06	8.4±0.09	8.6±0.14	8.6±0.12	8.7±0.08
40.0	7.7±0.16	7.7±0.17	8.0±0.06	8.0±0.06	8.1±0.06	8.2±0.04	8.4±0.08	8.6±0.12	8.6±0.08	8.7±0.09
50.0	7.6±0.09	7.7±0.1	8.0±0.05	8.0±0.05	8.1±0.06	8.2±0.03	8.4±0.07	8.6±0.08	8.6±0.04	8.7±0.08
60.0	7.6±0.09	7.7±0.14	8.0±0.03	8.05±0.05	8.1±0.04	8.2±0.0	8.4±0.04	8.6±0.09	8.6±0.06	8.7±0.06
70.0	7.6±0.06	7.7±0.12	8.0±0.05	8.0±0.05	8.1±0.03	8.2±0.0	8.4±0.04	8.5±0.08	8.6±0.05	8.7±0.06
80.0	7.7±0.06	7.7±0.08	8.0±0.04	8.0±0.05	8.1±0.02	8.2±0.0	8.4±0.04	8.6±0.06	8.6±0.05	8.7±0.06
90.0	7.6±0.06	7.7±0.17	8.0±0.0	8.0±0.04	8.1±0.0	8.2±0.0	8.4±0.04	8.55±0.08	8.6±0.03	8.7±0.05
100.0	7.6±0.05	7.7±0.0	8.0±0.04	8.0±0.05	8.1±0.0	8.2±0.02	8.4±0.0	8.5±0.06	8.6±0.04	8.7±0.06
S/N	8.8	8.9	9.0	9.1	9.2	9.3	9.4	9.5	9.6	9.7
10.0	8.8±0.2	8.9±0.32	9.15±0.33	9.15±0.37	9.2±0.37	9.2±0.4	9.4±0.43	9.4±0.44	9.9±0.42	10.0±0.42
20.0	8.8±0.09	8.9±0.17	9.0±0.17	9.2±0.25	9.3±0.27	9.5±0.26	9.5±0.35	9.6±0.37	9.7±0.27	10.1±0.29
30.0	8.8±0.09	8.9±0.1	9.0±0.14	9.05±0.15	9.25±0.17	9.3±0.19	9.5±0.28	9.6±0.24	9.75±0.26	9.8±0.23
40.0	8.8±0.06	8.9±0.06	9.0±0.07	9.2±0.14	9.2±0.18	9.3±0.15	9.5±0.23	9.6±0.17	9.6±0.21	9.8±0.17
50.0	8.8±0.06	8.9±0.06	9.0±0.11	9.2±0.13	9.25±0.14	9.4±0.13	9.5±0.17	9.6±0.16	9.7±0.16	9.8±0.21
60.0	8.8±0.04	8.9±0.04	9.0±0.08	9.2±0.1	9.2±0.1	9.3±0.11	9.5±0.16	9.55±0.12	9.7±0.14	9.8±0.16
70.0	8.8±0.04	8.9±0.04	9.0±0.05	9.2±0.08	9.2±0.07	9.3±0.09	9.5±0.1	9.6±0.12	9.7±0.15	9.8±0.14
80.0	8.8±0.04	8.9±0.04	9.0±0.09	9.2±0.07	9.3±0.1	9.3±0.08	9.5±0.06	9.6±0.08	9.7±0.13	9.8±0.12
90.0	8.8±0.04	8.9±0.02	9.0±0.04	9.2±0.08	9.2±0.05	9.3±0.08	9.5±0.1	9.6±0.1	9.7±0.09	9.8±0.12
100.0	8.8±0.04	8.9±0.03	9.0±0.03	9.2±0.04	9.2±0.05	9.3±0.07	9.5±0.09	9.6±0.08	9.7±0.1	9.8±0.1
S/N	9.8	9.9	10.0	10.1	10.2					
10.0	9.95±0.43	9.9±0.4	9.95±0.35	9.9±0.38	9.9±0.3					
20.0	10.0±0.36	9.9±0.26	10.0±0.25	9.9±0.28	10.1±0.23					
30.0	9.75±0.3	9.8±0.21	9.8±0.23	10.1±0.22	10.0±0.21					
40.0	9.8±0.22	9.9±0.16	10.0±0.16	10.1±0.17	10.0±0.16					
50.0	9.75±0.22	9.9±0.12	9.95±0.12	9.9±0.15	10.0±0.1					
60.0	9.8±0.13	9.9±0.11	10.0±0.13	9.9±0.15	10.0±0.1					
70.0	9.7±0.14	9.9±0.09	10.0±0.11	9.9±0.14	10.0±0.1					
80.0	9.8±0.15	9.9±0.1	9.95±0.1	9.9±0.14	10.0±0.11					
90.0	9.7±0.08	9.9±0.07	9.9±0.08	9.9±0.11	10.0±0.07					
100.0	9.75±0.09	9.9±0.06	9.9±0.08	10.0±0.13	10.0±0.07					

**Table 9.** Results - MIST models Padova clusters - wavelength: 5000-6200

S/N	6.8	6.9	7.0	7.1	7.2	7.3	7.4	7.5	7.6	7.7
10.0	7.15±0.72	7.1±0.59	7.3±0.62	7.25±0.52	7.1±0.44	7.5±0.66	7.35±0.64	7.7±0.53	7.45±0.58	7.55±0.61
20.0	7.7±0.53	7.4±0.56	7.4±0.42	7.3±0.43	7.3±0.38	7.3±0.43	7.6±0.29	7.7±0.36	7.65±0.4	7.6±0.46
30.0	8.0±0.5	7.6±0.49	7.3±0.3	7.3±0.33	7.3±0.25	7.35±0.26	7.7±0.2	7.75±0.42	7.75±0.34	7.6±0.4
40.0	8.1±0.35	7.5±0.42	7.3±0.27	7.15±0.25	7.4±0.27	7.4±0.21	7.65±0.25	7.8±0.28	7.65±0.29	7.5±0.32
50.0	7.9±0.32	7.6±0.45	7.3±0.32	7.3±0.24	7.2±0.25	7.3±0.21	7.6±0.21	7.8±0.21	7.7±0.19	7.55±0.22
60.0	8.0±0.28	7.6±0.38	7.3±0.2	7.4±0.23	7.1±0.22	7.3±0.19	7.4±0.23	7.8±0.2	7.6±0.2	7.5±0.21
70.0	8.0±0.28	7.6±0.36	7.5±0.21	7.2±0.2	7.2±0.23	7.3±0.19	7.6±0.18	7.8±0.28	7.7±0.22	7.6±0.17
80.0	8.25±0.26	7.6±0.45	7.3±0.19	7.0±0.2	7.0±0.2	7.3±0.12	7.5±0.19	7.8±0.17	7.7±0.13	7.6±0.24
90.0	8.25±0.22	7.6±0.38	7.3±0.25	7.15±0.19	7.2±0.23	7.3±0.13	7.7±0.2	7.8±0.27	7.7±0.19	7.6±0.21
100.0	8.3±0.23	7.6±0.38	7.3±0.18	7.15±0.19	7.0±0.19	7.3±0.14	7.3±0.16	7.8±0.16	7.7±0.17	7.6±0.21
S/N	7.8	7.9	8.0	8.1	8.2	8.3	8.4	8.5	8.6	8.7
10.0	7.3±0.61	7.5±0.67	7.55±0.7	7.8±0.64	7.3±0.69	8.1±0.7	7.65±0.76	8.55±0.62	7.8±0.7	7.6±0.79
20.0	7.7±0.45	7.5±0.61	7.55±0.48	7.65±0.49	8.0±0.54	8.35±0.56	8.5±0.66	8.45±0.61	8.35±0.61	8.75±0.54
30.0	7.45±0.38	7.55±0.4	7.8±0.44	7.9±0.41	8.3±0.43	8.3±0.48	8.3±0.49	8.6±0.53	8.15±0.51	8.6±0.54
40.0	7.55±0.3	7.6±0.4	7.6±0.44	7.9±0.33	8.2±0.31	8.3±0.36	8.25±0.37	8.3±0.44	8.6±0.38	8.65±0.43
50.0	7.6±0.29	7.5±0.34	7.9±0.39	7.9±0.31	8.1±0.32	8.4±0.33	8.0±0.32	8.5±0.42	8.35±0.37	8.65±0.36
60.0	7.6±0.36	7.55±0.25	7.7±0.39	7.9±0.29	8.2±0.26	8.25±0.31	8.4±0.36	8.5±0.4	8.6±0.34	8.65±0.36
70.0	7.6±0.26	7.5±0.28	7.6±0.34	7.9±0.26	8.2±0.21	8.3±0.21	8.3±0.31	8.5±0.37	8.4±0.4	8.7±0.29
80.0	7.55±0.28	7.5±0.3	7.8±0.41	7.9±0.26	8.2±0.18	8.4±0.23	8.0±0.35	8.45±0.4	8.55±0.38	8.65±0.38
90.0	7.6±0.25	7.6±0.27	7.8±0.3	7.9±0.26	8.2±0.18	8.35±0.19	7.8±0.34	8.5±0.35	8.5±0.36	8.7±0.22
100.0	7.6±0.16	7.5±0.27	7.7±0.31	7.9±0.26	8.3±0.17	8.4±0.2	8.25±0.34	8.5±0.32	8.6±0.39	8.6±0.3
S/N	8.8	8.9	9.0	9.1	9.2	9.3	9.4	9.5	9.6	9.7
10.0	8.7±0.66	8.9±0.74	9.0±0.83	9.1±0.81	9.15±0.82	9.4±0.94	9.5±0.43	9.6±0.49	9.6±0.53	9.7±0.94
20.0	8.6±0.6	8.9±0.18	9.0±0.29	9.1±0.56	9.1±0.57	9.4±0.13	9.5±0.11	9.6±0.11	9.65±0.19	9.8±0.48
30.0	8.8±0.39	8.9±0.07	9.0±0.08	9.1±0.07	9.1±0.34	9.4±0.08	9.5±0.08	9.6±0.1	9.6±0.14	9.8±0.19
40.0	8.8±0.33	8.9±0.11	9.0±0.29	9.1±0.09	9.2±0.12	9.4±0.06	9.5±0.06	9.6±0.08	9.7±0.08	9.8±0.13
50.0	8.8±0.09	8.9±0.04	9.0±0.29	9.1±0.08	9.15±0.12	9.4±0.08	9.5±0.06	9.6±0.08	9.65±0.13	9.8±0.18
60.0	8.8±0.09	8.9±0.02	9.0±0.03	9.1±0.07	9.2±0.09	9.4±0.07	9.5±0.08	9.6±0.07	9.7±0.15	9.8±0.15
70.0	8.8±0.09	8.9±0.0	9.0±0.0	9.1±0.08	9.2±0.1	9.4±0.06	9.5±0.07	9.55±0.07	9.7±0.07	9.8±0.15
80.0	8.8±0.07	8.9±0.02	9.0±0.02	9.15±0.08	9.2±0.11	9.4±0.07	9.5±0.07	9.6±0.07	9.7±0.15	9.8±0.08
90.0	8.8±0.11	8.9±0.0	9.0±0.0	9.2±0.07	9.2±0.09	9.4±0.07	9.5±0.06	9.6±0.08	9.7±0.17	9.8±0.06
100.0	8.8±0.07	8.9±0.0	9.0±0.0	9.2±0.06	9.2±0.08	9.4±0.07	9.5±0.06	9.6±0.07	9.7±0.12	9.8±0.07
S/N	9.8	9.9	10.0	10.1	10.2					
10.0	9.85±0.89	9.95±0.83	9.9±0.69	10.0±0.51	10.2±0.76					
20.0	9.8±0.25	9.85±0.15	10.0±0.16	10.1±0.13	10.2±0.12					
30.0	9.9±0.19	9.95±0.15	10.0±0.15	10.1±0.14	10.1±0.13					
40.0	9.85±0.21	9.9±0.11	10.0±0.12	10.1±0.1	10.1±0.1					
50.0	9.9±0.13	9.9±0.11	10.0±0.12	10.1±0.11	10.1±0.11					
60.0	9.8±0.16	9.9±0.11	9.95±0.07	10.05±0.11	10.1±0.1					
70.0	9.8±0.12	9.9±0.08	10.0±0.05	10.0±0.1	10.1±0.09					
80.0	9.9±0.09	9.95±0.08	10.0±0.07	10.1±0.08	10.1±0.1					
90.0	9.8±0.09	9.9±0.07	10.0±0.06	10.0±0.09	10.1±0.07					
100.0	9.8±0.07	9.9±0.07	9.9±0.08	10.0±0.09	10.1±0.06					

**Table 10.** Results - Padova models MIST clusters - wavelength: 3700-6200

S/N	6.8	6.9	7.0	7.1	7.2	7.3	7.4	7.5	7.6	7.7
10.0	6.85±0.12	6.9±0.11	7.0±0.13	6.9±0.19	7.3±0.28	7.3±0.18	6.9±0.42	7.5±0.54	8.05±0.72	8.4±0.59
20.0	6.8±0.14	6.95±0.13	7.1±0.11	6.9±0.22	7.5±0.26	7.4±0.12	6.9±0.0	8.3±0.56	8.4±0.52	8.5±0.79
30.0	6.8±0.17	6.9±0.08	7.1±0.1	7.3±0.25	7.5±0.19	7.3±0.11	6.9±0.0	8.4±0.46	8.4±0.47	8.5±0.42
40.0	6.8±0.09	6.9±0.06	7.1±0.15	7.3±0.23	7.5±0.24	7.3±0.1	6.9±0.0	8.4±0.5	8.45±0.43	8.5±0.57
50.0	6.8±0.14	6.9±0.05	7.1±0.12	7.3±0.23	7.5±0.2	7.4±0.1	6.9±0.0	8.4±0.23	8.45±0.29	8.5±0.3
60.0	6.8±0.14	6.9±0.03	7.1±0.1	7.3±0.21	7.5±0.18	7.4±0.07	6.9±0.0	8.4±0.31	8.5±0.06	8.55±0.31
70.0	6.8±0.05	6.9±0.04	7.1±0.11	7.3±0.15	7.5±0.24	7.4±0.09	6.9±0.0	8.4±0.27	8.5±0.06	8.55±0.05
80.0	6.8±0.05	6.9±0.04	7.2±0.07	7.3±0.24	7.5±0.18	7.35±0.09	6.9±0.0	8.4±0.04	8.45±0.05	8.5±0.05
90.0	6.8±0.0	6.9±0.02	7.2±0.08	7.3±0.2	7.5±0.18	7.3±0.11	6.9±0.0	8.4±0.04	8.5±0.05	8.5±0.04
100.0	6.8±0.0	6.9±0.02	7.2±0.05	7.35±0.18	7.5±0.15	7.4±0.09	6.9±0.0	8.4±0.04	8.5±0.04	8.5±0.05
S/N	7.8	7.9	8.0	8.1	8.2	8.3	8.4	8.5	8.6	8.7
10.0	8.35±0.78	8.65±0.32	8.55±0.29	8.6±0.31	8.6±0.33	8.3±0.36	8.65±0.34	8.7±0.26	8.7±0.18	8.7±0.18
20.0	8.5±0.32	8.65±0.11	8.6±0.12	8.7±0.19	8.6±0.15	8.7±0.15	8.5±0.18	8.75±0.19	8.7±0.15	8.7±0.13
30.0	8.5±0.42	8.65±0.08	8.6±0.07	8.65±0.07	8.6±0.11	8.6±0.16	8.7±0.13	8.75±0.17	8.7±0.14	8.7±0.11
40.0	8.6±0.31	8.7±0.06	8.6±0.06	8.6±0.11	8.6±0.1	8.65±0.08	8.7±0.13	8.75±0.14	8.7±0.12	8.7±0.07
50.0	8.6±0.05	8.7±0.04	8.6±0.05	8.6±0.04	8.6±0.06	8.7±0.05	8.5±0.13	8.7±0.11	8.7±0.14	8.75±0.07
60.0	8.6±0.06	8.7±0.04	8.6±0.05	8.6±0.06	8.6±0.04	8.65±0.05	8.5±0.11	8.7±0.09	8.7±0.12	8.75±0.07
70.0	8.6±0.06	8.7±0.04	8.6±0.05	8.6±0.04	8.6±0.05	8.7±0.05	8.6±0.11	8.7±0.09	8.7±0.1	8.7±0.08
80.0	8.6±0.05	8.7±0.03	8.6±0.05	8.6±0.04	8.6±0.05	8.7±0.05	8.5±0.1	8.7±0.09	8.7±0.1	8.8±0.05
90.0	8.6±0.05	8.7±0.04	8.6±0.04	8.6±0.05	8.6±0.03	8.6±0.05	8.5±0.11	8.7±0.1	8.7±0.1	8.8±0.07
100.0	8.6±0.06	8.7±0.02	8.6±0.05	8.6±0.05	8.6±0.03	8.6±0.05	8.7±0.1	8.7±0.08	8.7±0.09	8.8±0.05
S/N	8.8	8.9	9.0	9.1	9.2	9.3	9.4	9.5	9.6	9.7
10.0	8.7±0.22	8.8±0.16	9.0±0.12	9.1±0.14	9.1±0.14	9.3±0.14	9.4±0.25	9.45±0.25	9.5±0.32	9.5±0.38
20.0	8.7±0.12	8.9±0.09	9.0±0.1	9.2±0.09	9.2±0.11	9.3±0.08	9.4±0.11	9.4±0.13	9.6±0.21	9.6±0.16
30.0	8.75±0.08	8.9±0.08	9.0±0.1	9.2±0.07	9.2±0.11	9.3±0.11	9.4±0.07	9.4±0.07	9.5±0.11	9.7±0.15
40.0	8.75±0.07	8.8±0.06	9.0±0.08	9.1±0.07	9.2±0.09	9.3±0.06	9.4±0.09	9.4±0.09	9.5±0.1	9.7±0.09
50.0	8.7±0.08	8.85±0.07	9.0±0.05	9.2±0.07	9.2±0.08	9.3±0.08	9.4±0.08	9.4±0.05	9.5±0.08	9.65±0.09
60.0	8.7±0.08	8.8±0.05	9.0±0.05	9.2±0.08	9.2±0.09	9.3±0.07	9.4±0.09	9.4±0.07	9.5±0.09	9.7±0.09
70.0	8.7±0.07	8.8±0.06	9.0±0.05	9.1±0.07	9.2±0.06	9.3±0.07	9.3±0.09	9.4±0.05	9.6±0.1	9.7±0.09
80.0	8.7±0.05	8.8±0.05	9.0±0.05	9.1±0.07	9.2±0.07	9.3±0.08	9.3±0.09	9.4±0.08	9.5±0.09	9.6±0.1
90.0	8.7±0.03	8.8±0.06	9.0±0.02	9.1±0.08	9.2±0.07	9.3±0.08	9.3±0.08	9.4±0.06	9.6±0.11	9.6±0.09
100.0	8.7±0.04	8.8±0.05	9.0±0.02	9.1±0.06	9.2±0.06	9.3±0.07	9.35±0.09	9.4±0.06	9.6±0.1	9.6±0.09
S/N	9.8	9.9	10.0	10.1	10.2					
10.0	9.8±0.32	9.8±0.25	9.8±0.26	9.9±0.17	10.0±0.21					
20.0	9.8±0.21	9.85±0.17	10.05±0.21	9.9±0.14	10.0±0.16					
30.0	9.9±0.2	9.9±0.18	10.0±0.18	10.0±0.14	10.1±0.09					
40.0	9.8±0.15	9.9±0.18	10.1±0.18	10.0±0.15	10.1±0.1					
50.0	9.8±0.16	9.9±0.15	10.1±0.14	10.0±0.16	10.1±0.08					
60.0	9.8±0.17	9.9±0.16	10.1±0.12	10.2±0.16	10.1±0.08					
70.0	9.7±0.12	9.9±0.14	10.0±0.14	10.2±0.14	10.1±0.07					
80.0	9.7±0.1	9.9±0.13	10.0±0.14	10.2±0.15	10.1±0.1					
90.0	9.8±0.1	9.9±0.11	10.0±0.14	10.2±0.16	10.1±0.07					
100.0	9.7±0.06	9.9±0.13	10.0±0.13	10.2±0.15	10.1±0.06					

**Table 11.** Results - Padova models MIST clusters - wavelength: 3700-5000

S/N	6.8	6.9	7.0	7.1	7.2	7.3	7.4	7.5	7.6	7.7
10.0	7.1±0.19	7.0±0.17	7.05±0.13	7.0±0.21	7.2±0.26	7.3±0.22	7.3±0.26	7.5±0.33	7.6±0.31	7.6±0.49
20.0	7.1±0.14	6.9±0.14	7.0±0.07	7.1±0.24	7.25±0.24	7.3±0.1	7.4±0.22	7.5±0.16	7.5±0.16	7.8±0.27
30.0	7.0±0.13	6.8±0.13	7.0±0.06	7.2±0.24	7.25±0.28	7.3±0.09	7.5±0.23	7.5±0.08	7.5±0.09	7.5±0.2
40.0	7.1±0.1	6.8±0.12	7.0±0.04	6.8±0.25	7.3±0.2	7.3±0.07	7.5±0.16	7.5±0.04	7.5±0.07	7.65±0.15
50.0	7.1±0.1	6.8±0.05	7.0±0.05	7.05±0.25	7.25±0.18	7.3±0.07	7.5±0.11	7.5±0.04	7.5±0.04	7.5±0.15
60.0	7.1±0.07	6.8±0.08	7.0±0.04	7.05±0.25	7.2±0.2	7.3±0.06	7.5±0.04	7.5±0.02	7.5±0.03	7.65±0.15
70.0	7.1±0.1	6.8±0.05	7.0±0.04	7.3±0.25	7.5±0.19	7.3±0.05	7.5±0.0	7.5±0.03	7.5±0.06	7.65±0.15
80.0	7.1±0.11	6.8±0.0	7.0±0.03	6.8±0.25	7.5±0.16	7.3±0.04	7.5±0.0	7.5±0.02	7.5±0.03	7.5±0.14
90.0	7.1±0.08	6.8±0.0	7.0±0.04	7.3±0.25	7.5±0.16	7.3±0.04	7.5±0.0	7.5±0.0	7.5±0.02	7.5±0.15
100.0	7.1±0.05	6.8±0.0	7.0±0.02	7.3±0.25	7.5±0.12	7.3±0.04	7.5±0.0	7.5±0.0	7.5±0.0	7.5±0.15
S/N	7.8	7.9	8.0	8.1	8.2	8.3	8.4	8.5	8.6	8.7
10.0	7.8±0.58	8.2±0.62	8.2±0.43	8.3±0.36	8.3±0.43	8.45±0.35	8.7±0.24	8.75±0.2	8.6±0.17	8.65±0.18
20.0	8.3±0.38	8.4±0.4	8.3±0.31	8.3±0.1	8.3±0.21	8.3±0.2	8.5±0.14	8.6±0.21	8.8±0.16	8.7±0.14
30.0	8.3±0.39	8.4±0.29	8.3±0.17	8.3±0.09	8.3±0.1	8.6±0.21	8.4±0.13	8.6±0.17	8.6±0.14	8.7±0.11
40.0	7.8±0.35	8.4±0.05	8.0±0.11	8.3±0.08	8.3±0.09	8.6±0.14	8.45±0.14	8.6±0.16	8.6±0.13	8.65±0.11
50.0	8.4±0.32	8.5±0.05	8.0±0.14	8.3±0.07	8.3±0.11	8.6±0.17	8.5±0.11	8.6±0.14	8.6±0.12	8.7±0.09
60.0	8.4±0.31	8.4±0.05	8.0±0.14	8.3±0.05	8.3±0.0	8.6±0.17	8.5±0.1	8.6±0.14	8.6±0.1	8.7±0.08
70.0	8.4±0.29	8.4±0.04	8.0±0.12	8.3±0.0	8.3±0.05	8.6±0.16	8.5±0.07	8.6±0.13	8.5±0.1	8.7±0.1
80.0	8.1±0.31	8.4±0.05	8.0±0.12	8.3±0.04	8.3±0.05	8.6±0.15	8.5±0.09	8.6±0.15	8.55±0.11	8.7±0.04
90.0	8.4±0.27	8.4±0.05	8.0±0.1	8.3±0.0	8.3±0.0	8.6±0.14	8.5±0.09	8.6±0.09	8.5±0.07	8.7±0.06
100.0	7.8±0.3	8.4±0.04	8.0±0.0	8.3±0.0	8.3±0.0	8.6±0.15	8.5±0.07	8.6±0.09	8.5±0.07	8.7±0.07
S/N	8.8	8.9	9.0	9.1	9.2	9.3	9.4	9.5	9.6	9.7
10.0	8.7±0.21	8.8±0.25	9.0±0.26	9.1±0.31	9.3±0.39	9.3±0.45	9.9±0.49	9.2±0.51	9.45±0.45	9.95±0.51
20.0	8.8±0.15	8.9±0.13	9.0±0.12	9.1±0.16	9.2±0.27	9.2±0.21	9.3±0.35	9.4±0.29	9.4±0.34	9.6±0.28
30.0	8.8±0.15	8.9±0.11	9.0±0.14	9.1±0.12	9.2±0.14	9.2±0.16	9.5±0.17	9.4±0.25	9.4±0.29	9.6±0.22
40.0	8.8±0.09	8.9±0.07	9.0±0.08	9.1±0.08	9.15±0.14	9.4±0.17	9.3±0.12	9.4±0.17	9.55±0.19	9.6±0.23
50.0	8.8±0.06	8.9±0.08	9.0±0.07	9.1±0.06	9.2±0.11	9.25±0.12	9.3±0.14	9.4±0.14	9.5±0.14	9.6±0.16
60.0	8.8±0.07	8.85±0.06	9.0±0.06	9.1±0.05	9.15±0.08	9.3±0.08	9.3±0.13	9.4±0.13	9.5±0.16	9.6±0.16
70.0	8.7±0.07	8.9±0.06	9.0±0.04	9.1±0.06	9.2±0.08	9.2±0.06	9.3±0.1	9.4±0.11	9.5±0.16	9.6±0.15
80.0	8.7±0.06	8.9±0.06	9.0±0.04	9.1±0.05	9.2±0.08	9.2±0.06	9.3±0.1	9.4±0.12	9.5±0.13	9.6±0.14
90.0	8.7±0.06	8.9±0.05	9.0±0.06	9.1±0.03	9.2±0.05	9.3±0.05	9.3±0.09	9.4±0.06	9.5±0.09	9.6±0.13
100.0	8.8±0.05	8.9±0.06	9.0±0.03	9.1±0.03	9.2±0.06	9.3±0.06	9.3±0.09	9.4±0.09	9.5±0.12	9.6±0.15
S/N	9.8	9.9	10.0	10.1	10.2					
10.0	9.45±0.48	10.1±0.37	10.05±0.37	10.1±0.39	10.1±0.34					
20.0	9.75±0.37	10.1±0.27	9.9±0.32	10.2±0.27	10.0±0.25					
30.0	9.7±0.28	9.85±0.28	10.2±0.25	10.1±0.21	10.1±0.2					
40.0	9.8±0.26	9.9±0.16	10.2±0.17	10.1±0.16	10.1±0.15					
50.0	9.7±0.21	9.9±0.17	10.2±0.18	10.2±0.08	10.1±0.1					
60.0	9.8±0.14	9.9±0.15	10.2±0.15	10.15±0.06	10.1±0.12					
70.0	9.75±0.18	9.9±0.12	10.2±0.15	10.2±0.04	10.1±0.07					
80.0	9.8±0.13	9.9±0.12	10.2±0.1	10.2±0.04	10.1±0.14					
90.0	9.8±0.1	9.9±0.13	10.0±0.14	10.2±0.05	10.1±0.09					
100.0	9.7±0.08	9.9±0.11	10.2±0.14	10.2±0.06	10.1±0.05					

**Table 12.** Results - Padova models MIST clusters - wavelength: 5000-6200

S/N	6.8	6.9	7.0	7.1	7.2	7.3	7.4	7.5	7.6	7.7
10.0	6.8±0.53	7.0±0.69	6.95±0.66	7.05±0.6	7.3±0.6	7.25±0.75	9.1±0.76	7.3±0.88	7.6±0.94	7.55±0.89
20.0	6.85±0.44	7.3±0.5	7.05±0.38	7.2±0.53	7.5±0.6	7.3±0.53	9.0±0.61	7.25±0.77	7.2±0.91	8.8±0.85
30.0	6.8±0.17	7.4±0.46	7.2±0.36	7.2±0.49	7.5±0.59	7.4±0.41	9.0±0.07	7.0±0.8	7.25±0.92	8.8±0.84
40.0	6.9±0.07	7.6±0.38	7.0±0.17	7.1±0.29	7.5±0.42	7.45±0.38	9.0±0.07	7.55±0.83	7.1±0.91	8.8±0.86
50.0	6.8±0.08	7.7±0.48	7.0±0.16	7.1±0.43	7.5±0.44	7.4±0.37	9.05±0.08	8.7±0.81	7.85±0.94	8.9±0.58
60.0	6.8±0.08	7.7±0.4	7.0±0.15	7.1±0.27	7.5±0.39	7.4±0.29	9.1±0.09	8.7±0.76	8.7±0.91	8.9±0.76
70.0	6.8±0.06	7.7±0.38	7.05±0.17	7.1±0.31	7.5±0.39	7.4±0.26	9.1±0.08	7.5±0.8	8.7±0.91	8.9±0.67
80.0	6.9±0.07	7.6±0.41	7.2±0.18	7.1±0.29	7.5±0.35	7.4±0.3	9.1±0.08	8.7±0.72	8.75±0.87	8.9±0.66
90.0	6.9±0.07	7.7±0.41	7.2±0.19	7.1±0.18	7.5±0.21	7.4±0.16	9.1±0.09	8.75±0.82	8.7±0.68	8.9±0.08
100.0	6.85±0.06	7.55±0.45	7.2±0.2	7.1±0.26	7.5±0.05	7.4±0.25	9.1±0.07	8.7±0.71	8.7±0.65	8.9±0.07
S/N	7.8	7.9	8.0	8.1	8.2	8.3	8.4	8.5	8.6	8.7
10.0	8.8±0.87	8.85±0.95	7.55±0.89	8.15±0.85	7.55±0.83	7.3±0.86	8.6±0.92	7.5±0.88	8.5±0.82	7.6±0.87
20.0	7.5±0.85	8.8±0.86	8.8±0.77	8.8±0.74	7.6±0.81	7.55±0.81	7.6±0.74	8.05±0.81	8.6±0.77	7.6±0.74
30.0	7.6±0.86	8.9±0.52	8.8±0.73	7.55±0.84	7.6±0.75	7.6±0.76	8.7±0.68	7.6±0.76	8.05±0.73	8.7±0.77
40.0	8.8±0.86	8.8±0.62	8.8±0.74	8.2±0.85	8.7±0.8	8.7±0.67	8.65±0.72	8.7±0.65	8.7±0.75	8.7±0.7
50.0	7.5±0.87	8.9±0.05	8.8±0.83	8.8±0.56	7.5±0.7	8.7±0.51	8.6±0.69	8.7±0.56	8.7±0.56	8.7±0.55
60.0	8.8±0.79	8.9±0.49	8.8±0.62	8.8±0.71	8.8±0.58	8.7±0.51	8.7±0.52	8.7±0.39	8.7±0.59	8.7±0.4
70.0	8.8±0.74	8.9±0.05	8.8±0.35	8.8±0.24	8.7±0.67	8.7±0.45	8.7±0.45	8.7±0.34	8.65±0.2	8.7±0.4
80.0	8.8±0.59	8.9±0.05	8.8±0.35	8.8±0.47	8.7±0.45	8.7±0.37	8.65±0.45	8.7±0.2	8.7±0.36	8.7±0.22
90.0	8.8±0.53	8.9±0.05	8.8±0.05	8.8±0.4	8.7±0.38	8.7±0.42	8.7±0.36	8.7±0.28	8.7±0.2	8.7±0.37
100.0	8.8±0.67	8.9±0.05	8.8±0.05	8.8±0.0	8.8±0.41	8.7±0.42	8.7±0.29	8.7±0.36	8.7±0.22	8.7±0.0
S/N	8.8	8.9	9.0	9.1	9.2	9.3	9.4	9.5	9.6	9.7
10.0	8.7±0.84	8.85±0.87	9.0±0.82	9.1±0.74	9.2±0.75	9.25±0.71	9.4±0.62	9.4±0.57	9.6±0.57	9.6±0.79
20.0	8.8±0.67	8.9±0.58	9.0±0.37	9.2±0.41	9.3±0.11	9.3±0.1	9.4±0.11	9.4±0.24	9.5±0.21	9.65±0.21
30.0	8.8±0.22	8.9±0.46	9.0±0.51	9.2±0.09	9.2±0.06	9.3±0.08	9.4±0.09	9.45±0.14	9.5±0.2	9.6±0.19
40.0	8.8±0.48	8.9±0.08	9.0±0.05	9.2±0.07	9.2±0.06	9.3±0.07	9.35±0.11	9.4±0.1	9.5±0.12	9.6±0.15
50.0	8.8±0.33	8.9±0.07	9.0±0.05	9.2±0.07	9.2±0.06	9.3±0.08	9.4±0.08	9.4±0.11	9.6±0.1	9.6±0.14
60.0	8.8±0.24	8.9±0.07	9.0±0.05	9.2±0.07	9.2±0.07	9.3±0.07	9.4±0.09	9.45±0.09	9.5±0.11	9.7±0.14
70.0	8.8±0.24	8.9±0.08	9.0±0.05	9.2±0.07	9.2±0.06	9.3±0.07	9.3±0.09	9.4±0.12	9.5±0.11	9.6±0.13
80.0	8.8±0.0	8.9±0.08	9.0±0.04	9.2±0.06	9.2±0.05	9.3±0.07	9.3±0.09	9.4±0.09	9.5±0.09	9.6±0.1
90.0	8.8±0.0	8.9±0.06	9.0±0.03	9.2±0.06	9.2±0.05	9.3±0.06	9.3±0.08	9.4±0.1	9.5±0.09	9.65±0.13
100.0	8.8±0.24	8.9±0.08	9.0±0.04	9.2±0.06	9.2±0.06	9.3±0.06	9.3±0.09	9.4±0.08	9.5±0.09	9.6±0.1
S/N	9.8	9.9	10.0	10.1	10.2					
10.0	9.65±0.72	9.8±0.28	9.7±0.74	9.9±0.28	9.9±0.8					
20.0	9.7±0.29	9.7±0.28	9.95±0.25	10.0±0.18	10.0±0.22					
30.0	9.8±0.15	9.8±0.2	9.95±0.17	9.95±0.21	10.1±0.19					
40.0	9.85±0.11	9.9±0.18	9.9±0.2	10.0±0.16	10.1±0.16					
50.0	9.8±0.15	9.9±0.12	10.0±0.14	10.1±0.16	10.1±0.12					
60.0	9.8±0.12	9.9±0.1	10.1±0.15	10.1±0.14	10.1±0.15					
70.0	9.8±0.11	9.9±0.11	10.0±0.15	10.1±0.15	10.2±0.11					
80.0	9.8±0.11	9.8±0.11	10.0±0.14	10.2±0.07	10.2±0.12					
90.0	9.8±0.1	9.9±0.09	10.0±0.12	10.1±0.09	10.1±0.11					
100.0	9.7±0.1	9.9±0.09	10.0±0.11	10.1±0.1	10.2±0.06					

**Table 13.** Metallicity Results - Padova - wavelength: 3700-6200

S/N	6.8	6.9	7.0	7.1	7.2	7.3	7.4	7.5	7.6	7.7
10.0	-0.2±0.28	-0.2±0.32	-0.6±0.28	-0.6±0.29	-0.6±0.24	-0.4±0.23	-0.4±0.19	-0.4±0.27	-0.4±0.33	-0.4±0.37
20.0	-0.4±0.23	-0.4±0.41	-0.6±0.1	-0.6±0.25	-0.4±0.11	-0.4±0.09	-0.4±0.11	-0.4±0.22	-0.5±0.33	-0.4±0.33
30.0	-0.4±0.21	-0.4±0.28	-0.4±0.1	-0.4±0.13	-0.4±0.08	-0.4±0.12	-0.4±0.1	-0.4±0.16	-0.4±0.23	-0.4±0.2
40.0	-0.4±0.13	-0.4±0.13	-0.4±0.08	-0.4±0.07	-0.4±0.07	-0.4±0.06	-0.4±0.0	-0.4±0.1	-0.4±0.23	-0.4±0.14
50.0	-0.4±0.04	-0.4±0.16	-0.4±0.08	-0.4±0.08	-0.4±0.05	-0.4±0.05	-0.4±0.0	-0.4±0.1	-0.4±0.09	-0.4±0.12
60.0	-0.4±0.11	-0.4±0.04	-0.4±0.07	-0.4±0.04	-0.4±0.0	-0.4±0.06	-0.4±0.0	-0.4±0.06	-0.4±0.08	-0.4±0.1
70.0	-0.4±0.04	-0.4±0.04	-0.4±0.08	-0.4±0.04	-0.4±0.0	-0.4±0.05	-0.4±0.0	-0.4±0.04	-0.4±0.06	-0.4±0.06
80.0	-0.4±0.0	-0.4±0.0	-0.4±0.05	-0.4±0.0	-0.4±0.0	-0.4±0.04	-0.4±0.0	-0.4±0.04	-0.4±0.04	-0.4±0.09
90.0	-0.4±0.0	-0.4±0.0	-0.4±0.04	-0.4±0.0	-0.4±0.0	-0.4±0.0	-0.4±0.0	-0.4±0.04	-0.4±0.0	-0.4±0.06
100.0	-0.4±0.0	-0.4±0.0	-0.4±0.08	-0.4±0.0	-0.4±0.0	-0.4±0.0	-0.4±0.0	-0.4±0.04	-0.4±0.04	-0.4±0.08
S/N	7.8	7.9	8.0	8.1	8.2	8.3	8.4	8.5	8.6	8.7
10.0	-0.6±0.35	-0.4±0.4	-0.4±0.32	-0.4±0.21	-0.4±0.22	-0.4±0.28	-0.4±0.43	-0.4±0.28	-0.2±0.22	-0.2±0.2
20.0	-0.3±0.34	-0.3±0.27	-0.4±0.19	-0.4±0.19	-0.4±0.17	-0.4±0.26	-0.4±0.41	-0.4±0.23	-0.3±0.2	-0.4±0.21
30.0	-0.5±0.27	-0.4±0.15	-0.4±0.17	-0.4±0.17	-0.4±0.12	-0.4±0.28	-0.4±0.41	-0.4±0.21	-0.2±0.13	-0.4±0.19
40.0	-0.4±0.2	-0.4±0.14	-0.4±0.13	-0.4±0.14	-0.4±0.1	-0.4±0.24	-0.4±0.28	-0.4±0.25	-0.2±0.1	-0.4±0.16
50.0	-0.4±0.11	-0.4±0.11	-0.4±0.15	-0.4±0.17	-0.4±0.05	-0.4±0.19	-0.4±0.21	-0.4±0.16	-0.4±0.1	-0.4±0.15
60.0	-0.4±0.14	-0.4±0.06	-0.4±0.11	-0.4±0.1	-0.4±0.07	-0.4±0.14	-0.4±0.2	-0.4±0.15	-0.2±0.1	-0.4±0.16
70.0	-0.4±0.11	-0.4±0.07	-0.4±0.06	-0.4±0.07	-0.4±0.08	-0.4±0.13	-0.4±0.07	-0.4±0.19	-0.4±0.1	-0.4±0.09
80.0	-0.4±0.1	-0.4±0.07	-0.4±0.08	-0.4±0.17	-0.4±0.06	-0.4±0.07	-0.4±0.17	-0.4±0.17	-0.4±0.1	-0.4±0.1
90.0	-0.4±0.06	-0.4±0.06	-0.4±0.05	-0.4±0.15	-0.4±0.11	-0.4±0.09	-0.4±0.15	-0.4±0.13	-0.2±0.1	-0.4±0.11
100.0	-0.4±0.04	-0.4±0.05	-0.4±0.04	-0.4±0.12	-0.4±0.0	-0.4±0.06	-0.4±0.14	-0.4±0.08	-0.4±0.1	-0.4±0.09
S/N	8.8	8.9	9.0	9.1	9.2	9.3	9.4	9.5	9.6	9.7
10.0	-0.2±0.24	-0.4±0.29	-0.4±0.26	-0.4±0.23	-0.4±0.26	-0.4±0.25	-0.4±0.23	-0.4±0.34	-0.5±0.34	-0.6±0.24
20.0	-0.2±0.25	-0.2±0.24	-0.4±0.17	-0.4±0.18	-0.4±0.23	-0.4±0.17	-0.6±0.15	-0.4±0.12	-0.4±0.21	-0.6±0.22
30.0	-0.4±0.25	-0.4±0.21	-0.4±0.17	-0.4±0.23	-0.4±0.18	-0.4±0.24	-0.4±0.13	-0.4±0.15	-0.4±0.12	-0.4±0.13
40.0	-0.4±0.19	-0.4±0.19	-0.4±0.11	-0.4±0.21	-0.4±0.18	-0.5±0.23	-0.4±0.11	-0.4±0.12	-0.4±0.1	-0.4±0.11
50.0	-0.4±0.14	-0.4±0.19	-0.4±0.11	-0.4±0.18	-0.4±0.21	-0.4±0.19	-0.4±0.11	-0.4±0.1	-0.4±0.1	-0.4±0.15
60.0	-0.4±0.13	-0.4±0.14	-0.4±0.11	-0.4±0.17	-0.4±0.17	-0.4±0.17	-0.4±0.12	-0.4±0.08	-0.4±0.11	-0.4±0.1
70.0	-0.4±0.1	-0.4±0.17	-0.4±0.06	-0.4±0.17	-0.4±0.16	-0.4±0.23	-0.4±0.11	-0.4±0.11	-0.4±0.08	-0.4±0.14
80.0	-0.4±0.1	-0.4±0.17	-0.4±0.06	-0.4±0.15	-0.4±0.2	-0.4±0.12	-0.4±0.12	-0.4±0.09	-0.4±0.1	-0.4±0.06
90.0	-0.4±0.1	-0.4±0.17	-0.4±0.05	-0.4±0.1	-0.4±0.14	-0.4±0.16	-0.4±0.11	-0.4±0.09	-0.4±0.1	-0.4±0.14
100.0	-0.4±0.07	-0.4±0.17	-0.4±0.04	-0.4±0.07	-0.4±0.14	-0.4±0.17	-0.4±0.1	-0.4±0.11	-0.4±0.1	-0.4±0.07
S/N	9.8	9.9	10.0	10.1	10.2					
10.0	-0.4±0.29	-0.3±0.35	-0.4±0.3	-0.2±0.29	-0.2±0.23					
20.0	-0.6±0.13	-0.4±0.17	-0.4±0.19	-0.2±0.23	-0.2±0.2					
30.0	-0.6±0.18	-0.4±0.1	-0.4±0.15	-0.3±0.13	-0.2±0.16					
40.0	-0.4±0.14	-0.4±0.13	-0.4±0.09	-0.4±0.14	-0.4±0.11					
50.0	-0.4±0.1	-0.4±0.12	-0.4±0.08	-0.4±0.1	-0.2±0.14					
60.0	-0.4±0.13	-0.4±0.13	-0.4±0.1	-0.4±0.12	-0.4±0.14					
70.0	-0.4±0.08	-0.4±0.12	-0.4±0.09	-0.4±0.09	-0.4±0.13					
80.0	-0.4±0.1	-0.4±0.13	-0.4±0.09	-0.4±0.09	-0.4±0.11					
90.0	-0.4±0.13	-0.4±0.1	-0.4±0.07	-0.4±0.08	-0.4±0.12					
100.0	-0.4±0.1	-0.4±0.1	-0.4±0.09	-0.4±0.08	-0.4±0.08					

**Table 14.** Metallicity Results - Padova - wavelength: 3700-5000

S/N	6.8	6.9	7.0	7.1	7.2	7.3	7.4	7.5	7.6	7.7
10.0	-0.2±0.23	-0.2±0.26	-0.4±0.23	-0.4±0.32	-0.4±0.13	-0.4±0.22	-0.2±0.29	-0.4±0.32	-0.4±0.29	-0.4±0.35
20.0	-0.4±0.14	-0.4±0.26	-0.4±0.15	-0.4±0.18	-0.4±0.23	-0.4±0.18	-0.4±0.15	-0.4±0.17	-0.4±0.17	-0.4±0.15
30.0	-0.4±0.11	-0.4±0.23	-0.4±0.08	-0.4±0.08	-0.4±0.11	-0.4±0.14	-0.4±0.13	-0.4±0.16	-0.4±0.15	-0.4±0.17
40.0	-0.4±0.05	-0.4±0.16	-0.4±0.08	-0.4±0.04	-0.4±0.0	-0.4±0.0	-0.4±0.13	-0.4±0.14	-0.4±0.1	-0.4±0.12
50.0	-0.4±0.07	-0.4±0.24	-0.4±0.05	-0.4±0.0	-0.4±0.0	-0.4±0.05	-0.4±0.09	-0.4±0.1	-0.4±0.05	-0.4±0.14
60.0	-0.4±0.08	-0.4±0.11	-0.4±0.07	-0.4±0.0	-0.4±0.0	-0.4±0.05	-0.4±0.0	-0.4±0.07	-0.4±0.0	-0.4±0.0
70.0	-0.4±0.08	-0.4±0.0	-0.4±0.06	-0.4±0.0	-0.4±0.0	-0.4±0.0	-0.4±0.0	-0.4±0.1	-0.4±0.0	-0.4±0.0
80.0	-0.4±0.07	-0.4±0.0	-0.4±0.04	-0.4±0.0	-0.4±0.0	-0.4±0.0	-0.4±0.12	-0.4±0.0	-0.4±0.0	-0.4±0.07
90.0	-0.4±0.0	-0.4±0.0	-0.4±0.05	-0.4±0.0	-0.4±0.0	-0.4±0.0	-0.4±0.0	-0.4±0.07	-0.4±0.0	-0.4±0.0
100.0	-0.4±0.05	-0.4±0.0	-0.4±0.04	-0.4±0.0	-0.4±0.0	-0.4±0.0	-0.4±0.0	-0.4±0.0	-0.4±0.0	-0.4±0.0
S/N	7.8	7.9	8.0	8.1	8.2	8.3	8.4	8.5	8.6	8.7
10.0	-0.4±0.3	0.0±0.32	-0.2±0.17	-0.2±0.16	-0.2±0.26	-0.4±0.4	-0.6±0.43	-0.7±0.36	-0.4±0.31	-0.5±0.34
20.0	-0.4±0.14	-0.4±0.25	-0.2±0.15	-0.2±0.15	-0.3±0.19	-0.4±0.31	-0.4±0.51	-0.4±0.25	-0.4±0.23	-0.4±0.2
30.0	-0.4±0.13	-0.4±0.18	-0.4±0.11	-0.4±0.13	-0.4±0.17	-0.4±0.21	-0.4±0.44	-0.4±0.28	-0.2±0.24	-0.4±0.17
40.0	-0.4±0.07	-0.4±0.12	-0.4±0.12	-0.4±0.1	-0.4±0.19	-0.4±0.1	-0.4±0.36	-0.4±0.24	-0.4±0.17	-0.4±0.19
50.0	-0.4±0.0	-0.4±0.16	-0.4±0.09	-0.4±0.1	-0.4±0.15	-0.4±0.1	-0.4±0.31	-0.4±0.18	-0.4±0.16	-0.4±0.16
60.0	-0.4±0.07	-0.4±0.14	-0.4±0.04	-0.4±0.08	-0.4±0.13	-0.4±0.05	-0.4±0.28	-0.4±0.19	-0.4±0.18	-0.4±0.12
70.0	-0.4±0.0	-0.4±0.12	-0.4±0.08	-0.4±0.08	-0.4±0.1	-0.4±0.06	-0.4±0.25	-0.4±0.13	-0.4±0.11	-0.4±0.13
80.0	-0.4±0.0	-0.4±0.0	-0.4±0.05	-0.4±0.07	-0.4±0.07	-0.4±0.0	-0.4±0.22	-0.4±0.06	-0.4±0.15	-0.4±0.13
90.0	-0.4±0.0	-0.4±0.0	-0.4±0.0	-0.4±0.08	-0.4±0.0	-0.4±0.05	-0.4±0.21	-0.4±0.15	-0.4±0.11	-0.4±0.1
100.0	-0.4±0.0	-0.4±0.0	-0.4±0.05	-0.4±0.05	-0.4±0.0	-0.4±0.05	-0.4±0.13	-0.4±0.14	-0.4±0.08	-0.4±0.12
S/N	8.8	8.9	9.0	9.1	9.2	9.3	9.4	9.5	9.6	9.7
10.0	-0.2±0.36	-0.4±0.39	-0.5±0.43	-0.4±0.5	-0.3±0.46	-0.2±0.45	-0.2±0.42	-0.3±0.42	-0.6±0.34	-0.6±0.37
20.0	-0.2±0.18	-0.4±0.33	-0.4±0.29	-0.4±0.35	-0.6±0.36	-0.6±0.34	-0.4±0.41	-0.4±0.41	-0.4±0.22	-0.6±0.28
30.0	-0.4±0.21	-0.4±0.21	-0.4±0.18	-0.4±0.28	-0.4±0.24	-0.4±0.28	-0.4±0.35	-0.4±0.28	-0.5±0.21	-0.4±0.25
40.0	-0.4±0.15	-0.4±0.13	-0.4±0.1	-0.4±0.22	-0.4±0.23	-0.4±0.2	-0.4±0.26	-0.4±0.23	-0.4±0.12	-0.4±0.18
50.0	-0.4±0.14	-0.4±0.14	-0.4±0.13	-0.4±0.25	-0.4±0.15	-0.5±0.22	-0.4±0.23	-0.4±0.21	-0.4±0.13	-0.4±0.28
60.0	-0.4±0.12	-0.4±0.14	-0.4±0.11	-0.4±0.19	-0.4±0.2	-0.4±0.19	-0.4±0.22	-0.4±0.16	-0.4±0.12	-0.4±0.15
70.0	-0.4±0.11	-0.4±0.11	-0.4±0.09	-0.4±0.18	-0.4±0.15	-0.4±0.16	-0.4±0.13	-0.4±0.13	-0.4±0.09	-0.4±0.23
80.0	-0.4±0.11	-0.4±0.1	-0.4±0.12	-0.4±0.13	-0.4±0.17	-0.4±0.11	-0.4±0.13	-0.4±0.12	-0.4±0.07	-0.4±0.13
90.0	-0.4±0.08	-0.4±0.06	-0.4±0.06	-0.4±0.05	-0.4±0.12	-0.4±0.12	-0.4±0.15	-0.4±0.14	-0.4±0.06	-0.4±0.1
100.0	-0.4±0.1	-0.4±0.1	-0.4±0.05	-0.4±0.11	-0.4±0.12	-0.4±0.11	-0.4±0.08	-0.4±0.12	-0.4±0.06	-0.4±0.13
S/N	9.8	9.9	10.0	10.1	10.2					
10.0	-0.2±0.37	-0.2±0.36	-0.2±0.29	-0.2±0.22	0.0±0.22					
20.0	-0.6±0.39	-0.4±0.31	-0.3±0.28	-0.2±0.21	-0.2±0.21					
30.0	-0.4±0.32	-0.3±0.27	-0.2±0.27	-0.2±0.18	-0.2±0.19					
40.0	-0.4±0.29	-0.4±0.18	-0.4±0.2	-0.4±0.09	-0.4±0.14					
50.0	-0.4±0.23	-0.4±0.14	-0.4±0.15	-0.4±0.1	-0.4±0.1					
60.0	-0.4±0.15	-0.4±0.17	-0.4±0.16	-0.4±0.1	-0.4±0.1					
70.0	-0.4±0.16	-0.4±0.14	-0.4±0.12	-0.4±0.09	-0.4±0.09					
80.0	-0.4±0.13	-0.4±0.14	-0.4±0.14	-0.4±0.06	-0.4±0.09					
90.0	-0.4±0.09	-0.4±0.07	-0.4±0.13	-0.4±0.07	-0.4±0.08					
100.0	-0.4±0.11	-0.4±0.1	-0.4±0.12	-0.4±0.05	-0.4±0.1					

**Table 15.** Metallicity Results - Padova - wavelength: 5000-6200

S/N	6.8	6.9	7.0	7.1	7.2	7.3	7.4	7.5	7.6	7.7
10.0	-0.4±0.39	-0.3±0.36	-0.4±0.41	-0.4±0.34	-0.4±0.3	-0.2±0.34	-0.2±0.4	-0.2±0.36	-0.2±0.46	-0.3±0.34
20.0	-0.4±0.4	-0.4±0.41	-0.4±0.34	-0.5±0.33	-0.3±0.25	-0.4±0.24	-0.2±0.33	-0.2±0.29	-0.2±0.32	-0.4±0.29
30.0	-0.3±0.39	-0.4±0.4	-0.4±0.26	-0.4±0.33	-0.4±0.27	-0.2±0.16	-0.2±0.27	-0.2±0.29	-0.2±0.28	-0.3±0.23
40.0	-0.3±0.37	-0.4±0.34	-0.4±0.24	-0.5±0.25	-0.2±0.24	-0.2±0.24	-0.2±0.19	-0.2±0.25	-0.2±0.28	-0.2±0.28
50.0	-0.4±0.36	-0.4±0.32	-0.4±0.18	-0.4±0.3	-0.4±0.22	-0.3±0.16	-0.4±0.18	-0.2±0.22	-0.2±0.21	-0.3±0.24
60.0	-0.4±0.31	-0.4±0.3	-0.4±0.18	-0.4±0.2	-0.4±0.16	-0.2±0.19	-0.4±0.23	-0.4±0.24	-0.4±0.25	-0.4±0.29
70.0	-0.4±0.29	-0.4±0.27	-0.4±0.18	-0.4±0.17	-0.4±0.17	-0.2±0.1	-0.4±0.23	-0.4±0.26	-0.3±0.19	-0.4±0.2
80.0	-0.4±0.28	-0.4±0.26	-0.4±0.17	-0.4±0.13	-0.4±0.16	-0.4±0.16	-0.4±0.2	-0.4±0.24	-0.4±0.19	-0.4±0.22
90.0	-0.4±0.28	-0.4±0.26	-0.4±0.19	-0.4±0.14	-0.4±0.15	-0.4±0.1	-0.2±0.2	-0.4±0.2	-0.4±0.14	-0.4±0.19
100.0	-0.4±0.24	-0.4±0.26	-0.4±0.13	-0.4±0.12	-0.4±0.09	-0.4±0.16	-0.4±0.21	-0.4±0.17	-0.4±0.17	-0.4±0.2
S/N	7.8	7.9	8.0	8.1	8.2	8.3	8.4	8.5	8.6	8.7
10.0	-0.4±0.41	-0.2±0.37	-0.2±0.43	-0.3±0.39	-0.4±0.42	-0.2±0.48	0.0±0.5	-0.2±0.37	-0.4±0.45	0.2±0.51
20.0	-0.2±0.35	-0.3±0.28	-0.4±0.43	-0.6±0.41	-0.2±0.45	-0.2±0.38	-0.2±0.32	-0.3±0.33	-0.3±0.35	-0.2±0.36
30.0	-0.4±0.28	-0.4±0.29	-0.4±0.37	-0.5±0.38	-0.4±0.31	-0.4±0.32	-0.2±0.31	-0.2±0.31	-0.2±0.37	-0.4±0.35
40.0	-0.4±0.27	-0.2±0.28	-0.4±0.36	-0.6±0.35	-0.2±0.32	-0.4±0.3	-0.4±0.33	-0.4±0.29	-0.2±0.3	-0.4±0.23
50.0	-0.4±0.24	-0.5±0.3	-0.2±0.36	-0.4±0.34	-0.4±0.35	-0.4±0.25	-0.4±0.28	-0.4±0.22	-0.4±0.25	-0.4±0.22
60.0	-0.4±0.23	-0.5±0.24	-0.4±0.37	-0.4±0.34	-0.4±0.29	-0.4±0.27	-0.4±0.25	-0.4±0.2	-0.4±0.2	-0.4±0.25
70.0	-0.2±0.2	-0.4±0.25	-0.6±0.3	-0.4±0.32	-0.4±0.26	-0.4±0.24	-0.4±0.19	-0.4±0.14	-0.4±0.18	-0.4±0.15
80.0	-0.4±0.2	-0.4±0.24	-0.4±0.3	-0.4±0.35	-0.3±0.25	-0.4±0.27	-0.4±0.2	-0.4±0.14	-0.4±0.17	-0.4±0.2
90.0	-0.4±0.19	-0.4±0.24	-0.4±0.2	-0.4±0.32	-0.3±0.22	-0.4±0.27	-0.4±0.13	-0.4±0.14	-0.4±0.14	-0.4±0.17
100.0	-0.4±0.2	-0.6±0.22	-0.4±0.23	-0.4±0.33	-0.4±0.23	-0.4±0.2	-0.4±0.19	-0.4±0.13	-0.4±0.15	-0.4±0.16
S/N	8.8	8.9	9.0	9.1	9.2	9.3	9.4	9.5	9.6	9.7
10.0	-0.2±0.46	0.2±0.4	0.1±0.46	-0.4±0.45	-0.3±0.47	-0.4±0.41	-0.4±0.4	0.0±0.39	-0.4±0.45	-0.4±0.46
20.0	-0.4±0.47	-0.4±0.41	-0.5±0.43	-0.4±0.36	-0.6±0.38	-0.4±0.37	-0.4±0.34	-0.4±0.32	-0.4±0.35	-0.4±0.28
30.0	-0.4±0.39	-0.4±0.3	-0.4±0.37	-0.4±0.29	-0.4±0.22	-0.4±0.28	-0.4±0.31	-0.6±0.24	-0.4±0.18	-0.4±0.19
40.0	-0.5±0.31	-0.4±0.26	-0.4±0.21	-0.4±0.34	-0.4±0.21	-0.5±0.24	-0.4±0.24	-0.4±0.16	-0.4±0.11	-0.4±0.16
50.0	-0.4±0.19	-0.4±0.25	-0.4±0.34	-0.4±0.26	-0.4±0.28	-0.4±0.21	-0.4±0.15	-0.4±0.13	-0.4±0.11	-0.4±0.14
60.0	-0.4±0.17	-0.4±0.2	-0.4±0.26	-0.4±0.24	-0.4±0.12	-0.4±0.2	-0.4±0.19	-0.4±0.09	-0.4±0.09	-0.4±0.08
70.0	-0.4±0.17	-0.4±0.19	-0.4±0.2	-0.4±0.23	-0.4±0.16	-0.4±0.2	-0.4±0.13	-0.4±0.15	-0.4±0.09	-0.4±0.08
80.0	-0.4±0.19	-0.4±0.18	-0.4±0.19	-0.4±0.18	-0.4±0.13	-0.4±0.15	-0.4±0.14	-0.4±0.1	-0.4±0.1	-0.4±0.06
90.0	-0.4±0.2	-0.4±0.17	-0.4±0.21	-0.4±0.16	-0.4±0.09	-0.4±0.17	-0.4±0.13	-0.4±0.08	-0.4±0.08	-0.4±0.1
100.0	-0.4±0.15	-0.4±0.18	-0.4±0.19	-0.4±0.16	-0.4±0.15	-0.4±0.15	-0.4±0.1	-0.4±0.11	-0.4±0.06	-0.4±0.07
S/N	9.8	9.9	10.0	10.1	10.2					
10.0	-0.5±0.43	-0.4±0.47	-0.4±0.45	0.0±0.43	-0.2±0.41					
20.0	-0.6±0.3	-0.4±0.36	-0.4±0.36	-0.4±0.38	-0.2±0.28					
30.0	-0.4±0.29	-0.4±0.22	-0.4±0.34	-0.4±0.3	-0.2±0.32					
40.0	-0.4±0.11	-0.4±0.17	-0.4±0.24	-0.4±0.21	-0.4±0.19					
50.0	-0.4±0.08	-0.4±0.14	-0.4±0.12	-0.4±0.11	-0.2±0.19					
60.0	-0.4±0.09	-0.4±0.07	-0.4±0.11	-0.4±0.16	-0.4±0.19					
70.0	-0.4±0.08	-0.4±0.04	-0.4±0.07	-0.4±0.06	-0.4±0.13					
80.0	-0.4±0.06	-0.4±0.0	-0.4±0.1	-0.4±0.06	-0.4±0.13					
90.0	-0.4±0.07	-0.4±0.05	-0.4±0.07	-0.4±0.04	-0.4±0.09					
100.0	-0.4±0.08	-0.4±0.0	-0.4±0.0	-0.4±0.0	-0.4±0.06					

**Table 16.** Metallicity Results - MIST - wavelength: 3700-6200

S/N	6.8	6.9	7.0	7.1	7.2	7.3	7.4	7.5	7.6	7.7
10.0	-0.4±0.27	-0.3±0.2	-0.4±0.22	-0.2±0.27	-0.4±0.29	-0.3±0.29	-0.4±0.25	-0.3±0.26	-0.4±0.24	-0.4±0.35
20.0	-0.4±0.13	-0.4±0.19	-0.4±0.22	-0.4±0.2	-0.4±0.23	-0.4±0.27	-0.4±0.1	-0.4±0.16	-0.4±0.16	-0.4±0.14
30.0	-0.4±0.08	-0.4±0.16	-0.4±0.14	-0.4±0.11	-0.4±0.17	-0.4±0.23	-0.4±0.09	-0.4±0.09	-0.4±0.07	-0.4±0.1
40.0	-0.4±0.0	-0.4±0.19	-0.4±0.15	-0.4±0.08	-0.4±0.04	-0.4±0.18	-0.4±0.09	-0.4±0.1	-0.4±0.07	-0.4±0.08
50.0	-0.4±0.04	-0.4±0.07	-0.4±0.13	-0.4±0.17	-0.4±0.05	-0.4±0.08	-0.4±0.04	-0.4±0.06	-0.4±0.05	-0.4±0.08
60.0	-0.4±0.05	-0.4±0.12	-0.4±0.09	-0.4±0.11	-0.4±0.0	-0.4±0.09	-0.4±0.04	-0.4±0.08	-0.4±0.06	-0.4±0.06
70.0	-0.4±0.0	-0.4±0.12	-0.4±0.1	-0.4±0.08	-0.4±0.0	-0.4±0.08	-0.4±0.06	-0.4±0.06	-0.4±0.05	-0.4±0.05
80.0	-0.4±0.0	-0.4±0.14	-0.4±0.07	-0.4±0.12	-0.4±0.0	-0.4±0.08	-0.4±0.0	-0.4±0.0	-0.4±0.04	-0.4±0.08
90.0	-0.4±0.0	-0.4±0.0	-0.4±0.06	-0.4±0.08	-0.4±0.0	-0.4±0.08	-0.4±0.0	-0.4±0.04	-0.4±0.0	-0.4±0.08
100.0	-0.4±0.0	-0.4±0.0	-0.4±0.04	-0.4±0.0	-0.4±0.0	-0.4±0.08	-0.4±0.0	-0.4±0.0	-0.4±0.0	-0.4±0.04
S/N	7.8	7.9	8.0	8.1	8.2	8.3	8.4	8.5	8.6	8.7
10.0	-0.4±0.26	-0.4±0.43	-0.4±0.41	-0.4±0.4	-0.4±0.39	-0.6±0.46	-0.7±0.4	-0.4±0.41	-0.3±0.34	-0.3±0.29
20.0	-0.4±0.12	-0.4±0.16	-0.4±0.19	-0.4±0.21	-0.4±0.21	-0.4±0.24	-0.4±0.25	-0.4±0.36	-0.4±0.25	-0.4±0.25
30.0	-0.4±0.15	-0.4±0.09	-0.4±0.13	-0.4±0.12	-0.4±0.15	-0.4±0.19	-0.4±0.16	-0.4±0.33	-0.4±0.28	-0.4±0.21
40.0	-0.4±0.08	-0.4±0.04	-0.4±0.13	-0.4±0.12	-0.4±0.13	-0.4±0.12	-0.4±0.16	-0.4±0.28	-0.4±0.2	-0.4±0.13
50.0	-0.4±0.09	-0.4±0.0	-0.4±0.09	-0.4±0.09	-0.4±0.14	-0.4±0.08	-0.4±0.15	-0.4±0.21	-0.4±0.17	-0.4±0.12
60.0	-0.4±0.09	-0.4±0.0	-0.4±0.09	-0.4±0.08	-0.4±0.08	-0.4±0.08	-0.4±0.08	-0.4±0.17	-0.4±0.12	-0.4±0.09
70.0	-0.4±0.08	-0.4±0.04	-0.4±0.07	-0.4±0.04	-0.4±0.11	-0.4±0.06	-0.4±0.09	-0.4±0.15	-0.4±0.1	-0.4±0.09
80.0	-0.4±0.04	-0.4±0.0	-0.4±0.06	-0.4±0.05	-0.4±0.04	-0.4±0.06	-0.4±0.07	-0.4±0.13	-0.4±0.09	-0.4±0.1
90.0	-0.4±0.05	-0.4±0.0	-0.4±0.08	-0.4±0.04	-0.4±0.05	-0.4±0.0	-0.4±0.05	-0.4±0.13	-0.4±0.11	-0.4±0.07
100.0	-0.4±0.04	-0.4±0.0	-0.4±0.06	-0.4±0.0	-0.4±0.05	-0.4±0.0	-0.4±0.0	-0.4±0.11	-0.4±0.1	-0.4±0.08
S/N	8.8	8.9	9.0	9.1	9.2	9.3	9.4	9.5	9.6	9.7
10.0	-0.3±0.37	-0.4±0.29	-0.2±0.28	-0.2±0.32	-0.4±0.4	-0.3±0.29	-0.4±0.36	-0.6±0.34	-0.6±0.26	-0.4±0.31
20.0	-0.4±0.25	-0.2±0.2	-0.4±0.28	-0.4±0.25	-0.4±0.26	-0.6±0.22	-0.5±0.16	-0.4±0.21	-0.5±0.21	-0.4±0.16
30.0	-0.4±0.15	-0.3±0.18	-0.4±0.26	-0.4±0.17	-0.4±0.27	-0.4±0.23	-0.4±0.14	-0.4±0.14	-0.4±0.11	-0.4±0.17
40.0	-0.4±0.19	-0.4±0.16	-0.4±0.21	-0.4±0.17	-0.4±0.21	-0.4±0.19	-0.4±0.14	-0.4±0.1	-0.4±0.13	-0.4±0.13
50.0	-0.4±0.16	-0.4±0.11	-0.4±0.13	-0.4±0.09	-0.6±0.2	-0.6±0.15	-0.4±0.12	-0.4±0.12	-0.4±0.14	-0.4±0.12
60.0	-0.4±0.17	-0.4±0.16	-0.4±0.12	-0.4±0.09	-0.4±0.16	-0.5±0.17	-0.4±0.12	-0.4±0.11	-0.4±0.15	-0.4±0.14
70.0	-0.4±0.19	-0.4±0.17	-0.4±0.11	-0.4±0.07	-0.4±0.16	-0.4±0.14	-0.4±0.13	-0.4±0.14	-0.4±0.12	-0.2±0.14
80.0	-0.4±0.1	-0.4±0.14	-0.4±0.11	-0.4±0.07	-0.4±0.16	-0.4±0.11	-0.4±0.12	-0.4±0.12	-0.4±0.14	-0.3±0.11
90.0	-0.4±0.12	-0.4±0.1	-0.4±0.05	-0.4±0.05	-0.4±0.16	-0.4±0.14	-0.4±0.12	-0.4±0.13	-0.4±0.11	-0.4±0.13
100.0	-0.4±0.08	-0.4±0.07	-0.4±0.07	-0.4±0.05	-0.4±0.12	-0.4±0.13	-0.4±0.12	-0.4±0.13	-0.4±0.1	-0.4±0.1
S/N	9.8	9.9	10.0	10.1	10.2					
10.0	-0.4±0.23	-0.4±0.27	-0.4±0.3	-0.4±0.28	-0.2±0.35					
20.0	-0.4±0.15	-0.4±0.19	-0.4±0.21	-0.2±0.19	-0.2±0.21					
30.0	-0.4±0.15	-0.4±0.17	-0.4±0.13	-0.2±0.11	-0.4±0.13					
40.0	-0.4±0.15	-0.4±0.17	-0.4±0.12	-0.4±0.11	-0.4±0.09					
50.0	-0.4±0.14	-0.4±0.15	-0.4±0.14	-0.4±0.1	-0.4±0.09					
60.0	-0.4±0.14	-0.2±0.14	-0.4±0.13	-0.4±0.08	-0.4±0.09					
70.0	-0.4±0.16	-0.4±0.15	-0.4±0.12	-0.4±0.06	-0.4±0.09					
80.0	-0.4±0.13	-0.4±0.13	-0.4±0.1	-0.4±0.08	-0.4±0.08					
90.0	-0.3±0.11	-0.4±0.12	-0.4±0.1	-0.4±0.07	-0.4±0.05					
100.0	-0.4±0.08	-0.4±0.12	-0.4±0.1	-0.4±0.07	-0.4±0.09					

**Table 17.** Metallicity Results - MIST - wavelength: 3700-5000

S/N	6.8	6.9	7.0	7.1	7.2	7.3	7.4	7.5	7.6	7.7
10.0	-0.2±0.22	-0.4±0.18	-0.4±0.43	-0.2±0.17	-0.2±0.16	-0.2±0.17	-0.2±0.17	-0.2±0.15	-0.2±0.16	-0.2±0.36
20.0	-0.4±0.17	-0.4±0.13	-0.4±0.34	-0.4±0.11	-0.4±0.12	-0.3±0.16	-0.4±0.14	-0.2±0.14	-0.3±0.1	-0.4±0.16
30.0	-0.4±0.11	-0.4±0.11	-0.4±0.22	-0.4±0.11	-0.4±0.1	-0.4±0.1	-0.4±0.1	-0.4±0.11	-0.4±0.1	-0.4±0.15
40.0	-0.4±0.09	-0.4±0.13	-0.4±0.09	-0.4±0.07	-0.4±0.08	-0.4±0.1	-0.4±0.09	-0.4±0.11	-0.4±0.11	-0.4±0.1
50.0	-0.4±0.09	-0.4±0.1	-0.4±0.1	-0.4±0.06	-0.4±0.0	-0.4±0.11	-0.4±0.1	-0.4±0.1	-0.4±0.08	-0.4±0.04
60.0	-0.4±0.08	-0.4±0.12	-0.4±0.06	-0.4±0.09	-0.4±0.0	-0.4±0.08	-0.4±0.04	-0.4±0.07	-0.4±0.07	-0.4±0.04
70.0	-0.4±0.06	-0.4±0.04	-0.4±0.09	-0.4±0.0	-0.4±0.0	-0.4±0.09	-0.4±0.06	-0.4±0.09	-0.4±0.07	-0.4±0.04
80.0	-0.4±0.08	-0.4±0.0	-0.4±0.04	-0.4±0.08	-0.4±0.0	-0.4±0.09	-0.4±0.0	-0.4±0.07	-0.4±0.05	-0.4±0.04
90.0	-0.4±0.04	-0.4±0.0	-0.4±0.0	-0.4±0.04	-0.4±0.0	-0.4±0.09	-0.4±0.0	-0.4±0.06	-0.4±0.04	-0.4±0.0
100.0	-0.4±0.0	-0.4±0.0	-0.4±0.0	-0.4±0.0	-0.4±0.0	-0.4±0.1	-0.4±0.0	-0.4±0.07	-0.4±0.04	-0.4±0.0
S/N	7.8	7.9	8.0	8.1	8.2	8.3	8.4	8.5	8.6	8.7
10.0	-0.4±0.36	0.0±0.29	0.0±0.26	-0.4±0.23	-0.4±0.22	-0.4±0.36	-0.5±0.42	-0.5±0.39	-0.4±0.29	-0.4±0.32
20.0	-0.4±0.26	-0.4±0.31	-0.4±0.19	-0.4±0.17	-0.4±0.22	-0.4±0.21	-0.4±0.34	-0.4±0.36	-0.6±0.25	-0.4±0.23
30.0	-0.4±0.13	-0.4±0.13	-0.4±0.17	-0.4±0.19	-0.4±0.21	-0.4±0.15	-0.4±0.26	-0.4±0.31	-0.4±0.21	-0.4±0.2
40.0	-0.4±0.11	-0.4±0.13	-0.4±0.1	-0.4±0.12	-0.4±0.2	-0.4±0.08	-0.4±0.27	-0.4±0.27	-0.4±0.16	-0.4±0.17
50.0	-0.4±0.0	-0.4±0.06	-0.4±0.12	-0.4±0.14	-0.4±0.16	-0.4±0.08	-0.4±0.17	-0.4±0.21	-0.4±0.15	-0.4±0.12
60.0	-0.4±0.0	-0.4±0.06	-0.4±0.1	-0.4±0.11	-0.4±0.11	-0.4±0.07	-0.4±0.16	-0.4±0.25	-0.4±0.13	-0.4±0.13
70.0	-0.4±0.0	-0.4±0.05	-0.4±0.0	-0.4±0.0	-0.4±0.06	-0.4±0.07	-0.4±0.07	-0.4±0.23	-0.4±0.14	-0.4±0.15
80.0	-0.4±0.0	-0.4±0.0	-0.4±0.0	-0.4±0.0	-0.4±0.0	-0.4±0.06	-0.4±0.1	-0.4±0.21	-0.4±0.12	-0.4±0.07
90.0	-0.4±0.0	-0.4±0.05	-0.4±0.0	-0.4±0.0	-0.4±0.05	-0.4±0.0	-0.4±0.1	-0.4±0.1	-0.4±0.09	-0.4±0.1
100.0	-0.4±0.0	-0.4±0.0	-0.4±0.0	-0.4±0.0	-0.4±0.0	-0.4±0.05	-0.4±0.1	-0.4±0.14	-0.4±0.08	-0.4±0.08
S/N	8.8	8.9	9.0	9.1	9.2	9.3	9.4	9.5	9.6	9.7
10.0	-0.2±0.3	-0.4±0.36	-0.4±0.51	-0.4±0.33	-0.6±0.46	-0.5±0.4	-0.8±0.41	-0.2±0.46	-0.3±0.39	-0.6±0.35
20.0	-0.4±0.3	-0.4±0.34	-0.4±0.35	-0.4±0.32	-0.5±0.4	-0.4±0.31	-0.3±0.35	-0.4±0.34	-0.4±0.33	-0.4±0.33
30.0	-0.4±0.3	-0.4±0.28	-0.4±0.41	-0.4±0.24	-0.6±0.29	-0.4±0.24	-0.4±0.19	-0.4±0.25	-0.4±0.26	-0.4±0.32
40.0	-0.4±0.15	-0.4±0.18	-0.4±0.3	-0.4±0.21	-0.4±0.19	-0.6±0.22	-0.4±0.18	-0.4±0.16	-0.4±0.17	-0.4±0.28
50.0	-0.4±0.13	-0.4±0.15	-0.4±0.24	-0.4±0.24	-0.4±0.18	-0.4±0.19	-0.4±0.19	-0.4±0.23	-0.4±0.15	-0.4±0.24
60.0	-0.4±0.12	-0.4±0.19	-0.4±0.25	-0.4±0.11	-0.4±0.16	-0.4±0.14	-0.4±0.17	-0.4±0.17	-0.4±0.18	-0.4±0.2
70.0	-0.4±0.11	-0.4±0.16	-0.4±0.17	-0.4±0.06	-0.4±0.17	-0.4±0.13	-0.4±0.13	-0.4±0.07	-0.4±0.17	-0.4±0.2
80.0	-0.4±0.1	-0.4±0.13	-0.4±0.13	-0.4±0.12	-0.4±0.11	-0.4±0.1	-0.4±0.13	-0.4±0.08	-0.4±0.12	-0.4±0.15
90.0	-0.4±0.05	-0.4±0.1	-0.4±0.16	-0.4±0.0	-0.4±0.08	-0.4±0.13	-0.4±0.13	-0.4±0.05	-0.4±0.11	-0.4±0.13
100.0	-0.4±0.04	-0.4±0.14	-0.4±0.11	-0.4±0.0	-0.4±0.09	-0.4±0.13	-0.4±0.11	-0.4±0.05	-0.4±0.08	-0.4±0.16
S/N	9.8	9.9	10.0	10.1	10.2					
10.0	-0.2±0.38	-0.4±0.3	-0.2±0.24	0.0±0.23	0.0±0.22					
20.0	-0.4±0.34	-0.4±0.28	-0.2±0.24	-0.2±0.21	-0.2±0.2					
30.0	-0.4±0.28	-0.3±0.26	-0.4±0.19	-0.2±0.19	-0.2±0.18					
40.0	-0.4±0.26	-0.4±0.16	-0.4±0.19	-0.4±0.17	-0.2±0.12					
50.0	-0.4±0.23	-0.4±0.17	-0.4±0.19	-0.4±0.15	-0.4±0.11					
60.0	-0.4±0.16	-0.4±0.15	-0.4±0.18	-0.4±0.1	-0.4±0.1					
70.0	-0.4±0.21	-0.4±0.15	-0.4±0.18	-0.4±0.09	-0.4±0.09					
80.0	-0.4±0.15	-0.4±0.12	-0.4±0.12	-0.4±0.09	-0.4±0.09					
90.0	-0.4±0.16	-0.4±0.13	-0.4±0.17	-0.4±0.11	-0.4±0.07					
100.0	-0.4±0.1	-0.4±0.11	-0.4±0.17	-0.4±0.1	-0.4±0.05					

**Table 18.** Metallicity Results - MIST - wavelength: 5000-6200

S/N	6.8	6.9	7.0	7.1	7.2	7.3	7.4	7.5	7.6	7.7
10.0	-0.4±0.47	0.0±0.4	0.0±0.36	0.0±0.41	0.2±0.26	0.2±0.23	-0.2±0.28	0.2±0.29	-0.2±0.31	-0.2±0.29
20.0	-0.2±0.36	0.2±0.28	-0.3±0.38	0.1±0.24	-0.2±0.22	0.1±0.13	-0.4±0.27	-0.2±0.21	-0.4±0.27	-0.2±0.35
30.0	-0.4±0.35	0.0±0.23	-0.4±0.31	0.0±0.24	-0.2±0.22	0.0±0.28	-0.4±0.27	-0.4±0.21	-0.4±0.22	-0.4±0.18
40.0	-0.4±0.28	0.0±0.28	-0.4±0.29	-0.4±0.28	-0.2±0.21	0.0±0.28	-0.4±0.21	-0.4±0.23	-0.4±0.21	-0.4±0.28
50.0	-0.4±0.23	0.0±0.26	-0.4±0.33	0.0±0.27	-0.4±0.14	0.0±0.24	-0.4±0.22	-0.3±0.13	-0.4±0.2	-0.4±0.16
60.0	-0.6±0.26	-0.4±0.26	-0.5±0.26	0.0±0.26	-0.3±0.16	0.0±0.27	-0.4±0.16	-0.4±0.15	-0.4±0.11	-0.4±0.16
70.0	-0.4±0.25	-0.4±0.28	-0.4±0.22	0.0±0.29	-0.2±0.11	-0.4±0.24	-0.4±0.06	-0.2±0.14	-0.4±0.12	-0.4±0.07
80.0	-0.4±0.29	-0.4±0.33	-0.4±0.24	-0.2±0.3	-0.4±0.14	-0.4±0.23	-0.4±0.04	-0.4±0.1	-0.4±0.06	-0.4±0.1
90.0	-0.4±0.28	-0.4±0.23	-0.4±0.2	-0.2±0.27	-0.4±0.16	-0.4±0.25	-0.4±0.0	-0.4±0.11	-0.4±0.1	-0.4±0.0
100.0	-0.4±0.28	-0.4±0.21	-0.4±0.24	-0.4±0.25	-0.4±0.1	-0.4±0.25	-0.4±0.0	-0.4±0.1	-0.4±0.0	-0.4±0.07
S/N	7.8	7.9	8.0	8.1	8.2	8.3	8.4	8.5	8.6	8.7
10.0	0.0±0.33	0.2±0.36	0.0±0.33	-0.2±0.33	0.1±0.4	0.2±0.36	0.2±0.42	0.2±0.32	0.0±0.37	0.2±0.4
20.0	-0.4±0.33	-0.4±0.3	-0.4±0.39	-0.4±0.36	-0.4±0.34	-0.2±0.39	-0.2±0.38	-0.2±0.34	-0.4±0.31	-0.2±0.37
30.0	-0.4±0.27	-0.4±0.25	-0.5±0.25	-0.4±0.3	-0.4±0.29	-0.4±0.36	-0.4±0.25	-0.2±0.29	-0.4±0.37	-0.4±0.32
40.0	-0.4±0.25	-0.4±0.3	-0.5±0.22	-0.4±0.28	-0.4±0.25	-0.4±0.25	-0.4±0.27	-0.4±0.27	-0.4±0.26	-0.4±0.24
50.0	-0.4±0.19	-0.4±0.19	-0.4±0.3	-0.6±0.18	-0.6±0.24	-0.4±0.18	-0.4±0.27	-0.4±0.19	-0.4±0.26	-0.4±0.22
60.0	-0.4±0.16	-0.4±0.2	-0.4±0.18	-0.5±0.2	-0.5±0.15	-0.4±0.15	-0.4±0.18	-0.4±0.19	-0.4±0.23	-0.4±0.22
70.0	-0.4±0.16	-0.4±0.18	-0.4±0.15	-0.4±0.14	-0.4±0.19	-0.4±0.13	-0.4±0.23	-0.4±0.21	-0.4±0.22	-0.4±0.23
80.0	-0.4±0.09	-0.4±0.09	-0.4±0.13	-0.6±0.19	-0.4±0.18	-0.4±0.14	-0.4±0.2	-0.4±0.16	-0.4±0.16	-0.4±0.19
90.0	-0.4±0.11	-0.4±0.09	-0.4±0.16	-0.4±0.15	-0.4±0.17	-0.6±0.15	-0.4±0.2	-0.4±0.17	-0.4±0.14	-0.4±0.19
100.0	-0.4±0.15	-0.4±0.0	-0.4±0.14	-0.4±0.16	-0.4±0.14	-0.4±0.19	-0.4±0.14	-0.4±0.15	-0.4±0.18	-0.4±0.11
S/N	8.8	8.9	9.0	9.1	9.2	9.3	9.4	9.5	9.6	9.7
10.0	0.2±0.36	-0.2±0.38	-0.2±0.37	-0.4±0.45	-0.7±0.48	-0.2±0.51	-0.4±0.41	-0.6±0.47	-0.5±0.46	0.0±0.53
20.0	-0.2±0.44	-0.3±0.38	-0.4±0.34	-0.5±0.42	-0.4±0.39	-0.6±0.34	-0.4±0.35	-0.4±0.38	-0.4±0.45	-0.4±0.4
30.0	-0.4±0.33	-0.4±0.32	-0.4±0.38	-0.4±0.34	-0.4±0.41	-0.4±0.42	-0.4±0.34	-0.3±0.33	-0.4±0.38	-0.4±0.36
40.0	-0.4±0.33	-0.4±0.25	-0.4±0.26	-0.4±0.36	-0.3±0.36	-0.4±0.27	-0.4±0.26	-0.4±0.24	-0.4±0.17	-0.4±0.26
50.0	-0.4±0.3	-0.4±0.21	-0.4±0.27	-0.4±0.29	-0.4±0.3	-0.4±0.13	-0.4±0.19	-0.4±0.21	-0.4±0.16	-0.4±0.22
60.0	-0.4±0.33	-0.4±0.16	-0.4±0.22	-0.4±0.23	-0.4±0.31	-0.6±0.16	-0.4±0.18	-0.4±0.15	-0.4±0.2	-0.4±0.21
70.0	-0.4±0.3	-0.4±0.17	-0.3±0.25	-0.4±0.22	-0.4±0.21	-0.4±0.15	-0.4±0.13	-0.4±0.17	-0.4±0.19	-0.4±0.24
80.0	-0.4±0.17	-0.4±0.11	-0.4±0.18	-0.4±0.16	-0.4±0.23	-0.6±0.15	-0.4±0.14	-0.4±0.18	-0.4±0.14	-0.4±0.14
90.0	-0.4±0.17	-0.4±0.12	-0.4±0.16	-0.4±0.15	-0.4±0.25	-0.4±0.15	-0.4±0.11	-0.4±0.09	-0.4±0.13	-0.4±0.11
100.0	-0.4±0.19	-0.4±0.12	-0.4±0.18	-0.4±0.15	-0.4±0.2	-0.4±0.12	-0.4±0.14	-0.4±0.12	-0.4±0.13	-0.4±0.15
S/N	9.8	9.9	10.0	10.1	10.2					
10.0	-0.7±0.49	-0.3±0.49	-0.4±0.55	-0.6±0.48	-0.4±0.45					
20.0	-0.7±0.42	-0.4±0.46	-0.4±0.4	-0.3±0.42	-0.2±0.42					
30.0	-0.4±0.43	-0.5±0.33	-0.4±0.38	-0.3±0.35	-0.3±0.28					
40.0	-0.4±0.26	-0.4±0.31	-0.4±0.29	-0.4±0.29	-0.4±0.2					
50.0	-0.4±0.32	-0.4±0.24	-0.4±0.23	-0.4±0.25	-0.4±0.14					
60.0	-0.4±0.23	-0.4±0.19	-0.4±0.18	-0.4±0.13	-0.4±0.18					
70.0	-0.4±0.17	-0.4±0.21	-0.4±0.13	-0.4±0.17	-0.4±0.16					
80.0	-0.4±0.19	-0.4±0.12	-0.4±0.11	-0.4±0.15	-0.4±0.13					
90.0	-0.4±0.24	-0.4±0.11	-0.4±0.1	-0.4±0.11	-0.4±0.12					
100.0	-0.4±0.13	-0.4±0.1	-0.4±0.07	-0.4±0.13	-0.4±0.12					

**Table 19.** Metallicity Results - MIST models Padova clusters - wavelength: 3700-6200

S/N	6.8	6.9	7.0	7.1	7.2	7.3	7.4	7.5	7.6	7.7
10.0	-0.2±0.13	-0.2±0.2	-0.4±0.29	-0.3±0.31	-0.2±0.3	-0.4±0.31	-0.1±0.34	-0.6±0.38	-0.3±0.45	-0.6±0.4
20.0	-0.2±0.1	-0.4±0.11	-0.4±0.26	-0.3±0.25	-0.4±0.12	-0.6±0.35	-0.2±0.26	-0.4±0.31	-0.4±0.37	-0.6±0.37
30.0	-0.4±0.1	-0.4±0.15	-0.6±0.29	-0.4±0.16	-0.4±0.11	-0.6±0.29	-0.2±0.24	-0.4±0.28	-0.4±0.31	-0.6±0.39
40.0	-0.4±0.09	-0.4±0.18	-0.6±0.27	-0.4±0.11	-0.2±0.11	-0.6±0.23	-0.2±0.16	-0.4±0.3	0.0±0.29	0.0±0.39
50.0	-0.4±0.09	-0.4±0.16	-0.6±0.29	-0.4±0.11	-0.2±0.09	-0.6±0.17	-0.2±0.2	-0.4±0.24	-0.4±0.26	0.0±0.37
60.0	-0.4±0.08	-0.4±0.16	-0.6±0.21	-0.2±0.09	-0.2±0.08	-0.6±0.12	-0.2±0.23	-0.4±0.24	0.0±0.33	0.0±0.39
70.0	-0.4±0.08	-0.4±0.15	-0.8±0.14	-0.2±0.08	-0.2±0.06	-0.6±0.1	-0.2±0.23	-0.4±0.27	-0.4±0.33	-0.8±0.39
80.0	-0.4±0.08	-0.4±0.09	-0.6±0.1	-0.2±0.1	-0.2±0.08	-0.6±0.07	-0.2±0.23	-0.4±0.21	-0.4±0.27	-0.8±0.37
90.0	-0.4±0.06	-0.4±0.14	-0.6±0.21	-0.2±0.1	-0.2±0.05	-0.6±0.0	-0.2±0.19	-0.4±0.18	-0.4±0.3	-0.8±0.3
100.0	-0.4±0.05	-0.4±0.12	-0.7±0.1	-0.2±0.09	-0.2±0.05	-0.6±0.0	-0.2±0.24	-0.4±0.13	-0.4±0.28	-0.8±0.41
S/N	7.8	7.9	8.0	8.1	8.2	8.3	8.4	8.5	8.6	8.7
10.0	-0.4±0.42	0.0±0.42	0.0±0.47	0.0±0.53	0.0±0.47	-0.1±0.38	-0.2±0.46	-0.2±0.33	0.0±0.37	0.0±0.36
20.0	-0.6±0.4	0.0±0.35	0.0±0.54	0.0±0.55	0.0±0.31	-0.2±0.29	-0.2±0.31	-0.2±0.27	-0.1±0.24	-0.4±0.27
30.0	0.0±0.42	0.0±0.42	0.0±0.46	0.2±0.41	0.0±0.16	-0.1±0.16	-0.2±0.24	-0.2±0.25	0.0±0.21	-0.2±0.25
40.0	0.0±0.4	0.0±0.43	0.0±0.45	0.2±0.31	0.2±0.1	0.0±0.15	-0.2±0.15	-0.2±0.24	-0.2±0.23	-0.4±0.16
50.0	0.0±0.4	0.0±0.42	0.0±0.41	0.2±0.04	0.2±0.1	-0.2±0.13	-0.2±0.09	-0.2±0.19	0.0±0.19	-0.2±0.15
60.0	0.0±0.4	0.0±0.42	0.0±0.48	0.2±0.04	0.2±0.1	0.0±0.11	-0.2±0.13	-0.2±0.19	-0.2±0.17	-0.4±0.15
70.0	0.0±0.39	0.0±0.44	0.0±0.46	0.2±0.06	0.2±0.1	0.0±0.1	-0.2±0.05	-0.2±0.14	-0.2±0.17	-0.4±0.08
80.0	-0.8±0.4	0.0±0.45	0.0±0.33	0.2±0.04	0.0±0.1	0.0±0.1	-0.2±0.1	-0.2±0.14	-0.1±0.17	-0.4±0.09
90.0	-0.8±0.4	0.0±0.45	0.0±0.35	0.2±0.0	0.1±0.1	0.0±0.1	-0.2±0.05	-0.2±0.12	-0.2±0.15	-0.4±0.09
100.0	-0.8±0.4	0.0±0.38	0.0±0.38	0.2±0.0	0.2±0.1	0.0±0.1	-0.2±0.07	-0.2±0.12	0.0±0.15	-0.4±0.09
S/N	8.8	8.9	9.0	9.1	9.2	9.3	9.4	9.5	9.6	9.7
10.0	-0.2±0.31	-0.2±0.36	-0.4±0.27	-0.3±0.29	-0.2±0.29	-0.4±0.29	-0.4±0.24	-0.4±0.35	-0.5±0.3	-0.4±0.2
20.0	-0.2±0.26	-0.4±0.26	-0.4±0.26	-0.2±0.32	-0.4±0.34	-0.4±0.22	-0.4±0.19	-0.4±0.17	-0.4±0.23	-0.4±0.17
30.0	-0.2±0.22	-0.2±0.22	-0.2±0.24	-0.4±0.33	-0.4±0.23	-0.5±0.2	-0.4±0.14	-0.4±0.14	-0.4±0.13	-0.4±0.13
40.0	-0.4±0.19	-0.2±0.2	-0.4±0.2	-0.4±0.32	-0.4±0.18	-0.4±0.17	-0.4±0.13	-0.3±0.13	-0.4±0.13	-0.2±0.1
50.0	-0.5±0.15	-0.2±0.21	-0.4±0.17	-0.6±0.32	-0.4±0.18	-0.4±0.15	-0.4±0.14	-0.4±0.14	-0.4±0.1	-0.4±0.13
60.0	-0.4±0.13	-0.4±0.16	-0.4±0.17	-0.6±0.27	-0.5±0.19	-0.4±0.13	-0.4±0.14	-0.4±0.13	-0.2±0.14	-0.4±0.14
70.0	-0.6±0.15	-0.4±0.24	-0.4±0.06	-0.6±0.28	-0.4±0.18	-0.4±0.12	-0.4±0.14	-0.4±0.12	-0.4±0.11	-0.4±0.12
80.0	-0.4±0.11	-0.2±0.26	-0.4±0.1	-0.6±0.32	-0.6±0.19	-0.4±0.14	-0.4±0.11	-0.4±0.1	-0.4±0.11	-0.4±0.1
90.0	-0.6±0.14	-0.2±0.24	-0.4±0.08	-0.6±0.21	-0.4±0.13	-0.4±0.15	-0.4±0.11	-0.2±0.11	-0.2±0.11	-0.2±0.13
100.0	-0.4±0.1	-0.4±0.27	-0.4±0.07	-0.6±0.24	-0.4±0.14	-0.6±0.15	-0.4±0.11	-0.4±0.09	-0.3±0.1	-0.4±0.1
S/N	9.8	9.9	10.0	10.1	10.2					
10.0	-0.4±0.26	-0.4±0.35	-0.3±0.34	-0.2±0.24	-0.2±0.27					
20.0	-0.4±0.16	-0.4±0.15	-0.4±0.16	-0.4±0.11	-0.2±0.19					
30.0	-0.4±0.17	-0.4±0.17	-0.4±0.14	-0.2±0.1	-0.4±0.11					
40.0	-0.4±0.15	-0.4±0.14	-0.4±0.11	-0.2±0.1	-0.4±0.1					
50.0	-0.2±0.13	-0.3±0.17	-0.4±0.13	-0.3±0.1	-0.4±0.1					
60.0	-0.4±0.13	-0.2±0.16	-0.4±0.12	-0.4±0.1	-0.3±0.1					
70.0	-0.4±0.13	-0.4±0.14	-0.4±0.12	-0.4±0.09	-0.4±0.1					
80.0	-0.3±0.17	-0.2±0.14	-0.4±0.11	-0.4±0.1	-0.4±0.1					
90.0	-0.4±0.18	-0.4±0.11	-0.4±0.1	-0.2±0.1	-0.4±0.1					
100.0	-0.4±0.14	-0.2±0.1	-0.4±0.12	-0.2±0.1	-0.4±0.09					

**Table 20.** Metallicity Results - MIST models Padova clusters - wavelength: 3700-5000

S/N	6.8	6.9	7.0	7.1	7.2	7.3	7.4	7.5	7.6	7.7
10.0	-0.2±0.15	-0.2±0.21	0.2±0.51	-0.1±0.43	-0.2±0.18	-0.2±0.16	-0.2±0.21	-0.2±0.17	-0.2±0.22	-0.2±0.42
20.0	-0.2±0.13	-0.2±0.12	-0.4±0.37	-0.4±0.35	-0.4±0.22	-0.2±0.17	-0.2±0.18	-0.2±0.21	-0.2±0.24	0.0±0.44
30.0	-0.1±0.14	-0.2±0.1	-0.4±0.29	-0.3±0.34	-0.4±0.23	-0.2±0.18	-0.4±0.15	-0.4±0.27	-0.2±0.24	-0.3±0.41
40.0	-0.2±0.1	-0.2±0.1	-0.4±0.32	-0.2±0.31	-0.5±0.28	-0.2±0.18	-0.2±0.16	-0.2±0.28	-0.1±0.24	0.0±0.4
50.0	-0.2±0.11	-0.2±0.1	-0.4±0.26	-0.2±0.23	-0.6±0.24	-0.4±0.16	-0.4±0.15	0.0±0.27	-0.1±0.26	0.0±0.42
60.0	-0.2±0.07	-0.2±0.12	-0.4±0.24	-0.2±0.21	-0.6±0.26	-0.2±0.17	-0.4±0.13	0.0±0.29	0.0±0.23	0.0±0.39
70.0	-0.2±0.08	-0.2±0.1	-0.4±0.21	-0.2±0.17	-0.2±0.27	-0.2±0.16	-0.4±0.11	0.0±0.29	0.0±0.23	0.0±0.18
80.0	-0.2±0.04	-0.2±0.07	-0.4±0.18	-0.2±0.19	-0.2±0.3	-0.4±0.15	-0.4±0.11	0.0±0.28	0.0±0.15	0.0±0.27
90.0	-0.2±0.08	-0.2±0.08	-0.4±0.15	-0.2±0.2	-0.2±0.3	-0.2±0.16	-0.4±0.08	0.0±0.3	0.0±0.11	0.0±0.11
100.0	-0.2±0.04	-0.2±0.1	-0.4±0.11	-0.2±0.18	-0.6±0.28	-0.2±0.11	-0.4±0.07	0.0±0.23	0.0±0.11	0.0±0.18
S/N	7.8	7.9	8.0	8.1	8.2	8.3	8.4	8.5	8.6	8.7
10.0	-0.6±0.38	-0.6±0.41	0.0±0.19	0.0±0.2	-0.2±0.2	-0.2±0.19	-0.4±0.44	-0.6±0.37	-0.2±0.32	-0.5±0.34
20.0	-0.6±0.38	-0.6±0.42	0.1±0.26	0.0±0.18	0.0±0.19	-0.2±0.17	-0.3±0.37	-0.4±0.26	-0.3±0.26	-0.2±0.21
30.0	-0.6±0.34	0.0±0.43	0.2±0.13	0.0±0.17	-0.2±0.15	-0.2±0.19	-0.4±0.24	-0.4±0.28	-0.2±0.23	-0.4±0.16
40.0	-0.6±0.4	0.0±0.45	0.2±0.11	0.0±0.17	0.0±0.13	-0.4±0.18	-0.4±0.21	-0.4±0.19	-0.2±0.17	-0.4±0.18
50.0	0.0±0.28	0.0±0.3	0.2±0.1	0.0±0.12	-0.2±0.14	-0.2±0.16	-0.4±0.17	-0.4±0.15	-0.2±0.12	-0.4±0.16
60.0	0.0±0.33	0.0±0.35	0.2±0.07	0.1±0.11	0.0±0.14	-0.2±0.12	-0.4±0.12	-0.4±0.18	-0.2±0.12	-0.4±0.12
70.0	0.0±0.26	0.0±0.32	0.2±0.1	0.0±0.1	-0.2±0.11	-0.2±0.12	-0.4±0.14	-0.4±0.14	-0.2±0.05	-0.4±0.12
80.0	-0.6±0.32	0.0±0.18	0.2±0.08	0.0±0.11	0.0±0.1	-0.2±0.09	-0.4±0.12	-0.4±0.11	-0.2±0.13	-0.4±0.12
90.0	0.0±0.23	0.0±0.43	0.2±0.0	0.0±0.09	0.0±0.1	-0.2±0.1	-0.4±0.12	-0.4±0.14	-0.2±0.05	-0.4±0.1
100.0	0.0±0.28	0.0±0.0	0.2±0.08	0.0±0.1	-0.2±0.1	-0.2±0.08	-0.4±0.09	-0.4±0.12	-0.2±0.06	-0.4±0.12
S/N	8.8	8.9	9.0	9.1	9.2	9.3	9.4	9.5	9.6	9.7
10.0	-0.4±0.36	-0.4±0.46	-0.8±0.53	-0.4±0.47	-0.4±0.48	-0.4±0.41	-0.4±0.38	-0.2±0.36	-0.6±0.39	-0.6±0.36
20.0	-0.3±0.21	-0.4±0.42	-0.4±0.4	-0.4±0.36	-0.6±0.37	-0.6±0.28	-0.4±0.41	-0.4±0.38	-0.4±0.32	-0.6±0.28
30.0	-0.4±0.24	-0.3±0.3	-0.4±0.38	-0.2±0.37	-0.5±0.33	-0.4±0.23	-0.4±0.32	-0.4±0.24	-0.5±0.31	-0.4±0.26
40.0	-0.4±0.21	-0.4±0.19	-0.4±0.25	-0.5±0.35	-0.4±0.35	-0.4±0.2	-0.4±0.28	-0.4±0.2	-0.3±0.28	-0.4±0.22
50.0	-0.4±0.19	-0.3±0.19	-0.4±0.3	-0.5±0.34	-0.5±0.24	-0.5±0.17	-0.4±0.21	-0.4±0.18	-0.4±0.19	-0.4±0.27
60.0	-0.4±0.16	-0.2±0.15	-0.4±0.24	-0.6±0.29	-0.4±0.18	-0.4±0.15	-0.4±0.21	-0.3±0.13	-0.4±0.17	-0.4±0.19
70.0	-0.4±0.16	-0.4±0.14	-0.4±0.17	-0.6±0.25	-0.4±0.11	-0.4±0.14	-0.4±0.12	-0.4±0.15	-0.4±0.18	-0.4±0.18
80.0	-0.4±0.15	-0.4±0.15	-0.4±0.3	-0.6±0.27	-0.6±0.13	-0.4±0.14	-0.4±0.05	-0.4±0.1	-0.4±0.15	-0.4±0.15
90.0	-0.3±0.15	-0.4±0.1	-0.4±0.14	-0.6±0.3	-0.4±0.09	-0.4±0.13	-0.4±0.12	-0.4±0.12	-0.4±0.11	-0.4±0.15
100.0	-0.4±0.16	-0.4±0.13	-0.4±0.11	-0.6±0.16	-0.4±0.09	-0.4±0.11	-0.4±0.12	-0.4±0.1	-0.4±0.13	-0.4±0.13
S/N	9.8	9.9	10.0	10.1	10.2					
10.0	-0.4±0.37	-0.2±0.33	-0.2±0.3	-0.2±0.28	0.0±0.21					
20.0	-0.6±0.38	-0.4±0.27	-0.4±0.26	-0.2±0.29	-0.3±0.22					
30.0	-0.3±0.35	-0.2±0.21	-0.2±0.25	-0.4±0.24	-0.2±0.21					
40.0	-0.4±0.28	-0.4±0.19	-0.4±0.17	-0.4±0.21	-0.2±0.18					
50.0	-0.3±0.27	-0.4±0.15	-0.3±0.15	-0.2±0.18	-0.2±0.1					
60.0	-0.4±0.16	-0.4±0.14	-0.4±0.14	-0.2±0.19	-0.2±0.1					
70.0	-0.2±0.18	-0.4±0.12	-0.4±0.13	-0.2±0.17	-0.2±0.13					
80.0	-0.4±0.19	-0.4±0.14	-0.3±0.13	-0.2±0.18	-0.2±0.13					
90.0	-0.2±0.12	-0.4±0.11	-0.2±0.1	-0.2±0.15	-0.2±0.1					
100.0	-0.3±0.13	-0.4±0.1	-0.2±0.11	-0.4±0.17	-0.2±0.08					

**Table 21.** Metallicity Results - MIST models Padova clusters - wavelength: 5000-6200

S/N	6.8	6.9	7.0	7.1	7.2	7.3	7.4	7.5	7.6	7.7
10.0	0.2±0.14	0.0±0.49	0.2±0.16	0.0±0.34	0.0±0.36	0.2±0.21	0.2±0.24	0.2±0.19	0.2±0.13	0.1±0.26
20.0	0.0±0.38	0.0±0.48	0.0±0.22	0.0±0.29	0.0±0.21	0.0±0.22	0.0±0.12	0.1±0.2	0.1±0.16	0.0±0.23
30.0	0.0±0.42	-0.8±0.49	0.0±0.3	0.0±0.23	0.0±0.25	0.0±0.19	0.0±0.15	0.0±0.16	0.0±0.13	0.0±0.25
40.0	0.0±0.4	-0.8±0.37	0.0±0.34	-0.2±0.23	0.0±0.21	0.0±0.21	0.0±0.23	0.0±0.14	0.0±0.13	0.0±0.29
50.0	0.0±0.46	-0.8±0.35	0.0±0.32	0.0±0.25	-0.2±0.23	-0.2±0.19	0.0±0.23	0.0±0.12	0.0±0.14	0.0±0.23
60.0	0.0±0.46	-0.8±0.24	-0.4±0.33	0.0±0.22	-0.2±0.22	-0.2±0.18	0.0±0.29	0.1±0.11	0.0±0.21	0.0±0.31
70.0	0.0±0.47	-0.8±0.11	0.0±0.31	-0.2±0.26	-0.2±0.21	-0.2±0.19	0.0±0.26	0.0±0.14	0.0±0.2	0.0±0.27
80.0	0.0±0.48	-0.8±0.35	-0.4±0.28	-0.2±0.2	-0.2±0.21	-0.2±0.2	0.0±0.27	0.0±0.1	0.0±0.15	0.0±0.25
90.0	0.0±0.47	-0.8±0.19	-0.4±0.29	-0.3±0.23	-0.2±0.23	-0.2±0.12	0.0±0.22	0.0±0.12	0.0±0.21	0.0±0.26
100.0	0.0±0.49	-0.8±0.12	-0.4±0.32	-0.2±0.23	-0.2±0.21	-0.2±0.14	-0.4±0.28	0.2±0.1	0.0±0.22	0.0±0.27
S/N	7.8	7.9	8.0	8.1	8.2	8.3	8.4	8.5	8.6	8.7
10.0	0.2±0.33	0.0±0.39	0.2±0.33	0.0±0.37	0.2±0.28	0.2±0.38	0.2±0.35	0.0±0.32	0.2±0.34	0.2±0.45
20.0	0.0±0.23	0.0±0.35	0.2±0.36	0.2±0.38	0.1±0.37	-0.2±0.36	-0.2±0.37	-0.2±0.32	-0.2±0.35	-0.2±0.39
30.0	0.0±0.28	-0.1±0.38	0.0±0.4	0.0±0.42	-0.2±0.43	-0.2±0.34	-0.2±0.33	-0.2±0.33	-0.2±0.36	-0.2±0.38
40.0	0.0±0.27	0.0±0.29	0.0±0.42	-0.5±0.47	0.0±0.45	-0.2±0.38	-0.5±0.38	-0.2±0.35	-0.2±0.33	-0.4±0.28
50.0	0.0±0.26	0.0±0.38	0.0±0.4	0.0±0.45	0.0±0.46	-0.2±0.32	-0.6±0.29	-0.3±0.27	-0.2±0.28	-0.4±0.29
60.0	0.0±0.28	-0.4±0.36	0.0±0.44	-0.4±0.5	-0.5±0.51	-0.2±0.39	-0.4±0.28	-0.4±0.27	-0.2±0.25	-0.4±0.24
70.0	0.0±0.27	0.0±0.35	-0.7±0.38	-0.8±0.48	0.0±0.48	-0.2±0.38	-0.3±0.27	-0.3±0.2	-0.2±0.22	-0.4±0.17
80.0	0.0±0.3	0.0±0.34	-0.6±0.43	-0.8±0.46	0.0±0.47	-0.1±0.39	-0.6±0.28	-0.4±0.21	-0.2±0.25	-0.4±0.17
90.0	0.0±0.27	0.0±0.33	-0.8±0.35	-0.8±0.47	0.0±0.47	-0.2±0.42	-0.6±0.21	-0.2±0.29	-0.2±0.22	-0.4±0.19
100.0	0.0±0.31	-0.5±0.35	-0.8±0.33	-0.8±0.45	0.0±0.48	-0.2±0.37	-0.5±0.27	-0.2±0.19	-0.2±0.24	-0.4±0.18
S/N	8.8	8.9	9.0	9.1	9.2	9.3	9.4	9.5	9.6	9.7
10.0	-0.2±0.46	-0.2±0.41	-0.2±0.38	-0.5±0.44	-0.3±0.44	-0.1±0.38	-0.2±0.44	0.1±0.37	-0.3±0.52	-0.4±0.49
20.0	-0.3±0.5	-0.4±0.34	-0.4±0.38	-0.6±0.34	-0.6±0.43	-0.2±0.4	-0.6±0.37	-0.4±0.39	-0.4±0.46	-0.4±0.4
30.0	-0.3±0.47	-0.2±0.31	-0.4±0.35	-0.6±0.33	-0.4±0.28	-0.5±0.35	-0.4±0.32	-0.4±0.33	-0.4±0.27	-0.4±0.34
40.0	-0.6±0.35	-0.4±0.25	-0.4±0.24	-0.6±0.33	-0.4±0.35	-0.4±0.26	-0.4±0.28	-0.3±0.21	-0.4±0.29	-0.4±0.26
50.0	-0.2±0.33	-0.3±0.21	-0.4±0.26	-0.6±0.25	-0.3±0.36	-0.4±0.24	-0.4±0.21	-0.4±0.24	-0.4±0.23	-0.4±0.33
60.0	-0.4±0.27	-0.4±0.15	-0.4±0.28	-0.6±0.2	-0.4±0.25	-0.4±0.14	-0.4±0.21	-0.4±0.18	-0.4±0.24	-0.4±0.25
70.0	-0.4±0.22	-0.4±0.11	-0.4±0.18	-0.6±0.18	-0.4±0.22	-0.4±0.12	-0.4±0.14	-0.4±0.16	-0.4±0.14	-0.4±0.23
80.0	-0.4±0.23	-0.2±0.18	-0.5±0.19	-0.6±0.2	-0.4±0.24	-0.4±0.12	-0.4±0.15	-0.4±0.13	-0.4±0.21	-0.4±0.1
90.0	-0.4±0.24	-0.2±0.1	-0.4±0.17	-0.6±0.11	-0.4±0.18	-0.4±0.09	-0.4±0.14	-0.4±0.14	-0.4±0.24	-0.4±0.12
100.0	-0.4±0.22	-0.4±0.11	-0.4±0.17	-0.6±0.13	-0.4±0.15	-0.4±0.11	-0.4±0.11	-0.4±0.13	-0.4±0.16	-0.4±0.1
S/N	9.8	9.9	10.0	10.1	10.2					
10.0	-0.6±0.49	-0.1±0.47	-0.4±0.47	-0.1±0.47	-0.2±0.48					
20.0	-0.4±0.47	-0.5±0.41	-0.4±0.44	-0.2±0.47	-0.4±0.37					
30.0	-0.4±0.43	-0.4±0.36	-0.4±0.41	-0.4±0.35	-0.2±0.38					
40.0	-0.6±0.38	-0.4±0.28	-0.4±0.33	-0.4±0.23	-0.4±0.24					
50.0	-0.4±0.23	-0.4±0.21	-0.4±0.21	-0.4±0.26	-0.4±0.28					
60.0	-0.4±0.26	-0.4±0.17	-0.4±0.15	-0.4±0.2	-0.4±0.22					
70.0	-0.4±0.19	-0.4±0.17	-0.4±0.14	-0.4±0.13	-0.4±0.18					
80.0	-0.4±0.16	-0.4±0.11	-0.4±0.13	-0.4±0.17	-0.4±0.17					
90.0	-0.4±0.16	-0.4±0.12	-0.4±0.1	-0.4±0.13	-0.4±0.1					
100.0	-0.4±0.11	-0.4±0.1	-0.4±0.1	-0.4±0.13	-0.4±0.09					

**Table 22.** Metallicity Results - Padova models MIST clusters - wavelength: 3700-6200

S/N	6.8	6.9	7.0	7.1	7.2	7.3	7.4	7.5	7.6	7.7
10.0	-0.4±0.39	-0.2±0.37	-0.6±0.21	-0.6±0.39	-0.2±0.28	-0.2±0.13	0.0±0.24	-0.2±0.35	-0.9±0.46	-1.0±0.37
20.0	-0.3±0.4	-0.6±0.41	-0.6±0.24	-1.0±0.36	-0.2±0.31	-0.2±0.11	0.0±0.1	-0.8±0.41	-0.8±0.36	-0.8±0.46
30.0	-1.0±0.38	-0.4±0.29	-0.4±0.18	-0.6±0.37	-0.6±0.29	-0.2±0.11	0.0±0.08	-1.0±0.36	-1.0±0.3	-1.0±0.25
40.0	-1.0±0.36	-0.4±0.2	-0.6±0.21	-0.6±0.23	-0.6±0.25	-0.2±0.11	0.0±0.05	-1.0±0.37	-1.0±0.29	-0.8±0.33
50.0	-1.0±0.3	-0.4±0.14	-0.6±0.23	-1.0±0.27	-0.6±0.21	-0.2±0.11	0.0±0.0	-1.0±0.2	-1.0±0.19	-0.8±0.19
60.0	-1.0±0.38	-0.4±0.06	-0.6±0.19	-1.0±0.2	-0.6±0.19	-0.2±0.04	0.0±0.0	-1.0±0.28	-1.0±0.05	-1.0±0.19
70.0	-1.0±0.24	-0.4±0.08	-0.6±0.22	-0.8±0.2	-0.6±0.19	-0.2±0.06	0.0±0.0	-1.0±0.24	-1.0±0.06	-1.0±0.1
80.0	-1.0±0.15	-0.4±0.09	-0.6±0.13	-1.0±0.19	-0.6±0.14	-0.2±0.06	0.0±0.0	-1.0±0.0	-1.0±0.0	-0.8±0.1
90.0	-1.0±0.0	-0.4±0.04	-0.6±0.15	-1.0±0.2	-0.6±0.14	-0.2±0.08	0.0±0.0	-1.0±0.0	-1.0±0.0	-0.8±0.09
100.0	-1.0±0.15	-0.4±0.04	-0.6±0.09	-1.0±0.2	-0.6±0.12	-0.2±0.06	0.0±0.0	-1.0±0.0	-1.0±0.0	-0.8±0.1
S/N	7.8	7.9	8.0	8.1	8.2	8.3	8.4	8.5	8.6	8.7
10.0	-0.8±0.45	-1.0±0.12	-1.0±0.19	-1.0±0.27	-0.9±0.27	-0.5±0.32	-0.6±0.24	-0.6±0.37	-0.2±0.2	-0.2±0.25
20.0	-1.0±0.19	-1.0±0.08	-1.0±0.1	-1.0±0.2	-1.0±0.17	-1.0±0.19	-0.6±0.34	-0.6±0.29	-0.4±0.21	-0.4±0.23
30.0	-1.0±0.25	-1.0±0.05	-1.0±0.09	-1.0±0.1	-1.0±0.16	-0.8±0.24	-0.8±0.29	-0.6±0.23	-0.4±0.2	-0.4±0.22
40.0	-1.0±0.19	-1.0±0.0	-1.0±0.07	-1.0±0.17	-1.0±0.16	-1.0±0.14	-0.8±0.22	-0.6±0.2	-0.4±0.19	-0.4±0.2
50.0	-1.0±0.09	-1.0±0.0	-1.0±0.0	-1.0±0.07	-1.0±0.07	-1.0±0.1	-0.6±0.23	-0.6±0.13	-0.4±0.12	-0.5±0.21
60.0	-1.0±0.08	-1.0±0.0	-1.0±0.04	-1.0±0.08	-0.8±0.1	-1.0±0.1	-0.6±0.2	-0.6±0.17	-0.4±0.21	-0.5±0.2
70.0	-1.0±0.1	-1.0±0.0	-1.0±0.0	-0.8±0.1	-1.0±0.1	-1.0±0.1	-0.7±0.21	-0.6±0.09	-0.4±0.24	-0.4±0.13
80.0	-1.0±0.1	-1.0±0.0	-1.0±0.0	-1.0±0.08	-1.0±0.1	-1.0±0.1	-0.6±0.18	-0.6±0.11	-0.4±0.17	-0.6±0.11
90.0	-1.0±0.1	-1.0±0.0	-1.0±0.0	-1.0±0.09	-0.8±0.1	-0.8±0.1	-0.6±0.19	-0.6±0.11	-0.4±0.2	-0.6±0.17
100.0	-1.0±0.1	-1.0±0.0	-1.0±0.0	-1.0±0.1	-0.8±0.1	-0.8±0.1	-0.8±0.19	-0.6±0.09	-0.4±0.21	-0.6±0.1
S/N	8.8	8.9	9.0	9.1	9.2	9.3	9.4	9.5	9.6	9.7
10.0	-0.2±0.33	-0.3±0.27	-0.6±0.24	-0.2±0.21	-0.2±0.25	-0.2±0.24	-0.4±0.32	-0.4±0.34	-0.4±0.28	-0.4±0.35
20.0	-0.2±0.26	-0.4±0.21	-0.4±0.2	-0.4±0.2	-0.4±0.2	-0.6±0.21	-0.5±0.22	-0.4±0.2	-0.6±0.21	-0.4±0.19
30.0	-0.2±0.19	-0.4±0.22	-0.4±0.22	-0.4±0.16	-0.4±0.26	-0.2±0.19	-0.5±0.18	-0.4±0.13	-0.4±0.13	-0.6±0.12
40.0	-0.3±0.21	-0.2±0.18	-0.4±0.17	-0.4±0.13	-0.4±0.19	-0.4±0.24	-0.4±0.2	-0.4±0.15	-0.5±0.13	-0.5±0.11
50.0	-0.2±0.24	-0.3±0.15	-0.4±0.1	-0.4±0.17	-0.4±0.19	-0.4±0.25	-0.6±0.17	-0.4±0.12	-0.4±0.11	-0.4±0.1
60.0	-0.2±0.22	-0.2±0.1	-0.4±0.13	-0.4±0.19	-0.4±0.2	-0.5±0.23	-0.6±0.19	-0.4±0.11	-0.4±0.1	-0.4±0.1
70.0	-0.2±0.21	-0.2±0.16	-0.4±0.09	-0.4±0.19	-0.4±0.15	-0.4±0.22	-0.2±0.19	-0.4±0.12	-0.4±0.12	-0.4±0.1
80.0	-0.2±0.13	-0.2±0.09	-0.4±0.13	-0.4±0.2	-0.4±0.17	-0.4±0.26	-0.2±0.2	-0.4±0.13	-0.4±0.11	-0.4±0.13
90.0	-0.2±0.07	-0.2±0.14	-0.4±0.04	-0.4±0.21	-0.4±0.17	-0.4±0.25	-0.2±0.19	-0.4±0.09	-0.6±0.14	-0.4±0.1
100.0	-0.2±0.11	-0.2±0.1	-0.4±0.04	-0.3±0.16	-0.4±0.15	-0.4±0.2	-0.3±0.2	-0.4±0.08	-0.6±0.14	-0.4±0.1
S/N	9.8	9.9	10.0	10.1	10.2					
10.0	-0.6±0.27	-0.4±0.27	-0.2±0.27	-0.2±0.21	-0.2±0.31					
20.0	-0.6±0.19	-0.4±0.22	-0.4±0.21	-0.2±0.17	-0.2±0.18					
30.0	-0.6±0.18	-0.4±0.16	-0.4±0.11	-0.2±0.15	-0.2±0.09					
40.0	-0.4±0.14	-0.5±0.16	-0.4±0.14	-0.2±0.14	-0.2±0.09					
50.0	-0.4±0.15	-0.4±0.14	-0.4±0.1	-0.2±0.17	-0.2±0.09					
60.0	-0.4±0.15	-0.4±0.16	-0.4±0.07	-0.4±0.16	-0.2±0.07					
70.0	-0.4±0.1	-0.4±0.13	-0.4±0.14	-0.4±0.15	-0.2±0.08					
80.0	-0.4±0.09	-0.4±0.16	-0.4±0.13	-0.4±0.15	-0.2±0.11					
90.0	-0.4±0.1	-0.4±0.12	-0.4±0.13	-0.4±0.16	-0.2±0.08					
100.0	-0.4±0.05	-0.4±0.13	-0.4±0.13	-0.4±0.15	-0.2±0.06					

**Table 23.** Metallicity Results - Padova models MIST clusters - wavelength: 3700-5000

S/N	6.8	6.9	7.0	7.1	7.2	7.3	7.4	7.5	7.6	7.7
10.0	-0.4±0.37	-0.2±0.39	-0.4±0.28	-0.4±0.5	-0.2±0.2	-0.2±0.2	-0.2±0.15	-0.2±0.22	-0.2±0.21	-0.1±0.34
20.0	-0.2±0.46	0.0±0.47	-0.4±0.2	-0.6±0.3	-0.2±0.17	-0.2±0.17	-0.2±0.18	-0.2±0.14	-0.2±0.15	-0.2±0.19
30.0	-0.3±0.44	-0.4±0.49	-0.4±0.09	-0.6±0.33	-0.4±0.19	-0.2±0.15	-0.2±0.19	-0.2±0.08	-0.2±0.0	-0.2±0.08
40.0	0.2±0.35	-0.3±0.48	-0.4±0.1	-0.6±0.36	-0.2±0.19	-0.2±0.0	-0.2±0.19	-0.2±0.07	-0.2±0.07	-0.2±0.06
50.0	0.2±0.35	0.0±0.52	-0.4±0.1	-0.6±0.35	-0.2±0.2	-0.2±0.07	-0.2±0.2	-0.2±0.0	-0.2±0.0	-0.2±0.1
60.0	0.2±0.28	-0.2±0.49	-0.4±0.09	-0.6±0.35	-0.2±0.2	-0.2±0.0	-0.2±0.18	-0.2±0.0	-0.2±0.0	-0.2±0.06
70.0	0.2±0.36	-0.2±0.5	-0.4±0.07	-0.6±0.31	-0.6±0.2	-0.2±0.0	-0.2±0.2	-0.2±0.0	-0.2±0.0	-0.2±0.08
80.0	0.2±0.36	0.0±0.51	-0.4±0.05	-0.6±0.39	-0.6±0.19	-0.2±0.0	-0.2±0.19	-0.2±0.0	-0.2±0.0	-0.2±0.05
90.0	0.2±0.25	0.0±0.51	-0.4±0.04	-0.6±0.34	-0.6±0.16	-0.2±0.0	-0.2±0.2	-0.2±0.0	-0.2±0.0	-0.2±0.09
100.0	0.2±0.15	-0.5±0.51	-0.4±0.05	-0.6±0.31	-0.6±0.16	-0.2±0.0	-0.2±0.16	-0.2±0.0	-0.2±0.0	-0.2±0.07
S/N	7.8	7.9	8.0	8.1	8.2	8.3	8.4	8.5	8.6	8.7
10.0	0.0±0.5	0.0±0.49	-0.2±0.35	-0.4±0.36	-0.4±0.46	-0.6±0.44	-1.0±0.46	-0.7±0.32	-0.4±0.29	-0.4±0.34
20.0	-1.0±0.48	-0.9±0.38	-0.6±0.27	-0.4±0.21	-0.4±0.35	-0.4±0.41	-0.5±0.4	-0.5±0.31	-0.6±0.27	-0.4±0.25
30.0	-0.9±0.48	-0.9±0.2	-0.6±0.22	-0.4±0.19	-0.4±0.23	-0.8±0.35	-0.4±0.32	-0.6±0.22	-0.4±0.24	-0.4±0.21
40.0	-0.2±0.49	-1.0±0.1	-0.2±0.15	-0.4±0.16	-0.4±0.2	-0.8±0.23	-0.5±0.35	-0.6±0.2	-0.4±0.21	-0.4±0.18
50.0	-1.0±0.5	-0.8±0.1	-0.2±0.19	-0.4±0.14	-0.4±0.21	-0.8±0.27	-0.6±0.22	-0.6±0.18	-0.4±0.19	-0.4±0.12
60.0	-1.0±0.51	-1.0±0.1	-0.2±0.19	-0.4±0.11	-0.4±0.0	-0.8±0.26	-0.6±0.2	-0.6±0.19	-0.4±0.18	-0.4±0.13
70.0	-1.0±0.49	-1.0±0.09	-0.2±0.16	-0.4±0.0	-0.4±0.11	-0.8±0.24	-0.6±0.13	-0.6±0.17	-0.4±0.18	-0.4±0.15
80.0	-0.5±0.51	-1.0±0.1	-0.2±0.16	-0.4±0.07	-0.4±0.11	-0.8±0.2	-0.6±0.19	-0.6±0.2	-0.4±0.21	-0.4±0.09
90.0	-1.0±0.45	-1.0±0.1	-0.2±0.14	-0.4±0.0	-0.4±0.0	-0.8±0.19	-0.6±0.17	-0.6±0.13	-0.4±0.16	-0.4±0.12
100.0	0.0±0.51	-1.0±0.08	-0.2±0.0	-0.4±0.0	-0.4±0.0	-0.8±0.21	-0.6±0.14	-0.6±0.12	-0.4±0.19	-0.4±0.1
S/N	8.8	8.9	9.0	9.1	9.2	9.3	9.4	9.5	9.6	9.7
10.0	-0.2±0.31	-0.2±0.34	-0.4±0.46	-0.4±0.4	-0.6±0.47	-0.5±0.41	-0.8±0.44	-0.1±0.49	-0.4±0.42	-0.6±0.41
20.0	-0.4±0.33	-0.4±0.31	-0.4±0.24	-0.4±0.27	-0.4±0.36	-0.2±0.31	-0.2±0.4	-0.4±0.33	-0.3±0.35	-0.4±0.21
30.0	-0.4±0.32	-0.4±0.25	-0.4±0.28	-0.4±0.19	-0.4±0.23	-0.4±0.26	-0.6±0.24	-0.4±0.29	-0.4±0.31	-0.4±0.17
40.0	-0.4±0.2	-0.4±0.14	-0.4±0.16	-0.4±0.12	-0.4±0.21	-0.6±0.23	-0.2±0.21	-0.4±0.23	-0.5±0.2	-0.4±0.2
50.0	-0.4±0.13	-0.4±0.17	-0.4±0.13	-0.4±0.09	-0.4±0.19	-0.3±0.19	-0.2±0.24	-0.4±0.21	-0.4±0.18	-0.4±0.11
60.0	-0.4±0.13	-0.3±0.13	-0.4±0.13	-0.4±0.09	-0.4±0.15	-0.4±0.15	-0.4±0.21	-0.4±0.2	-0.4±0.18	-0.4±0.11
70.0	-0.2±0.14	-0.4±0.12	-0.4±0.08	-0.4±0.08	-0.4±0.15	-0.2±0.11	-0.2±0.19	-0.4±0.15	-0.4±0.19	-0.4±0.09
80.0	-0.2±0.11	-0.4±0.12	-0.4±0.08	-0.4±0.07	-0.4±0.17	-0.2±0.13	-0.2±0.2	-0.4±0.16	-0.4±0.16	-0.4±0.1
90.0	-0.2±0.11	-0.4±0.1	-0.4±0.11	-0.4±0.04	-0.4±0.1	-0.4±0.1	-0.2±0.18	-0.4±0.09	-0.4±0.15	-0.4±0.08
100.0	-0.4±0.1	-0.4±0.11	-0.4±0.05	-0.4±0.04	-0.4±0.12	-0.4±0.11	-0.2±0.19	-0.4±0.14	-0.4±0.18	-0.4±0.1
S/N	9.8	9.9	10.0	10.1	10.2					
10.0	-0.2±0.39	-0.3±0.3	-0.2±0.26	0.0±0.17	0.0±0.15					
20.0	-0.4±0.34	-0.6±0.21	-0.2±0.25	-0.2±0.21	0.0±0.17					
30.0	-0.4±0.28	-0.4±0.26	-0.4±0.23	-0.2±0.17	-0.2±0.15					
40.0	-0.4±0.25	-0.4±0.15	-0.6±0.17	-0.2±0.13	-0.2±0.11					
50.0	-0.4±0.19	-0.4±0.17	-0.6±0.18	-0.4±0.1	-0.2±0.09					
60.0	-0.4±0.12	-0.4±0.16	-0.6±0.15	-0.3±0.1	-0.2±0.1					
70.0	-0.4±0.17	-0.4±0.13	-0.6±0.16	-0.4±0.09	-0.2±0.09					
80.0	-0.4±0.1	-0.4±0.15	-0.6±0.11	-0.4±0.08	-0.2±0.09					
90.0	-0.4±0.07	-0.4±0.17	-0.4±0.16	-0.4±0.09	-0.2±0.06					
100.0	-0.4±0.05	-0.4±0.14	-0.6±0.15	-0.4±0.1	-0.2±0.04					

**Table 24.** Metallicity Results - Padova models MIST clusters - wavelength: 5000-6200

S/N	6.8	6.9	7.0	7.1	7.2	7.3	7.4	7.5	7.6	7.7
10.0	-0.6±0.34	-0.4±0.41	-0.4±0.39	-0.8±0.32	0.2±0.35	-0.2±0.39	0.0±0.44	0.2±0.34	0.2±0.38	0.2±0.43
20.0	-0.6±0.36	-0.4±0.48	-0.7±0.34	-0.6±0.34	-0.1±0.28	-0.2±0.32	0.2±0.43	0.2±0.25	0.0±0.34	0.1±0.36
30.0	-0.8±0.31	0.0±0.43	-0.8±0.37	-0.4±0.32	-0.2±0.26	-0.2±0.23	-0.2±0.45	0.0±0.28	0.0±0.3	-0.2±0.33
40.0	-0.8±0.29	-0.1±0.4	-0.8±0.31	-0.4±0.21	-0.2±0.33	-0.2±0.25	-0.6±0.4	0.0±0.32	0.0±0.28	-0.2±0.36
50.0	-0.8±0.35	-0.6±0.33	-0.8±0.26	-0.6±0.28	-0.2±0.23	-0.2±0.19	-0.6±0.41	-0.1±0.3	0.0±0.32	-0.6±0.33
60.0	-0.6±0.24	-0.6±0.33	-0.8±0.31	-0.4±0.23	-0.2±0.25	-0.2±0.18	-0.6±0.43	-0.4±0.3	0.0±0.33	-0.6±0.31
70.0	-0.7±0.35	-0.6±0.36	-0.8±0.25	-0.4±0.23	-0.2±0.27	-0.4±0.18	-0.7±0.35	-0.4±0.3	0.0±0.29	-0.6±0.31
80.0	-1.0±0.3	-0.6±0.38	-0.8±0.34	-0.6±0.2	-0.2±0.2	-0.4±0.16	-0.6±0.35	-0.2±0.28	-0.3±0.33	-0.6±0.34
90.0	-1.0±0.27	-0.6±0.33	-0.8±0.3	-0.5±0.16	-0.2±0.19	-0.4±0.16	-0.6±0.36	-0.4±0.28	0.0±0.3	-0.6±0.27
100.0	-1.0±0.29	-0.6±0.29	-0.8±0.42	-0.6±0.1	-0.2±0.21	-0.4±0.2	-0.6±0.29	-0.6±0.29	0.0±0.31	-0.6±0.24
S/N	7.8	7.9	8.0	8.1	8.2	8.3	8.4	8.5	8.6	8.7
10.0	0.0±0.38	0.2±0.37	0.2±0.38	0.0±0.42	-0.1±0.46	0.2±0.47	0.0±0.46	-0.1±0.41	0.0±0.39	0.0±0.42
20.0	0.0±0.36	-0.2±0.38	-0.2±0.38	-0.2±0.36	-0.2±0.36	-0.2±0.32	-0.2±0.38	-0.1±0.3	-0.2±0.31	-0.2±0.31
30.0	-0.4±0.34	-0.5±0.34	-0.6±0.3	-0.4±0.27	-0.2±0.32	-0.5±0.35	-0.3±0.27	-0.2±0.3	-0.2±0.34	-0.2±0.31
40.0	-0.6±0.3	-0.2±0.3	-0.6±0.31	-0.4±0.3	-0.2±0.29	-0.3±0.27	-0.4±0.28	-0.2±0.3	-0.2±0.28	-0.2±0.23
50.0	-0.4±0.27	-0.5±0.23	-0.5±0.29	-0.6±0.14	-0.6±0.26	-0.6±0.21	-0.6±0.29	-0.4±0.2	-0.4±0.23	-0.4±0.18
60.0	-0.4±0.3	-0.6±0.27	-0.5±0.25	-0.6±0.23	-0.6±0.21	-0.6±0.2	-0.6±0.2	-0.4±0.19	-0.4±0.21	-0.4±0.17
70.0	-0.4±0.32	-0.6±0.23	-0.4±0.23	-0.4±0.13	-0.6±0.24	-0.6±0.21	-0.5±0.19	-0.6±0.16	-0.6±0.17	-0.5±0.19
80.0	-0.5±0.29	-0.6±0.24	-0.4±0.21	-0.6±0.17	-0.2±0.21	-0.6±0.19	-0.6±0.15	-0.4±0.14	-0.4±0.15	-0.2±0.18
90.0	-0.4±0.26	-0.6±0.21	-0.4±0.19	-0.4±0.11	-0.6±0.21	-0.6±0.18	-0.6±0.16	-0.5±0.16	-0.6±0.17	-0.4±0.15
100.0	-0.5±0.3	-0.6±0.2	-0.5±0.22	-0.4±0.14	-0.6±0.18	-0.6±0.17	-0.4±0.14	-0.4±0.11	-0.5±0.16	-0.4±0.15
S/N	8.8	8.9	9.0	9.1	9.2	9.3	9.4	9.5	9.6	9.7
10.0	-0.1±0.38	-0.2±0.4	0.2±0.39	-0.5±0.46	-0.4±0.45	0.0±0.45	-0.4±0.43	-0.4±0.46	-0.4±0.39	0.0±0.47
20.0	-0.3±0.37	-0.2±0.37	-0.4±0.39	-0.4±0.39	-0.4±0.33	-0.6±0.25	-0.4±0.3	-0.4±0.26	-0.4±0.36	-0.4±0.29
30.0	-0.4±0.27	-0.4±0.31	-0.4±0.39	-0.4±0.32	-0.4±0.32	-0.4±0.35	-0.4±0.28	-0.4±0.28	-0.4±0.29	-0.6±0.18
40.0	-0.4±0.21	-0.3±0.29	-0.4±0.33	-0.4±0.28	-0.4±0.27	-0.4±0.24	-0.4±0.25	-0.4±0.2	-0.5±0.16	-0.4±0.13
50.0	-0.4±0.24	-0.3±0.27	-0.4±0.26	-0.4±0.23	-0.4±0.17	-0.4±0.15	-0.4±0.23	-0.4±0.12	-0.4±0.11	-0.4±0.11
60.0	-0.4±0.18	-0.4±0.24	-0.4±0.26	-0.4±0.2	-0.4±0.2	-0.4±0.21	-0.4±0.17	-0.4±0.1	-0.4±0.16	-0.4±0.09
70.0	-0.4±0.22	-0.4±0.25	-0.2±0.29	-0.4±0.16	-0.4±0.15	-0.4±0.18	-0.4±0.12	-0.4±0.12	-0.4±0.15	-0.4±0.11
80.0	-0.4±0.14	-0.4±0.24	-0.4±0.21	-0.4±0.15	-0.4±0.17	-0.4±0.17	-0.4±0.16	-0.4±0.17	-0.4±0.11	-0.4±0.09
90.0	-0.4±0.1	-0.4±0.18	-0.4±0.2	-0.4±0.14	-0.4±0.13	-0.4±0.14	-0.2±0.17	-0.4±0.12	-0.4±0.11	-0.4±0.08
100.0	-0.4±0.1	-0.4±0.23	-0.4±0.19	-0.4±0.17	-0.4±0.13	-0.4±0.12	-0.4±0.15	-0.4±0.12	-0.4±0.13	-0.4±0.11
S/N	9.8	9.9	10.0	10.1	10.2					
10.0	-0.6±0.44	-0.4±0.46	0.0±0.45	-0.4±0.4	0.2±0.44					
20.0	-0.5±0.31	-0.4±0.38	-0.4±0.33	-0.2±0.34	-0.2±0.36					
30.0	-0.4±0.3	-0.4±0.23	-0.4±0.27	-0.2±0.27	-0.2±0.25					
40.0	-0.4±0.11	-0.4±0.11	-0.4±0.26	-0.3±0.27	-0.2±0.13					
50.0	-0.4±0.1	-0.4±0.08	-0.4±0.16	-0.2±0.2	-0.2±0.12					
60.0	-0.4±0.1	-0.4±0.09	-0.4±0.13	-0.4±0.1	-0.2±0.16					
70.0	-0.4±0.09	-0.4±0.08	-0.4±0.08	-0.4±0.14	-0.2±0.12					
80.0	-0.4±0.09	-0.4±0.04	-0.4±0.11	-0.4±0.07	-0.2±0.13					
90.0	-0.4±0.09	-0.4±0.05	-0.4±0.05	-0.4±0.1	-0.2±0.13					
100.0	-0.4±0.07	-0.4±0.04	-0.4±0.06	-0.4±0.09	-0.2±0.09					